

**THE EFFECT OF POTASSIUM HYDROXIDE ON THE  
POLYMERIZATION OF TRICHLOROPHENOL, PYRROLE AND  
THIOPHENE BY MICROWAVE INITIATION**

**A THESIS SUBMITTED TO  
THE GRADUATE SCHOOL OF NATURAL AND APPLIED SCIENCES  
OF  
MIDDLE EAST TECHNICAL UNIVERSITY**

**BY**

**MÜFİDE ELİF (ÜNSAL) GÜNGÖR**

**IN PARTIAL FULFILLMENT OF THE REQUIREMENTS  
FOR  
THE DEGREE OF DOCTOR OF PHILOSOPHY  
IN  
CHEMISTRY**

**JUNE 2008**

**Approval of the Thesis:**

**THE EFFECT OF POTASSIUM HYDROXIDE ON THE  
POLYMERIZATION OF TRICHLOROPHENOL, PYRROLE AND  
THIOPHENE BY MICROWAVE INITIATION**

submitted by **M. ELİF (ÜNSAL) GÜNGÖR** in partial fulfillment of the requirements for the degree of **Doctor of Philosophy in Chemistry Department, Middle East Technical University** by,

Prof. Dr. Canan Özgen \_\_\_\_\_  
Dean, Graduate School of **Natural and Applied Science**

Prof. Dr. Ahmet Önal \_\_\_\_\_  
Head of Department, **Chemistry**

Prof. Dr. Duygu Kısakürek \_\_\_\_\_  
Supervisor, **Chemistry Department, METU**

**Examining Committee Members**

Prof. Dr. Oya Şanlı  
Chemistry Department,  
Gazi University \_\_\_\_\_

Prof. Dr. Duygu Kısakürek  
Chemistry Department, METU \_\_\_\_\_

Prof. Dr. Leyla Aras  
Chemistry Department, METU \_\_\_\_\_

Prof. Dr. Ali Usanmaz  
Chemistry Department, METU \_\_\_\_\_

Prof. Dr. Levent Toppare  
Chemistry Department, METU \_\_\_\_\_

**Date:** \_\_\_\_\_ 24.06.2008

**I hereby declare that all information in this document has been obtained and presented in accordance with academic rules and ethical conduct. I also declare that, as required by these rules and conduct, I have fully cited and referenced all material and results that are not original to this work.**

Name, Last name : M. Elif (Ünsal) Güngör

Signature :

## ABSTRACT

### THE EFFECT OF POTASSIUM HYDROXIDE ON THE POLYMERIZATION OF TRICHLOROPHENOL, PYRROLE AND THIOPHENE BY MICROWAVE INITIATION

Güngör, (Ünsal) M. Elif

Ph.D., Chemistry Department

Supervisor : Prof. Dr. Duygu Kısakürek

June 2008, 114 pages

The synthesis of black conducting polymer (**CP**) and/or crosslinked polymers (**CLP**) and/or radical ion polymer (**RIP**) and/or white polymers (**WP**) and/or orange polymer (**OP**) were achieved by using KOH with TCP, pyrrole and thiophene via microwave energy in a very short time interval.

Polymerizations were carried out by constant microwave energy with different time intervals varying from 1 to 25 min; or at constant time intervals with variation of microwave energy from 90 to 900 watt; or varying the water content from 0, 0.5 to 5 ml at constant time intervals and microwave energy, or at constant time interval, water content, microwave energy with variation of amount of KOH 0.03 mol to  $6 \times 10^{-4}$  mol. The effects of heating time, microwave energy, water content and amount of KOH on the percent conversion and the polymer synthesis were also investigated.

White, orange polymers and radical ion polymers were characterized by FTIR (Fourier Transform Infrared),  $^1\text{H}$ -NMR (Proton Nuclear Magnetic Resonance),  $^{13}\text{C}$ -NMR (Carbon-13 Nuclear Magnetic Resonance), TGA/ FTIR (Thermal Gravimetric Analysis / Fourier Transform Infrared), DSC (Differential Scanning Calorimeter), SEM (Scanning Electron Microscope), ESR (Electron Spin Resonance), GPC (Gel Permeation Chromatography), UV-Vis (UV-Visible Spectroscopy) and Light Scattering. Conducting and crosslinked polymers were characterized by FTIR, TGA/ FTIR, DSC, SEM, ESR, XRD (Powder Diffraction X-Ray) and conductivity.

Keywords: Microwave energy; conducting polymer; crosslinked polymer; radical ion polymer.

## ÖZ

### MİKRODALGA BAŞLATICISI İLE POTASYUM HİDROSİTİN TRİKLOROFENOL, PİROL, TİYOFEN POLİMERİZASYONUNDAKİ ETKİLERİ

Güngör, (Ünsal) M. Elif

Doktora, Kimya Bölümü

Tez Yöneticisi: Prof. Dr. Duygu Kısakürek

Haziran 2008, 114 sayfa

Siyah iletken polimer (**CP**) ve/veya çapraz bağlı (**CLP**) ve/veya iyon radikal (**RIP**) ve/veya beyaz (**WP**) ve/veya portakal (**OP**) polimerlerin sentezi mikrodalga enerjisi yoluyla KOH ile TCP, pirol ve tiyofen kullanılarak çok kısa zaman aralığında gerçekleştirildi.

Polimerleşmeler 1 ile 25 dakika arasında değişen zaman aralıklarında, sabit mikrodalga enerjisinde veya 90 ile 900 watt arasında değişen mikrodalga enerjilerinde, sabit sürelerde veya 0, 0.5 ile 5 ml su miktarları değiştirilerek, sabit süre ve mikrodalga enerjisinde ya da süre, mikrodalga enerjisi ve su miktarı sabit iken  $0.03$  ile  $6 \times 10^{-4}$  mol aralığında KOH kullanılarak gerçekleştirilmiştir Aynı zamanda ısıtma zamanı, mikrodalga enerjisi, su içeriği ve KOH miktarının polimer sentezi ve yüzde dönüşümüne etkisi incelenmiştir.

Sentezlenen polimerlerden, beyaz, portakal ve radikal iyon polimerleri FTIR (Fourier Transform Infrared Spektroskopisi),  $^1\text{H-NMR}$  (Proton Nükleer

Manyetik Rezonans),  $^{13}\text{C}$ -NMR( Karbon-13 Nükleer Manyetik Rezonans), TGA/ FTIR (Termogravimetrik Analiz / Fourier Transform Infrared), DSC (Diferansiyel Taramalı Kalorimetri), SEM (Taramalı Elektron Mikroskop), ESR (Elektron Spin Rezonans), UV-Vis (UV-Görünür Bölge Spektroskopisi) ve Işık Saçılması ile karakterize edilmiştir . İletken ve çapraz bağlı polimerler ise FTIR, TGA/ FTIR, DSC, SEM, ESR, XRD (Toz X-ışınları Kırınımı Spektroskopisi) ve İletkenlik Ölçümü ile karakterize edilmiştir.

Anahtar Kelimeler: Mikrodalga enerjisi; iletken polimer, çapraz bağlı polimer, iyon radikal polimer.

**Kızıma ve Eşime,**

**To My Daughter and Husband,**

## ACKNOWLEDGMENTS

I would like to express my sincere gratitude and respect to my supervisors Prof. Dr. Duygu KISAKÜREK for her unceasing interest, guidance, encouragement and support during the course of this study.

I would like to thank Prof. Dr. Levent TOPPARE for his advices and comments.

I would like to express my special thanks to all my research group friends Dr. Güler (BAYRAKLI) ÇELİK, Binnur ÖZKAN and Leyla MOLU for their support, friendship during the days of my hard study.

I would like to thank to Dr. Ece DÜZGÜN for her friendship, help and valuable discussions.

I would like to thank sincerely to current colleagues in SANAEM/TAEK; Dr. Gülten KAHRAMAN, Dr. Uğur Adnan SEVİL, Dr. Yusuf AGUŞ, Alper Nazmi YÜKSEL, Ülkü Rabia YÜCE for their help whenever I needed, their moral support and friendship.

I am much indebted to my parents, Türkay and Hayri ÜNSAL, for their love, encouragement, trust and support. I could not have completed this work without their help. Also I would like to thank to my brother Murat and his wife Burcu for their love and encouragement.

Finally, I would like to express sincere appreciation to my husband Murat GÜNGÖR for his everlasting encouragement, support, intelligence and love which made this work possible. Also great thanks to my daughter Müge GÜNGÖR for her patience and understanding my frequent absences.

## TABLE OF CONTENTS

ABSTRACT .....	iv
ÖZ.....	iv
ACKNOWLEDGMENTS .....	ix
TABLE OF CONTENTS .....	x
LIST OF TABLES .....	xiii
LIST OF FIGURES .....	xiv
LIST OF ABBREVIATIONS .....	xviii
CHAPTER	
1.INTRODUCTION.....	1
1.1 Conducting Polymer .....	1
1.1.1 History of Conducting Polymers .....	1
1.1.2 Synthesis of Conducting Polymers .....	2
1.1.3 Applications of Conducting Polymers.....	4
1.2 Electrical Cunduction in Conducting Polymers .....	5
1.2.1 Conductivity .....	5
1.2.2 Band Theory and Doping-Induced Transitions in Conjugated Polymers .....	7
1.2.3. Doping .....	10
1.3 Polypyrrole .....	11
1.4 Synthesis of Polypyrrole .....	12
1.4.1 Chemical Polymerization of PPy.....	13
1.4.2 Electrochemical Polymerization of PPy .....	15
1.5 Polythiophene .....	17
1.6 Synthesis of Polythiophene.....	18
1.6.1 Organometallic Coupling.....	18
1.6.2 Oxidative Coupling.....	19
1.6.3 Electrochemical Polymerization of PTh.....	20

1.7 Phenol .....	22
1.8 Poly(phenylene oxide)s and Their Synthesis.....	23
1.8.1 History of poly(phenylene oxide)s .....	25
1.9 Crosslinked Polymers .....	29
1.9.1 Formation of network structure .....	29
1.9.2 Crosslinking Mechanism .....	31
1.10 Microwave-assisted Polymerization.....	32
1.10.1 Fundamental Concept of Microwave.....	32
1.10.2 Application of Microwave on Polymeric Materials .....	34
1.11 Aim of the study .....	36
2. EXPERIMENTAL .....	37
2.1 Chemicals .....	37
2.1.1 2,4,6 – Trichlorophenol (TCP), Pyrrole(Py) and Thiophene(Th) .....	37
2.1.2 Potassium Hydroxide (KOH) .....	37
2.1.3 Toluene .....	37
2.1.4 Ethyl Alcohol.....	37
2.1.5 Hydrochloric Acid .....	37
2.1.6 Deuterated Chloroform (CDCl <sub>3</sub> ).....	38
2.1.7 Potassium Bromide (KBr) .....	38
2.2 Apparatus and Instruments .....	38
2.2.1 Microwave Oven .....	38
2.2.2 Differential Scanning Calorimeter (DSC) .....	38
2.2.3 Thermogravimetry Analysis and Fourier – Transform Infrared Spectrophotometer (TGA/FTIR) System.....	38
2.2.4 Fourier – Transform Infrared Spectrophotometer (FTIR) .....	39
2.2.5 NMR Spectrophotometer.....	39
2.2.6 Mass Spectrometer.....	39
2.2.7 Powder Diffraction X-ray .....	39
2.2.8 Light Scattering .....	40
2.2.9 ESR.....	40

2.2.10 SEM .....	40
2.2.11 UV-Vis.....	40
2.2.12 Conductivity Measurement.....	40
2.3 Procedure .....	42
2.3.1 Synthesis of Polymers by using TCP and KOH .....	42
2.3.2 Synthesis of Polymers by using pyrrole and KOH.....	42
2.3.3 Synthesis of Polymers by using Thiophene and KOH .....	43
2.3.4 Characterization of the Polymers .....	43
3. RESULTS AND DISCUSSION .....	44
3.1 Synthesis of Polymer with TCP and KOH .....	45
3.1.1 Characterization .....	47
3.2 Synthesis of Polymer with Pyrrole and KOH .....	58
3.2.1 Characterization .....	60
3.3 Synthesis of Polymer with Thiophene and KOH .....	77
3.3.1 Characterization .....	79
4. CONCLUSIONS .....	94
REFERENCES .....	98
APPENDIX.....	106
VITA .....	114

## LIST OF TABLES

### TABLES

Table 3.1.1 The effect of polymerization time and energy on the % conversion and % weight loss of CP and CLP of TCP .....	46
Table 3.2.1 The effect of polymerization time, energy and amount of KOH on the % conversion and % weight loss of CP and RIP of pyrrole ...	59
Table 3.3.1 The effect of polymerization time, energy and amount of KOH on the % conversion and % weight loss of CP, WP and OP of thiophene.....	78

## LIST OF FIGURES

### FIGURES

Figure 1.1 Some common CPs.....	2
Figure 1.2 Applications of CPs.....	5
Figure 1.3 Magnitude of conductivity of different types of conducting polymer. ....	6
Figure 1.4 Band structure of a metal, a semiconductor and an insulator .....	8
Figure1.5 The structure of a polaron and bipolaron in polypyrrole and its corresponding energy bands.....	10
Figure1.6 Chemical Polymerization of PPy.....	14
Figure1.7 Electrochemical Polymerization of PPy .....	16
Figure1.8 The First Chemical Synthesis of PTh.....	18
Figure1.9 Chemical Polymerization of PTh. ....	20
Figure1.10 Electrochemical Polymerization of PTh.....	21
Figure1.11 The Oxidation Products of Phenols.....	23
Figure1.12 Oxidative Coupling Reactions of Phenols.....	27
Figure1.13 Crosslinked Structure .....	31
Figure1.14 Schematic representation of the microwave heating of water.....	34
Figure2.1 Four-probe conductivity measurement set up .....	41
Figure3.1.1 % conversion of CP and CLP.....	47
Figure3.1.2 FTIR spectrum of (a) CLP, (b) CP and (c) released gases during polymerization.....	49
Figure3.1.3 DSC thermograms of (a) CP and (b) CLP.....	50

Figure3.1.4 TGA thermograms of (a) CP and (b) CLP. ....	52
Figure3.1.5 X-ray powder diffraction spectrum of (a) unwashed CP, (b) washed CP and (c) CLP.....	53
Figure3.1.6 The effect of energy on conductivity of CP. ....	54
Figure3.1.7 ESR spectra of (a) CP and (b) CLP at room temp.....	55
Figure3.1.8 UV-Vis spectra of (a) TCP and (b) CLP* at room temperature...	56
Figure3.1.9 SEM micrographs of (a) washed CP, (b) unwashed CP, (c) washed CLP and (d) unwashed CLP .....	57
Figure3.2.1 % conversion of CPs of pyrrole at different concentration of KOH.....	60
Figure 3.2.2 FTIR spectra of (a) Pyrrole, (b) RIP of pyrrole, (c) CP (with low concentration of KOH) of pyrrole and (d) released gases during polymerization. ....	62
Figure 3.2.3 (a) <sup>1</sup> H NMR of RIP and (b) <sup>13</sup> C NMR of RIP of pyrrole .....	64
Figure 3.2.4 (a) Ion-temperature profile of RIP, (b) Direct pyrolysis mass spectrum of RIP at 428 °C and (c) Indirect pyrolysis mass spectrum of RIP of pyrrole at 428 °C .....	67
Figure 3.2.5 DSC thermograms of (a) RIP and (b) CP of pyrrole .....	68
Figure 3.2.6 TGA thermograms of (a) RIP and (b) CP of pyrrole.....	70
Figure 3.2.7 The effect of energy on conductivity of CP of pyrrole (a) CP (with low concentration of KOH) and (b) CP (with high concentration of KOH) .....	71
Figure 3.2.8 X-ray powder diffraction spectra of (a) unwashed CP and (b) washed CP of pyrrole.....	72
Figure 3.2.9 ESR spectra of (a) CP, (b) RIP and (c) RIP of pyrrole	

at room temperature. ....	74
Figure 3.2.10 UV-Vis spectra of (a) Pyrrole, (b) 6 min. RIP, (c) 8 min. RIP and (d) 10 min. RIP of pyrrole at room temperature. ....	75
Figure 3.2.11 SEM micrographs of (a), (b), (c) unwashed CP, (d) washed CP, (e) and (f) unwashed RIP. ....	76
Figure 3.3.1 % conversion of CPs of thiophene at different concentration of KOH. ....	79
Figure 3.3.2 FTIR spectra of (a) Thiophene, (b) CP (with low concentration of KOH) and (c) released gases during polymerization. ....	81
Figure 3.3.3 FTIR spectra of (a) white polymer WP and (b) orange polymer OP of thiophene. ....	82
Figure 3.3.4 (a) <sup>1</sup> H NMR of WP and (b) <sup>1</sup> H NMR of OP of thiophene. ....	83
Figure 3.3.5 DSC thermograms of (a) CP, (b) white polymer WP and (c) orange polymer OP of thiophene. ....	84
Figure 3.3.6 TGA thermograms of (a) CP, (b) WP and (c) OP of thiophene. ....	87
Figure 3.3.7 The effect of energy on conductivity of CP of thiophene (a) CP (with low concentration of KOH) and (b) CP (with high concentration of KOH). ....	88
Figure 3.3.8 X-ray powder diffraction spectra of (a) unwashed CP and (b) washed CP of thiophene. ....	89
Figure 3.3.9 X-ray powder diffraction spectra of (a) unwashed WP and	

(b) unwashed OP of thiophene. ....	90
Figure 3.3.10 ESR spectra of (a) CP and (b) OP at room temperature. ....	91
Figure 3.3.11 SEM micrographs of (a) washed CP, (b) unwashed CP, (c) and (d) WP, (e) WP, (f) X-ray microanalysis of WP, (g) and (h) OP of thiophene. ....	93
Figure A.1 In situ FTIR spectrum of evolved volatile components during TGA of CP synthesized from potassium 2,4,6-trichlorophenolate at (a) 31 °C (b) 166 °C (c) 360 °C (d) 453 °C (e) 562 °C (f) 795 °C. ....	108
Figure A.2 In situ FTIR spectrum of evolved volatile components during TGA of CLP synthesized from potassium 2,4,6-trichlorophenolate at (a) 120 °C (b) 403 °C (c) 578 °C (d) 802 °C. ....	110
Figure A.3 In situ FTIR spectrum of evolved volatile components during TGA of <b>RIP</b> synthesized from pyrrole and KOH at (a) 190 °C. ....	111
Figure A.4 In situ FTIR spectrum of evolved volatile components during TGA of <b>WP</b> synthesized from KOH and thiophene at (a) 185 °C. ....	112
Figure A.5 In situ FTIR spectrum of evolved volatile components during TGA of orange polymer <b>OP</b> synthesized from KOH and thiophene at (a) 45 °C. ....	113

## LIST OF ABBREVIATIONS

TCP	Trichlorophenol
CP	Conducting Polymer
RIP	Radical Ion Polymer
CLP	Crosslinked Polymer
WP	White Polymer
OP	Orange Polymer
MW	Microwave
PPy	Polypyrrole
PA	Polyacetylene
PTh	Polythiophene
PANI	Polyaniline
LED	Light Emitting Diode
DSC	Differential Scanning Calorimeter
TGA	Thermal Gravimetric Analysis
NMR	Nuclear Magnetic Resonance

FTIR    Fourier Transform Infrared

SEM    Scanning Electron Microscope

VB    Valance Band

CB    Conduction Band

$E_g$     Band Gap

## CHAPTER 1

### INTRODUCTION

#### 1.1. Conducting Polymers

##### 1.1.1. History of Conducting Polymers

Conjugated polymers have led to an explosive growth in research effort during the last two decades, both scientific and industrial [1]. This interest is due to substantial  $\pi$ -electron delocalization along their  $\pi$ -conjugated backbones, which gives rise to fascinating optical and non-linear optical properties and allows them to become good electrical conductors, typically when oxidized or reduced. The discovery of conducting polymers (CP)s as a class of materials and of their properties was honoured in the year 2000 with the awarding of the Nobel Prize in chemistry to Alan McDiarmid, Alan J. Heeger and Hideki Shirakawa [2]. In 1977, they showed that poly(acetylene), which is the simplest polyconjugated system can be rendered conductive by the reaction with bromine and iodine vapors [3]. Due to limitations (unstability in the presence of oxygen which destroys conjugation and causes degradation of polymeric chains) of polyacetylene, many other CPs so called 'synthetic metals' have been developed and extensively investigated such as poly-(para-phenylene), poly(phenylenevinylene), polypyrrole, polythiophene, polyfuran, polyaniline (Figure 1.1) [4].

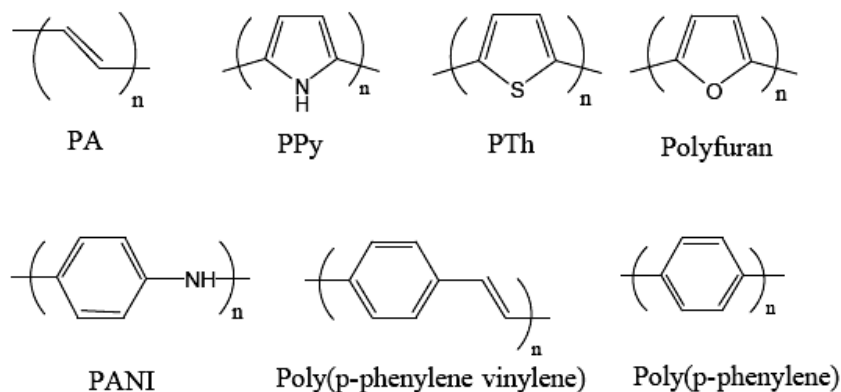


**Figure 1.1** Some common CPs.

### 1.1.2. Synthesis of Conducting Polymers

Conducting polymers(CP)s can be synthesized by any one of the following techniques:

- a) Chemical polymerization
- b) Electrochemical polymerization
- c) Photochemical polymerization
- d) Metathesis polymerization
- e) Concentrated emulsion polymerization
- f) Inclusion polymerization
- g) Solid-state polymerization
- h) Plasma polymerization
- i) Pyrolysis
- j) Soluble precursor polymer preparation
- k) Microwave initiation

Among all the above categories, chemical polymerization [5-8] is the most useful method for preparing large amount of conducting polymers. Chemical

polymerization (oxidative coupling) is followed by the oxidation of monomers to a cation radical and their coupling to form dications and the repetition of this process generates a polymer. All the classes of conjugated polymers may be synthesized by this technique.

Electrochemical polymerization is normally carried out in a single- or dual-compartment cell by adopting a standard three-electrode configuration in a supporting electrolyte, both dissolved in an appropriate solvent. Electrochemical polymerization can be carried out potentiometrically by using a suitable power supply (potentiogalvanostat) [1,9-10]. The electrochemical technique has received wider attention both because of the simplicity and the added advantage of obtaining a conductive polymer being simultaneously doped. Beside this, wider choice of cations and anions for use as 'dopant ions' are available in the electrochemical polymerization process. Using this novel technique, a variety of CPs like polypyrrole, polythiophene, polyphenylene oxide, polyaniline have been generated.

Photochemical polymerization [11] takes place in the presence of sunlight. This technique utilises photons to initiate a polymerization reaction in the presence of photosensitisers.

Plasma polymerization is a technique for preparing ultrathin uniform layers that strongly adhere to an appropriate substrate. The advantage of this method is that it eliminates various steps needed for the conventional coating process.

Metathesis polymerization is unique, differing all other polymerizations in that all the double bonds in the monomer remain in the polymer. Metathesis polymerization is further divided into three classes: ring-opening metathesis of cyclo-olefins (ROMP); metathesis of alkynes, acyclic or cyclic; and metathesis of diolefins.

Pyrolysis is probably one of the oldest approaches utilised to synthesize conductive polymers by eliminating heteroatoms from the polymer by heating it to form

extended aromatic structures. The product of polymer hydrolysis can be a film, powder or a fibre depending on the form and nature of the starting polymer including the pyrolysis condition [12].

Microwave heating has shown a great potential, still far from being extensively used as it could, for accelerated industrial processing of the entire variety of commercial (both commodity and high-performance) plastics, rubbers, thermosetting resins and conductive polymers [13].

### **1.1.3. Applications of Conducting Polymers**

The conductive polymers have been attracting the attention of countless groups of researchers all over the world because of their potential application in the modern technology [14]. The very low density of polymers as compared to that of metals attracted the attention of the first investigators looking for possible applications of the newly discovered electrically conductive polymeric materials. However, poor stability vitiated their attempts to use them in batteries or energy storage devices. Stability problems were solved with the discovery of the very stable PANI and its analogues, of PThs and PPys that are sensitive to oxygen only in their neutral forms. Such polymers exhibit mechanical, electrical, optical and magnetic properties, which sometimes resemble metals and semiconductors. These characteristics turn conducting polymers into a category of so-called synthetic metals and make them suitable for great number of applications.

There is growing interest in using conducting polymers as nanowires, for rechargeable batteries and energy storage, for photoelectrodes and antistatic coatings, dissipation of spacecraft charging, printed board surface finish (Figure 1.2) [12,15,16].

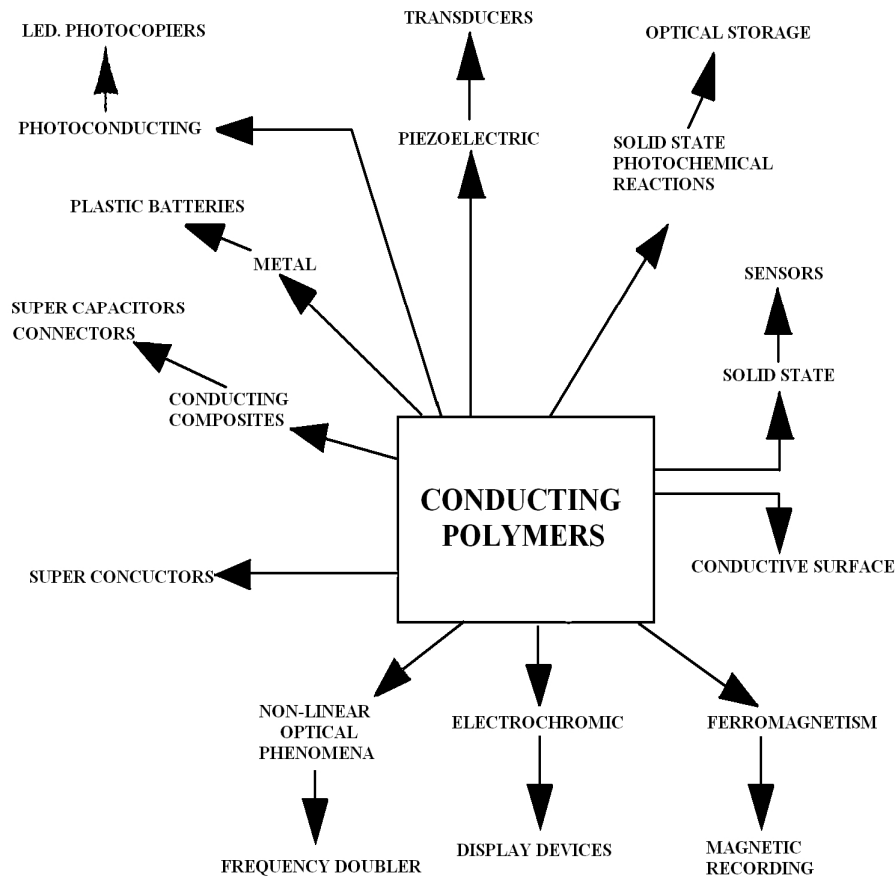


**Figure 1.2** Applications of CPs.

## 1.2 Electrical Conduction in Conducting Polymers

### 1.2.1. Conductivity

Electrical conductivity or specific conductivity is a measure of a material's ability to conduct an electric current. When an electrical potential difference is placed across a conductor, its movable charges flow, giving rise to an electric current. The conductivity  $\sigma$  is defined as the ratio of the current density ( $J$ ) to the electric field strength ( $E$ ):

$$\mathbf{J} = \sigma \mathbf{E} \tag{1}$$

In polymeric materials conduction may occur through the movement of either electrons or ions. In both cases electrical conductivity depends on a number of fundamental parameters, such as the number density of mobile charge carriers  $n$ , the charge  $q$ , and the carrier mobility  $\mu$ . The relationship between conductivity  $\sigma$  ( $S\ m^{-1}$ ) and three latter quantities is expressed by the general relationship:

$$\sigma = n q \mu \quad (2)$$

The magnitude of the room temperature conductivity for different types of conducting polymer is shown in Figure 1.3 and compared to the conductivity of copper, iron, and the range of conductivities for typical amorphous conventional metals [17]. The conductivity of a polymer can be increased several fold by “doping” it with oxidizing/ reducing substituents or by donor/ acceptor radicals. As the doping level increases, the conductivity of conjugated polymers increases. The “doped” form of polyacetylene had a conductivity of  $10^3\ S\ cm^{-1}$ , which was higher than that of any previously known polymers. As a comparison, teflon has a conductivity of  $10^{-16}\ S\ cm^{-1}$  and silver and copper  $10^5\ S\ cm^{-1}$ .

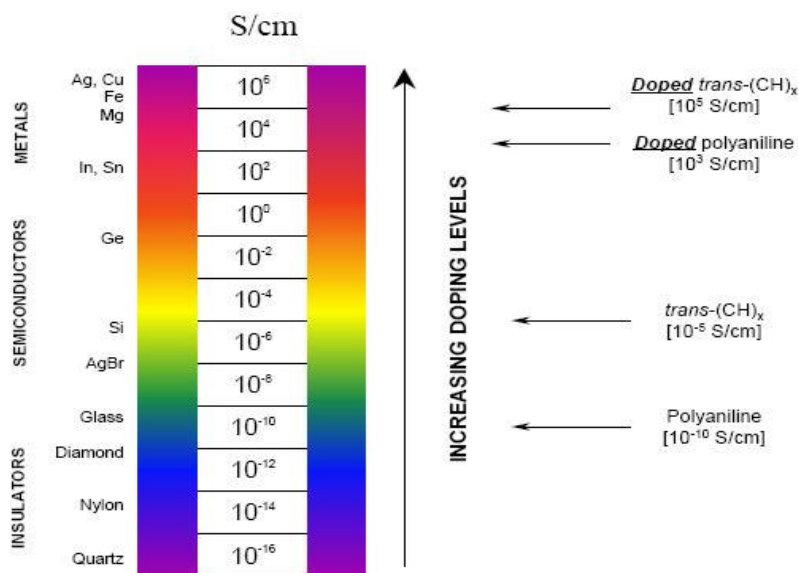


**Figure 1.3** Magnitude of conductivity of different types of conducting polymer.

### **1.2.2. Band Theory and Doping-Induced Transitions in Conjugated Polymers**

Band theory has been used to describe the properties of insulators, metals, and semiconductors. The energy spacing between the highest occupied and the lowest unoccupied bands, is called the band gap ( $E_g$ ). The lowest unoccupied band is called the conduction band (CB) and the highest occupied one the valence band (VB). The width of the forbidden band, or band gap ( $E_g$ ) between the VB and CB determines the intrinsic electrical properties of the material.

The conductivity of the metal is due either to only-partly-filled valence or conduction bands, or to the band gap being near zero, so that with even a weak electric field the electrons easily redistribute: electrons at higher energy and holes at lower energy. This situation is ideal for rapid transport of a charge: An electron injected at a certain position into a conduction orbital, which is delocalised over macroscopic dimensions, could leave the same orbital instantaneously at any other point in that orbital's space. Semiconductors have filled VBs and empty CBs and the movement of electrons from VB to CB provides the conduction. The gap energy is small ( $E_g < 3\text{eV}$ ) as compared to the larger gap in insulators ( $E_g > 3\text{eV}$ ) (Figure 1.4) [18].

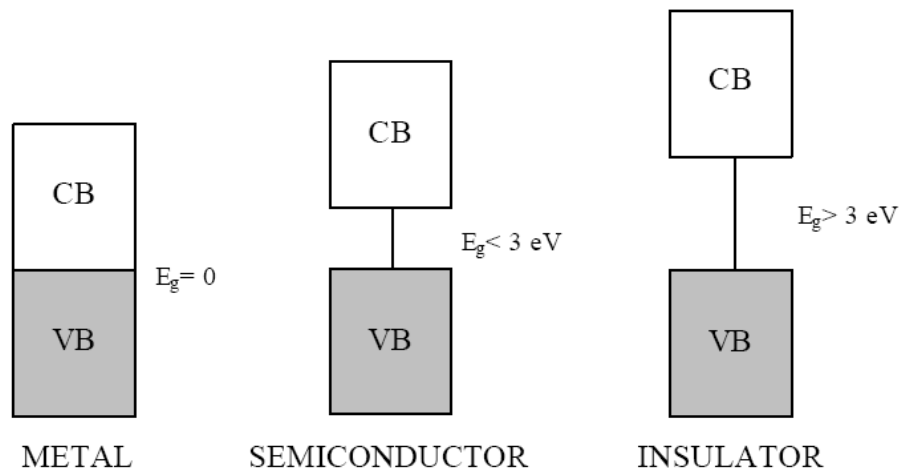


**Figure 1.4** Band structure of a metal, a semiconductor and an insulator.

The polymer is transformed into a conductor by doping it with either an electron donator or an electron acceptor. This is reminiscent of doping of silicon based semiconductors where silicon is doped with either arsenic or boron. However, while the doping of silicon produces a donor energy level close to the conduction band or a acceptor level close to the valence band, this is not the case with conducting polymers. The evidence for this is that the resulting polymers do not have a high enough concentration of free spins, as determined by electron spin spectroscopy. Initially the free spins concentration increases with concentration of dopant. At larger concentrations, however, the concentration of free spins levels off at a maximum. To understand this it is necessary to examine the way in which charge is stored along the polymer chain and its effect. The polymer may store charge in two ways. In an oxidation process it could either lose an electron from one of the bands or it could localize the charge over a small section of the chain. Localizing the charge causes a local distortion due to a change in geometry, which costs the polymer some energy. However, the generation of this local geometry decreases the ionization energy of the polymer chain and increases its electron affinity making it more able to accommodate the newly formed charges. This method increases the energy of the polymer less than it

would if the charge was delocalized and, hence, takes place in preference of charge delocalization.

The oxidative doping of polypyrrole proceeds in the following way. An electron is removed from the p-system of the backbone producing free radical and a spinless positive charge. The radical and cation are coupled to each other via local resonance of the charge and the radical. In this case, a sequence of quinoid-like rings is used. The distortion produced by this is of higher energy than the remaining portion of the chain. The creation and separation of these defects costs a considerable amount of energy. This limits the number of quinoid-like rings that can link these two bound species together. In the case of polypyrrole it is believed that the lattice distortion extends over four pyrrole rings. This combination of a charge site and a radical is called a polaron. This could be either a radical cation or radical anion. This creates a new localized electronic states in the gap, with the lower energy states being occupied by a single unpaired electrons. The polaron state of polypyrrole are symmetrically located about 0.5 eV from the band edges. Upon further oxidation the free radical of the polaron is removed, creating a new spinless defect called a bipolaron. This is of lower energy than the creation of two distinct polarons. At higher doping levels it becomes possible that two polarons combine to form a bipolaron. Thus at higher doping levels the polarons are replaced with bipolarons. The bipolarons are located symmetrically with a band gap of 0.75 eV for polypyrrole. This eventually, with continued doping, forms into a continuous bipolaron bands. Their band gap also increases as newly formed bipolarons are made at the expense of the band edges. For a very heavily dope polymer it is conceivable that the upper and the lower bipolaron bands will merge with the conduction and the valence bands respectively to produce partially filled bands and metallic like conductivity (Figure1.5) [19].

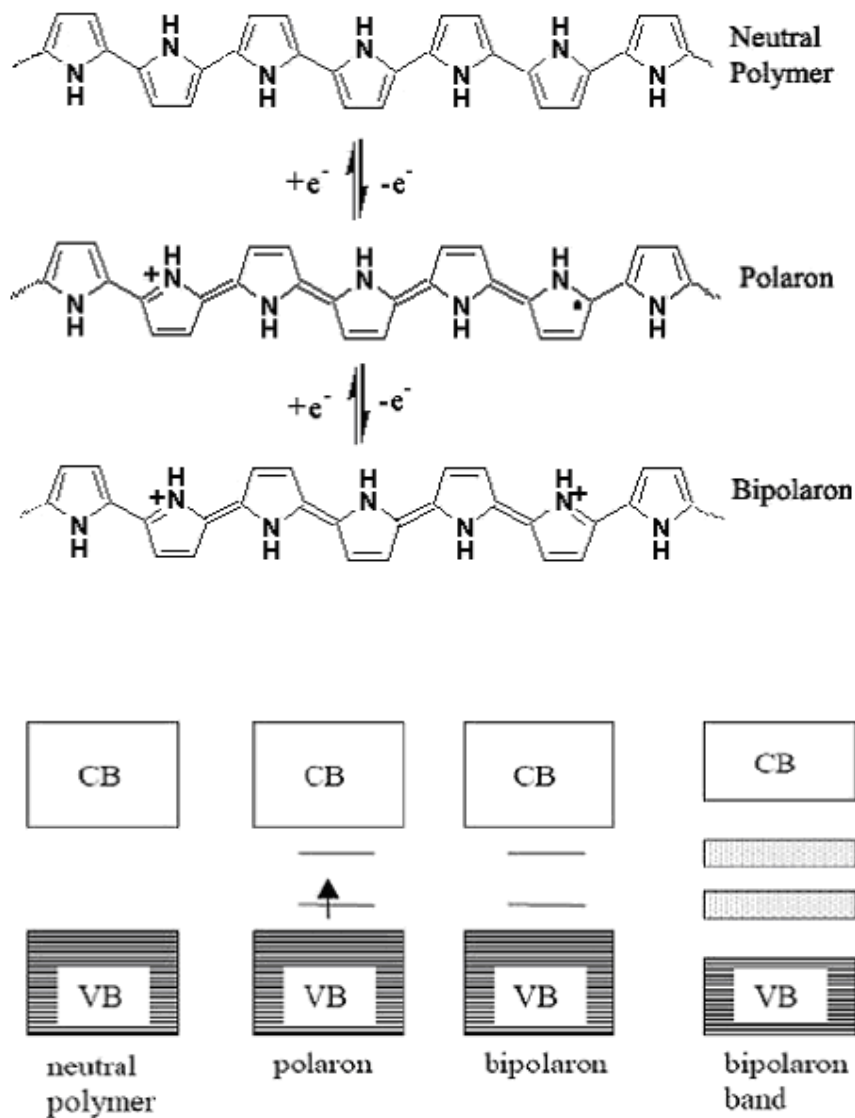


**Figure 1.5** The structure of a polaron and bipolaron in polypyrrole and its corresponding energy bands.

### 1.2.3. Doping

The concept of doping is the unique, central, underlying and unifying theme which distinguishes conducting polymers from all other types of polymers[20]. During the doping process, an organic polymer, either an insulator or semiconductor having a small conductivity, typically in the range  $10^{-10}$  to  $10^{-5}$  S

$\text{cm}^{-1}$ , is converted into a polymer which is in the 'metallic' conducting regime (1 to  $10^4 \text{ S cm}^{-1}$ ). The controlled addition of known, usually small ( $\leq 10\%$ ) nonstoichiometric quantities of chemical species results in dramatic changes in the electronic, electrical, magnetic, optical, and structural properties of the polymer. Doping is reversible to produce the original polymer with little or no degradation of the polymer backbone. Both doping and undoping processes, involving dopant counterions which stabilize the doped state, may be carried out chemically or electrochemically [21]. Transitory doping by methods which introduce no dopant ions are also known [22].

Doping agents or dopants are either strong reducing agents or strong oxidizing agents. They may be neutral molecules and compounds or inorganic salts which can easily form ions, organic dopants and polymeric dopants [12]. Polymers may be doped by the following techniques: gaseous, solution, electrochemical, self, radical-induced and ion-exchange doping. The first three techniques are widely used because of convenience and low cost.

Certain dopants could give rise to magnetic ordering in these polymers along with the electron acceptor e.g. iodine,  $\text{FeCl}_3$ ,  $\text{AsF}_5$ , etc. (p-type) or electron donor such as Na, Li, etc. (n-type) to the polymer which is considered to generate positive carriers (holes) or negative carriers (electrons) in the  $\pi$ -conjugated system [23].

### **1.3 Polypyrrole**

Pyrrole is a heterocyclic five membered ring with four carbon and one nitrogen atoms in an aromatic configuration. Pyrrole is known to polymerize to give black conducting powder referred to as 'pyrrole black'. Polypyrrole is one of the most used conducting polymers for applications due to the good stability of its properties and because it can be easily synthesized as a homopolymer and also as a composite. The success of PPy applications depends on the improvement of the properties and the processability of this material. Therefore one of the main

research goal is the correlation between the synthesis parameters and the molecular architecture of PPy in order to obtain the required properties for a specific application [24].

PPy can often be used as biosensors [25], gas sensors [26], wires [27], microactuators [28], antielectrostatic coatings [29], solid electrolytic capacitor [30], electrochromic windows and displays, packaging, polymeric batteries, electronic devices and functional membranes, etc. [1].

PPy can be easily prepared by either an oxidatively chemical or electrochemical polymerization of pyrrole. However synthetically conductive PPy is insoluble and infusible, which restricts its processing and applications in other fields. Therefore, electrical, dielectric, microwave and morphological properties of the PPy can be tailored by adjusting the synthesis parameters such as dopant and monomer concentration, dopant type, synthesis time, synthesis temperature and electrolyte pH [31].

#### **1.4 Synthesis of Polypyrrole**

The polymerization of pyrrole, forming polypyrrole (PPy), can be carried out via chemical or electrochemical oxidation. Both polymerization techniques use pyrrole that has been dissolved in solvents including water, organic solutions and ionic liquids [32]. Chemical polymerization uses a chemical initiator that is reduced by the monomer [33], whereas electrochemical polymerization uses electrodes submerged in a solution of dopant to initiate polymerization [32]. Lower conductivities are generally achieved when chemical oxidation is used, but the economic gain and simplicity of production gives this method an advantage over electrochemical polymerization [34]. Advantages in using electrochemical polymerization including the ease in controlling growth rate and PPy film thicknesses[35].

#### 1.4.1 Chemical Polymerization of PPy

Pyrrole can also be polymerized chemically with an oxidizing agent such as ferric chloride ( $\text{FeCl}_3$ ), diazonium salts, ozone, nitrous acid, quinone or lead dioxide [36,37].  $\text{FeCl}_3$  is the most commonly used oxidant. The product PPy may be obtained as powder or a film, and the conductivity depends on the molar ratio of pyrrole /  $\text{FeCl}_3$  and the solvent used [38- 41]. The solvent also influences the form of the PPy aggregates that are formed [42]. High conductivity may be attained when strong acid anions are used for the charge-compensating dopant. For example, Walker *et al.* [43] reported conductivity as high as 62 S/cm for PPy powder prepared by using various ferric salts.

Compared with the electrochemical polymerization method, the oxidative polymerization approach for producing conductive blends has received considerably less attention. One reason may be that PPy is usually obtained as a powder by the chemical polymerization route and its conductivity is generally lower than for that obtained from electrochemical polymerization [33]. Machida *et al.* [44], however, reported that when ferrous chloride ( $\text{FeCl}_2$ ) was added to control the oxidation potential of the oxidant before the reaction, PPy powder with a conductivity of 220 S/cm was obtained. Free standing films with reasonable conductivity may also be prepared by an interfacial polymerization in which two immiscible solutions, one containing pyrrole and the other the oxidant, are brought into contact [45,46].

Because of the low solubility of PPy and its intermediates, the reaction mechanism for the chemical polymerization of pyrrole is uncertain, but it is expected to essentially be the same as for the electrochemical polymerization (Figure 1.6) [45]. The pyrrole radical cation, which is an intermediate during the oxidation reaction, also plays an important role in the oxidative polymerization [36]. The protons produced by the polymerization reaction combine with  $\text{Cl}^-$  that results from the reduction of  $\text{FeCl}_3$  to produce HCl as a by product.

The first stage in the polymerization involves an initiation reaction and then generation of the pyrrole cation radical by ferric chloride although numerous other oxidants, such as aluminium and silver ions can be used. Once a number of pyrrole radicals have formed, propagation takes place with a pseudo first order reaction rate. Propagation involves two step process beginning with the dimerization of two pyrrole radicals. After two radicals have joined, stabilization of the dimer/ oligomer takes place through hydrogen loss from each radical. After deprotonation of the pyrrole dimer, re-initiation and further propagation/ deprotonation reaction steps take place. Finally, termination occurs to end up with polypyrrole (Figure 1.6) [45].

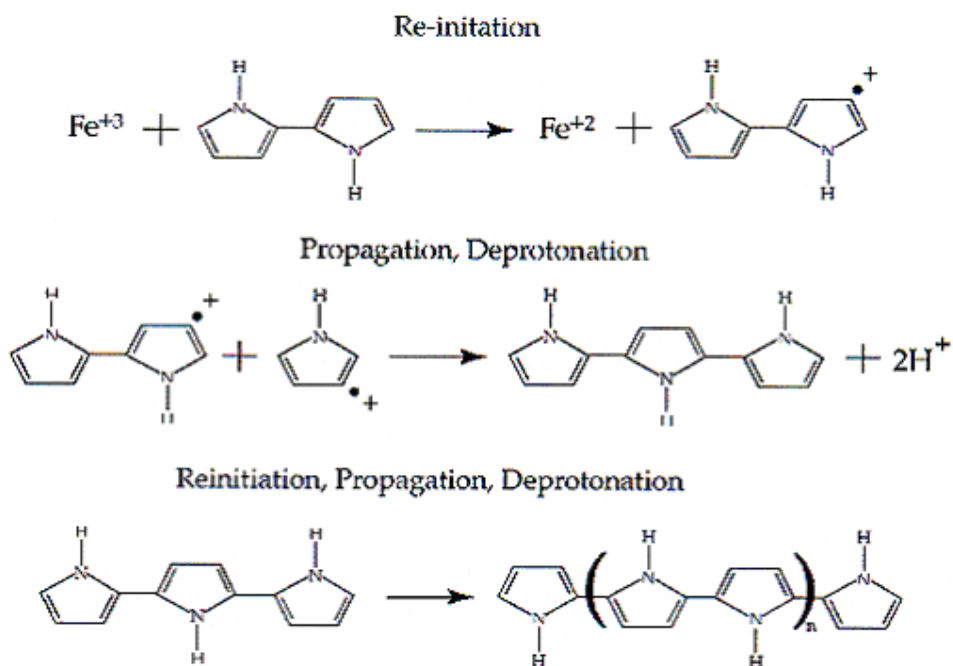


**Figure 1.6** Chemical Polymerization of PPy.

In chemical polymerization, the oxidants used generally are as follows:  $(\text{NH}_4)_2\text{S}_2\text{O}_8$ ,  $\text{H}_2\text{O}_2$  and many kinds of salts containing transition metal ions, for example,  $\text{Fe}^{3+}$ ,  $\text{Cu}^{2+}$ ,  $\text{Cr}^{6+}$ ,  $\text{Ce}^{4+}$ ,  $\text{Ru}^{3+}$  and  $\text{Mn}^{7+}$ [31]. Poor processibility of PPy due to its insolubility and infusibility has retarded further investigation on the

structure and structure-physical properties. To improve the processibility, many researchers have been engaged in the development of soluble or swollen PPy and dispersible fine-powdered PPy. At the same time, the electric properties and/or stability of chemically prepared PPy have also been investigated at many laboratories because the stability of conducting polymers seems to be the main limiting factor in their practical applications [47]. Several methods for PPy were introduced and several kinds of soluble PPy have been synthesized, such as poly(3-alkylpyrrole) with an alkyl group equal to or greater than a butyl group [48].

#### **1.4.2 Electrochemical Polymerization of PPy**

PPy is commonly synthesized by electrochemical methods, in which pyrrole is dissolved in an appropriate solvent in the presence of an electrolyte [39,49,50]. The conductive form of the polymer is directly generated at the anode of an electrochemical cell and incorporates the electrolyte as a counterion. The properties of the film can be controlled by varying the electrolyte, concentration, temperature or the current used in the polymerization. Aromatic sulfonate derivatives have often been used for the electrolyte in the electrochemical polymerization of pyrrole [51-53].

The electropolymerization of conductive polypyrrole films proceeds via the electrochemically activated step-growth coupling mechanism shown by Figure 1.7 [36]. The first step of the reaction is the oxidation of pyrrole to form a radical cation, which then couples with another radical cation or reacts with another monomer molecule to form a dimer. The double charged dimer can then lose two protons to rearomatize and form a stable dimer, which is more easily oxidized than the monomer and may participate in additional oxidation/radical coupling reactions to form oligomers and eventually polymer. The polymer precipitates as a film on the electrode surface. Partial oxidation of the polymer produces positive charges on some of the pyrrole rings that generate polarons and bipolarons, and the charge is balanced by an anion from the electrolyte to

maintain neutrality of the polymer. In general, the conductive form of PPy has one charge for every three or four pyrrole rings.

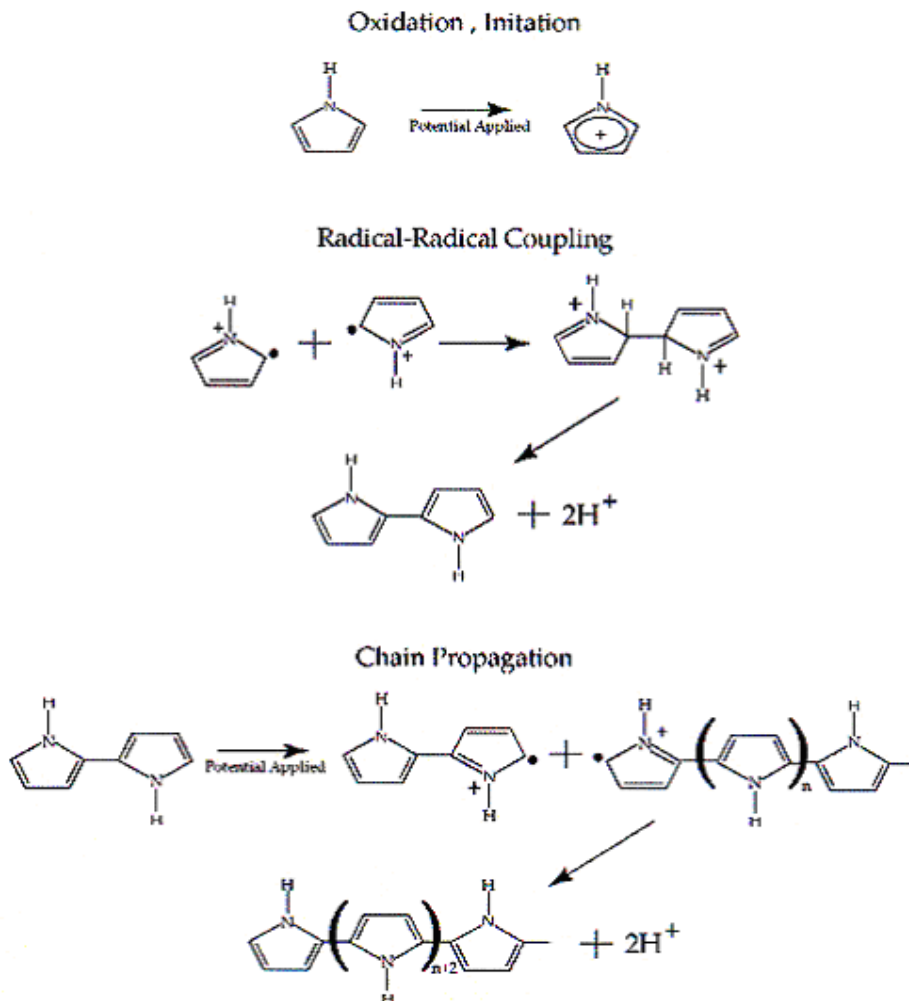


**Figure 1.7** Electrochemical Polymerization of PPy.

In the series of conducting polymers, considerable attention has been drawn to the polypyrrole family prepared by electrochemical oxidation such as PPy, poly (*N*-methyl pyrrole) and their copolymers for their application in solid state devices. Several investigations [54,55] have been performed to observe the effect of various parameters such as solvent, electrolyte choice of monomer, polymerizing temperature, annealing temperature, etc. , on the mechanical

strength, stability, and conductivity of the films prepared. Surface morphology studies suggest 3D-type growth and it is found that there is no change in conductivity and good handling strength after a certain annealing time [55]. A one-step synthesis of adherent PPy films on zinc electrodes is achieved by electrooxidation of pyrrole in aqueous oxalate solution [56].

### **1.5 Polythiophene**

Polythiophenes are to date one of the most extensively investigated classes of conjugated materials. Their chemical stability in various redox states and excellent electronic and charge transport properties make them good candidates for application such as electrical conductors, nonlinear optical devices, polymer LEDs, electrochromic or smart windows, photoresists, antistatic coatings, sensors, batteries, electromagnetic shielding materials, artificial noses and muscles, solar cells, electrodes, microwave absorbing materials, new types of memory devices, nanoswitches, optical modulators and valves, imaging materials, polymer electronic interconnects, nanoelectronic and optical devices, and transistors[1,4]. Polythiophene and its derivatives work very well in some of the above applications and less impressively in other devices.

The first polythiophene synthesis has been described in 1883. Washing of benzene with sulfuric acid afforded after further treatment with sulfuric acid a black insoluble material [57]. Oligomerization of thiophene induced by phosphoric acid leads to the formation of the trimer [58]. It was not until the early 1980's, however, that any well-defined polymeric material was obtained. After the first syntheses by Yamamoto [59] and Lin [60], using the Grignard-type coupling of 2,5-dibromothiophene, a vast number of articles concerning synthesis and properties of polythiophenes has been published.

## 1.6 Synthesis of Polythiophene

For the preparation of polythiophenes three main synthetic routes have been employed, namely: organometallic coupling, oxidative coupling and electrochemical synthesis.

### 1.6.1 Organometallic Coupling

One of the first chemical preparations of unsubstituted polythiophene (PTh) was reported in 1980 by two groups [59,60]. Both synthesized polythiophene by a metal-catalyzed polycondensation polymerization of 2,5-dibromothiophene (Figure 1.8). Yamamoto's synthesis treats 2,5-dibromothiophene with Mg in tetrahydrofuran (THF) in the presence of nickel(bipyridine) dichloride. The Mg reacts with either bromide to form either 2-bromo-5-magnesiobromothiophene or 2-magnesiobromo-5-bromothiophene, which is self-coupled with the  $\text{Ni}^{\text{II}}$  catalyst to form a thiophene dimer carrying a MgBr at one end and a Br at the other. This condensation reaction is propagated and eventually low molecular weight PTh is formed.

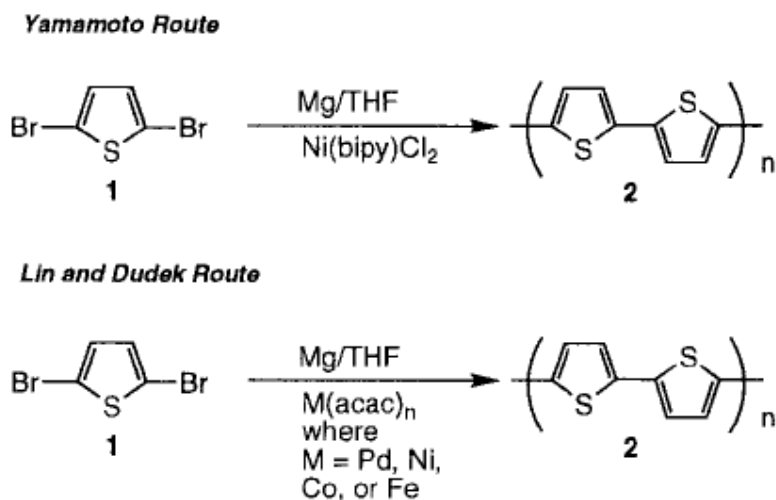


**Figure 1.8** The First Chemical Synthesis of PTh.

Systematic studies of the polymerization of 2,5-dihalothiophene have subsequently been performed primarily by Yamamoto's group[61] but also by others [62]. Varying the amounts of Mg[62], solvent[63], type of metal (i.e., Mg, Zn, etc.)[64], concentration of monomer [62], type of halogen on the monomer, temperature, reaction time and type of catalyst used [65] has led to some good chemical methods for the synthesis of PTh. The extension of these chemical methods to the synthesis of poly(3-alkylthiophene)s (PATs) and other polythiophenes will be noted later.

Due to the improved properties of regioregular 3-substituted polythiophenes, the polymerization based on the organometallic coupling of thiophene monomers is now by far the most interesting method. A number of polymers with functional groups in the side chain has been synthesized using this method as well; ethyleneglycol units give rise to conductivities [65] as high as  $5500 \text{ Scm}^{-1}$ . The high conductivity is believed to result from the oxygen containing side chains, which act like a crown ether and complex the dopant counter ion [66].

### **1.6.2 Oxidative Coupling**

Conducting polythiophenes are formed in the oxidation of thiophene or bithienyl with arsenic(V) fluoride. The observation that the material can be reduced with ammonia clearly displays that polymerization has occurred [67]. Due to the poisonous properties of arsenic(V) fluoride the method is not very practical. A more convenient method has been developed by Yoshino et al. [68], by using iron(III) chloride as oxidizing agent and chloroform as solvent under anhydrous conditions. Subsequent reduction with ammonia provides the neutral polymer in good yields. The reaction is easily carried out and this method has now widely been employed in the synthesis of polythiophenes from thiophene with alkyl[69], alkoxy[70] and alkylsulphonic acid [71] substituents.

Early on, Sugimoto[72] described the synthesis of PTh by treating thiophene with  $\text{FeCl}_3$  (Figure 1.9). The treatment of thiophene with butyl lithium provides

2,5-dilithiothiophene that can be polymerized with  $\text{CuCl}_2$  [73]. The acid-induced polymerization of thiophene was reported as early as 1883, but produces tetrahydrothiophene units [57]. A novel polymerization of thiophene vapor can produce encapsulated PTh in zeolites that contain transition metals [74].

*Sugimoto and Yoshino*

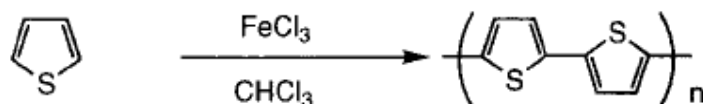


**Figure 1.9** Chemical Polymerization of PTh.

### 1.6.3 Electrochemical Polymerization of PTh

The synthesis of polythiophenes by electrochemical oxidation has been widely used since it was first described by Diaz [75]. Although the mechanism is not completely understood, the polymerization is proposed to proceed via the coupling of two radical cations, formed by the oxidation of the monomer as is outlined in Figure 1.10 [76]. The rearomatization of the dihydro dimer is the driving force in the coupling. The dimer, which has a lower oxidation potential than the monomer, is readily oxidized and undergoes further coupling. The polymer is deposited in its oxidized, and hence conducting, form onto the electrode, allowing the polymerization to proceed.

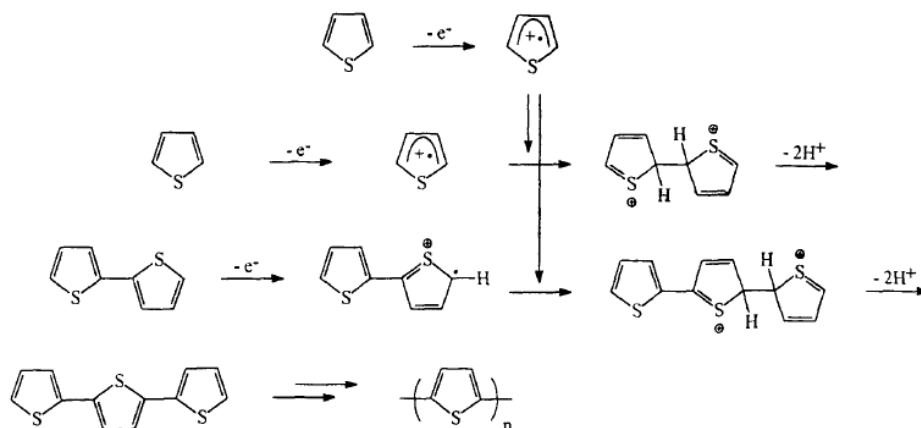


**Figure 1.10** Electrochemical Polymerization of PTh.

This method has the advantage that during the polymerization homogeneous, stable films are formed. The films can be characterized by optical and electrochemical methods. Electrochemical polymerization has been used for the synthesis of unsubstituted polythiophene [77,78] and substituted polythiophenes including poly-(3-methylthiophene) [79], poly-(3-ethylthiophene) [80] and of a number of different soluble poly-(3-alkylthiophenes) [81]. However, in all cases reported so far, the polymers obtained possess a regiorandom structure.

In electrochemical method, PTh is directly obtained in its oxidized or reduced state and its thickness as well as its doping level can be well controlled by the electrolysis time and potential, respectively. The polymerization is carried out in an electrolysis cell with constant potential or constant current using a working electrode such as Pt, Au, graphite or glass coated with  $\text{SnO}_2$  or  $\text{In}_2\text{O}_3$ . Saturated calomel electrodes (SCE)s on  $\text{Ag}/\text{Ag}^+$  can serve as reference electrodes and Pt, Ni or graphite can serve as the auxiliary electrode. The electrolytic medium typically consisted of an organic solvent, a supporting electrolyte and the monomer.

## 1.7 Phenol

Phenols are colorless solids or liquids at 25 °C [82]. They form strong hydrogen bonds via hydroxyl group present in the molecules of phenols. This hydrogen bonding causes phenols to have higher boiling points, melting points and densities than hydrocarbons of the same molecular weight [83]. They are distinguished from alcohols by their weak acidic character because of the resonance effect of hydroxyl group and which is enhanced by substitution of the negative groups as halides or nitro on the ring and reduced by substitution of the alkyl groups.

Sterically hindered phenols have little or no acidic character. The ability to form strong hydrogen bonds to molecules of water confers on phenols a modest solubility in water. These compounds are soluble in sodium hydroxide but do not dissolve in aqueous sodium carbonate. They are also soluble in polar solvents like lower alcohols, ketones, esters, pyridine, etc., but have very limited solubility in nonpolar aliphatic hydrocarbons. The solubility in hydrocarbons enhanced by alkyl substitution on the ring.

A variety of synthetic polymers can be formed from phenols by reactions at the ortho- and para-positions on the aromatic nucleus and by the reaction with hydroxyl group. The phenol molecule has four active sites for reaction and a combination of C-C or C-O coupling reactions or oxygenation reactions where the coupling occurs fastest at the position of highest density of free electrons, except where there is steric hindrance of approach [84].

The oxidation of phenols by using a catalyst can result in a variety of products, by a proper choice of catalyst, solvent and phenol [85]. For example; tetraalkyldiphenoquinones (1), polyphenylene ethers (2) and ortho-benzoquinone (3) can be prepared from catalyst autooxidation of phenol by using different copper salts and amines (Figure 1.11).

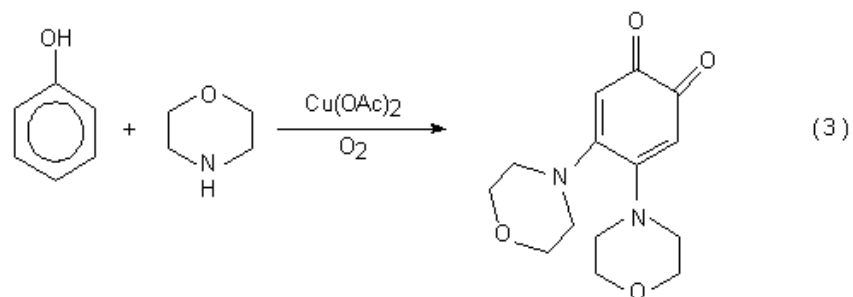
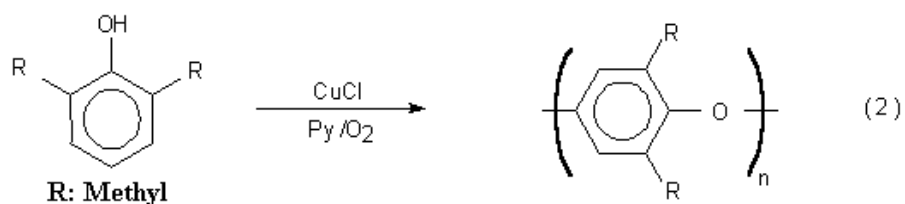
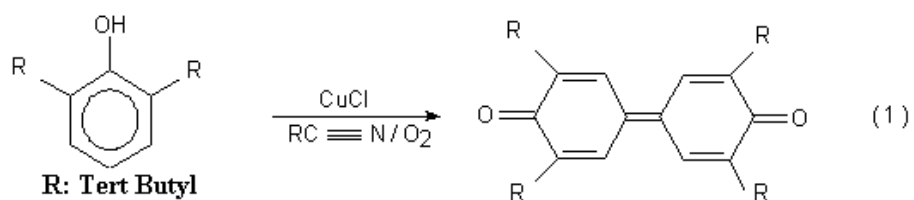
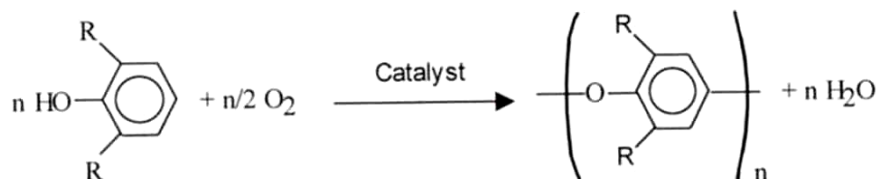


**Figure 1.11** The Oxidation Products of Phenols

### 1.8. Poly(phenylene oxide)s and Their Synthesis

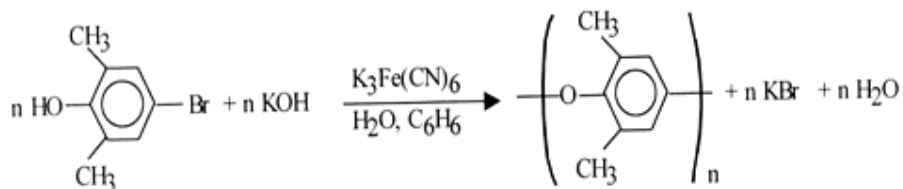
Poly (phenylene oxide)s have developed into important engineering thermoplastics in the short period of time since the discovery of the oxidative coupling of phenols [86]. They are polyesters having aromatic groups connected by an oxygen linkage at the backbone.

Poly (phenylene oxide) polymerisation is frequently based on the oxidative coupling of 2,6-disubstituted phenols with hydrogen atoms in the 4 position.

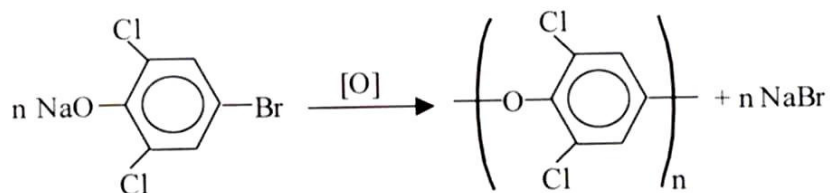


R:alkyl

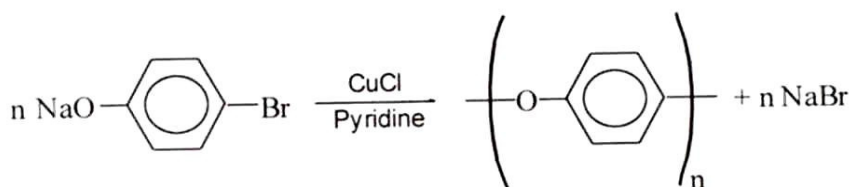
Some phenols with substituents in the 4 position can also be polymerised, such as phenol 4-aryloxy group. Another method is based on a free-radical initiated displacement process in which a halo group is removed from the 4 position of a 2,4,6-trisubstituted phenol salt. Oxidizing agents are only used in catalytic amounts as initiators. With 4-bromo-2,6-dimethylphenol, the reaction can be represented as



2,4,6 – Trihalophenols can be converted to poly(dihalophenylene oxide)s by a reaction that resembles free-radical-initiated displacement polymerisation. Either a copper or silver complex of the phenols heated to produce a branched product [87]. Oxidizing agent is used in catalytic amounts.



Oxidative displacement polymerisation of 4-halophenols (without 2, 6 – substitution) is not possible. To prepare poly (phenylene oxide) from 4 – halophenols Ullmann ether synthesis is used instead of a radical – anion chain process. It does not require a 2, 6–substituted phenol, but high temperatures are necessary; stoichiometry must be carefully controlled and the system must be free of moisture and oxygen.

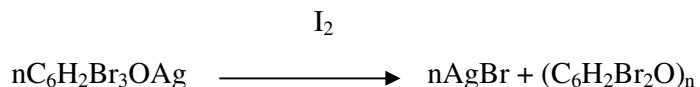


Oxidizing agent for the polymerisation of phenols is usually molecular oxygen and a transition – metal catalyst such as copper or manganese compound combined with ligands. Stoichiometric amounts of metal oxides and certain other oxidizing agents are also employed. The type of oxidizing system, its composition (metal – to – ligand ratio), concentration, and other reaction variables can have a large effect on reaction rate, selectivity, and product quality [86].

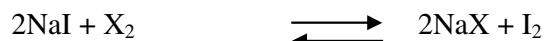
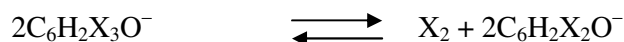
### 1.8.1. History of poly(tri halophenylene oxide)s

Synthesis of poly (phenylene oxide)s from alkyl substituted or halogenated phenols have been reported since 1916. In 1916 Hunter et. al. [88] was the first to

prepare a poly (phenylene oxide) by the ethyl iodide – induced decomposition of anhydrous silver 2,4,6– tribromophenoxide:



Silver salts of trichlorophenol and tribromoresorcinol were also decomposed to give poly (dihalophenylene oxide)s. Then, Hunter and his colleagues worked on the polymerization of mixed halophenols and they reported that iodine was displaced more readily than bromine and the latter more rapidly than chlorine and para – halogen reacted more rapidly than ortho group [89]. The actions of the iodine on polymerisation were also investigated by Hunter et.al. [90]. They proposed the following equations to clear up the effect of iodine:



Where X: halogen

In 1932, Hunter and Dahlen reported that only the halogen in the hydroxyl–bearing nucleus could be displaced in the catalytic decomposition of metallic salts of halogenated phenols [91].

In 1959, Staffin and Price, studied the polymerisation of 4 – bromo – 2,6 – disubstituted phenol with several oxidizing agents such as ferricyanide,  $\text{PbO}_2$ ,  $\text{I}_2$ ,  $\text{O}_2$  and light. Sterically hindered halogenated phenols failed to polymerise under the same conditions. They proposed a radicalic mechanism for the

polymerisation by displacement of bromine ion by phenoxy radical at the propagation step [92].

In 1962, Hay [93] was the first to report that oxidative coupling of 2,6-disubstituted phenols gave high molecular weight 2,6-disubstituted 1,4-phenylene oxides (for R=CH<sub>3</sub>). When the substituents are bulky, then only C – C coupling occurs to give diphenoquinones as the sole product (Figure 1.12).

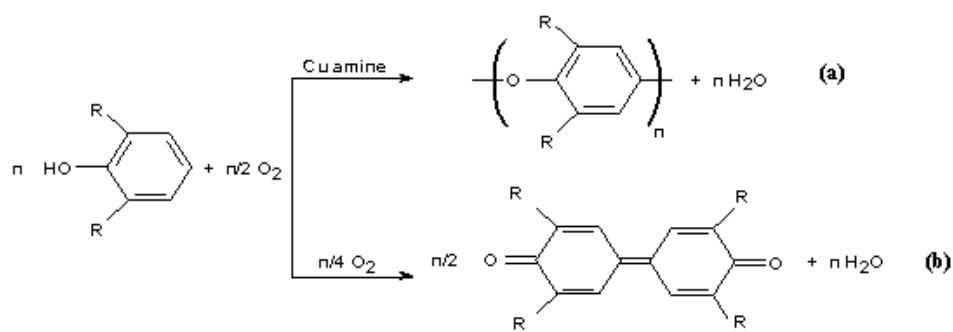


**Figure 1.12** Oxidative Coupling Reactions of Phenols

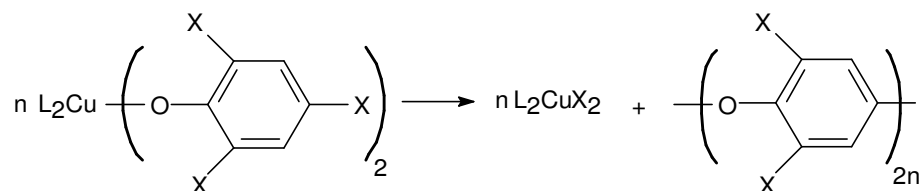
(a) Carbon-oxygen coupling, poly(phenylene oxide)s, R= Unhindered alkyl aryl groups, halogens

(b) Carbon-carbon coupling, diphenoquinone, R= Large and bulky groups

Blanchard et.al. studied the preparation and characterization of bis(phenolato)bis(pyridine)copper(II) complexes [87]. These complexes were decomposed to produce branched polymer under a variety of conditions. They also proposed a radicalic mechanism for the decomposition.

In 1969, Harrod studied the thermal decomposition of several trihalophenoxy copper (II) complexes containing various amine ligands [94]. Amine ligands increase the oxidizing power of copper (II) so thermal stability become lower.

Thermal stability of the complexes depends on the nature of the neutral ligand. The phenoxo complexes with chelating are highly resistant to decomposition compared to non-chelating ligands. These copper complexes undergo thermal decomposition to give poly(dihalophenylene oxide). The general chemical reaction for the preparation of these polymers was suggested as:



Harrod et.al. [95] reported that the molecular weights (Mn) of poly(phenylene oxide)s produced by thermal decomposition of bis(2,4,6 – trichlorophenoxy) bis(pyridine)copper(II) complex were found to increase with increasing concentration of complex, decreasing concentration of free impurity trichlorophenol, changing solvent from cumene to toluene, to benzene and changing the amine ligand from N,N,N',N'-tetramethyl- ethylenediamine to pyridine. Decomposition temperature had little effect on Mn.

Since 1980's Kısakürek et.al. made progress in synthesis and characterisation of poly(dihalophenylene oxide)s by decomposition of the isolated transition metal complex of phenols with various amine ligands by using various methods. Electroinitiation in solution [96, 97], thermal decomposition in solution [98], or in solid state [99] and also microwave-assisted polymerization [100-102] were studied. It was found that besides decomposition method, type of amine ligand and the type of halogen substituted on the phenol ring were found to be effective on the structure, molecular weight and the conversion of the polymer. The lowest molecular weight polymers are obtained in electroinitiated polymerization and the highest with thermal decomposition in solution, where the solid state polymerisation is close to electroinitiation with slightly higher values. Glass

transition temperatures ( $T_g$ ) of the polymers obtained are higher than 160°C and do not depend on the molecular weight.

The effect of the transition metal was also examined. Copper, cobalt and nickel were studied as transition metal. It was found that in solid state Cu complexes decompose much more easily than Co and Ni complexes. The type of metal was found to be effective on the structure of the polymer and on the % conversion.

## **1.9 Crosslinked Polymers**

Polymer networks or crosslinked polymers rank among the most complex macromolecular systems. A polymer network is defined as a structure in which essentially all mers are connected to all other mers and to the macroscopic phase boundary by many paths through the polymer's phase; the number of such paths increases with the average number of intervening bonds and the paths much on the average be co-extensive with the polymer phase [103]. Control of their formation and properties is often empirical due to a large variety of technologies and applications such as vulcanized elastomers, thermosets, matrices in high-performance composites, sorbents, organic coating films, polymers for electronics, synthetic and biological gels. Special features of polymer networks in comparison with uncrosslinked polymers include their dimensional stability, increased thermal, physical and chemical stability and ability to store information about their shape and formation history when the gel point is surpassed [104].

### **1.9.1. Formation of network structure**

For the formation of a 3D polymer network, at least one of the starting components must have the number of functional groups per molecule (called component functionality,  $f$ ), larger than two[105]. This is a necessary but often not sufficient condition. In order that an infinite paths of bonds may exist (which is condition for gelation), infinite repetitions of certain sequences of units connected by bonds should be possible. Small molecules carrying functional

groups (monomers) or preformed larger molecules carrying functional groups serve as polymer network precursors.

Polymer networks are formed from functional precursors by reactions between their functional groups resulting in bond formation [105]. Branched and crosslinked structures are formed by this process. First, molecular weights and polydispersity of branched molecules increase; the largest molecule progressively becomes larger and larger than any other one in the system until the critical state, the gel point, is reached when the largest molecule becomes “infinite”, i.e. commensurable with the macroscopic dimensions of the system. At this point, an infinite structure (molecule), gel, is formed for the first time. Beyond this point, if the degree of conversion and connectivity of the system further increase, the gel fraction increases at the expense of still finite (soluble) molecules called sol. The sol molecules become gradually bound to the gel and, eventually, under certain conditions, all precursor molecules can be parts of the gel (the network). This happens in the case when formation of finite molecules carrying no functional groups can be excluded (e.g. systems with monofunctional components, or off-stoichiometric alternate systems). Along with a decrease in the sol fraction, the network structure becomes “denser”, containing increasing amounts of crosslinks and strands between them called elastically active network chains. The concentration of elastically active network chains determines equilibrium mechanical properties of networks in the rubbery state (Figure 1.13).

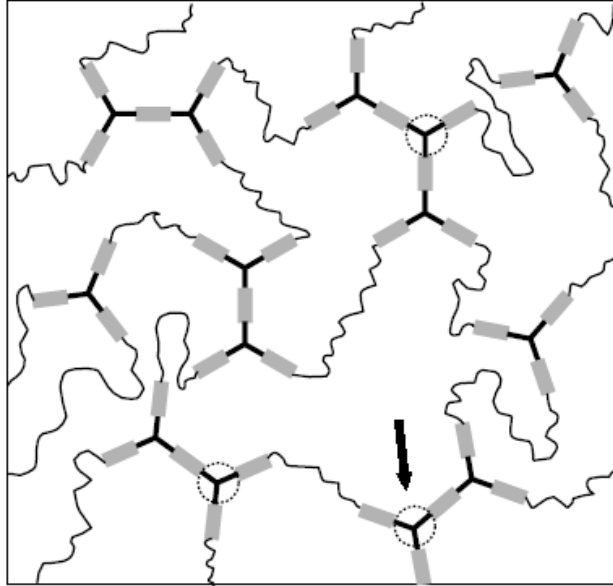


**Figure 1.13** Crosslinked Structure

### 1.9.2. Crosslinking Mechanism

Network formation exhibits some common features despite of the differences in the functionality and structure of precursors and chemical mechanism of the crosslinking reaction [103].

1. Increase in molecular weight averages and broadening of the molecular weight distribution.
2. Occurrence of the gel point at which an insoluble infinite structure is formed for the first time; the gel point is characterized by a divergence of the weight-average and higher-average molecular weight.
3. Transformation of finite molecules (sol) into the network structure (gel) by reactions between sol molecules and the gel which results in:
  - decrease in the soluble fraction (sol).
  - decrease in the molecular weight averages of the sol.

#### 4. Build-up of the structure of the gel by gel–gel reactions:

- formation of closed circuits (cycles).
- increase in the concentration of elastically active crosslinks.
- increase in the concentration of elastically active network chains.
- decrease in the fraction of material in so-called dangling chains.

### **1.10 Microwave-assisted Polymerization**

#### **1.10.1 Fundamental Concept of Microwave**

Microwave ovens operate with electromagnetic nonionizing radiation with frequencies between 300 GHz and 300 MHz. The corresponding wavelengths span a range from 1 mm to 1 m, exhibiting the medial position of microwaves between infrared and radio waves. Most commercial microwave systems, however, utilize an irradiation with a frequency of 2450 MHz (wavelength  $\lambda = 0.122$  m) in order to avoid interferences with telecommunication devices. The corresponding electric fields oscillate  $4.9 \times 10^9$  times per second and consequently subject dipolar species and ionic particles (as well as holes and electrons in semiconductors or metals) to perpetual reorientation cycles. This strong agitation leads to a fast noncontact heating that is (approximately) uniform throughout the radiation chamber [106].

From the viewpoint of frequency, resonance for electronic polarization takes place in the UV region and atomic polarization in IR region, both have very small dielectric loss in MW region. MW as heating source is dominated mainly by mechanism of the dipole polarization. As for the interfacial polarization, it only occurs in an even lower frequency region [107]. For the essence of dipole polarization, it can be further understood that the molecules undergo reorientation under the electric field, whereby friction takes place which causes transfer of electromagnetic energy into thermal heat [107].

Mechanism for MW interacting with materials determines that the power dissipation takes place in the molecule level. This nature offers MW heating process numerous advantages over the commonly used thermal treatment. First of all, MW heating of materials is volumetric which saves the trouble of thermal conduction/convection from external to internal in the handled material, a rather high heating rate is therefore obtainable. Another benefit arises from MW heating every portion of material concurrently, therefore there is no temperature gradient, and the consequent thermal stress is not to be produced inside the sample. In addition, MW as compared to the other band of electromagnetic waves shows more appropriate heating capacity for polymers. Gamma radiation is the most penetrative, it is however considered hazardous due to its continuous nature and long half time. X-rays are more penetrative but the dose rates obtainable in most X-ray system are of little. UV source has a poor penetration capability (0.4 mm for epoxies) limiting the extensive use of UV in industry [108]. For MW, the low frequency (< 2.45 GHz) has better penetration and lower attenuation (the decay is not significant for thickness of up to 10 mm), while for the high frequency above 2.45 GHz, the power attenuation is significant only if power is at low input [108]. So MW provides an alternative to the other radiant for wide application in industry.

The applied microwave frequency is in the same range as the rotational frequencies (relaxation times) of molecules. Thus, molecules (that have a permanent dipole moment) will try to align with the applied field leading to rotation and collision of molecules (Figure 1.14), which results in fast and efficient heating of the reaction mixture [109]. The use of microwave heating excludes many heat-transfer processes and thus energy losses that are present with conventional oilbath heating. Moreover, the direct heating under microwave irradiation provides a more homogeneous heat profile when compared to oilbath heating where the vessel walls are significantly warmer than the contents [110]. Besides fast and efficient heating, the occurrence of non-thermal microwave effects were reported in which the use of microwave irradiation changed the

selectivity of reactions with a polar transition state [111]. Another major advantage of the currently available commercial microwave reactors is their ability to work with closed reaction vessels. This allows safe exploration of superheated, heating a reaction beyond the boiling point of the solvents and/or reagents, reaction conditions under microwave irradiation.

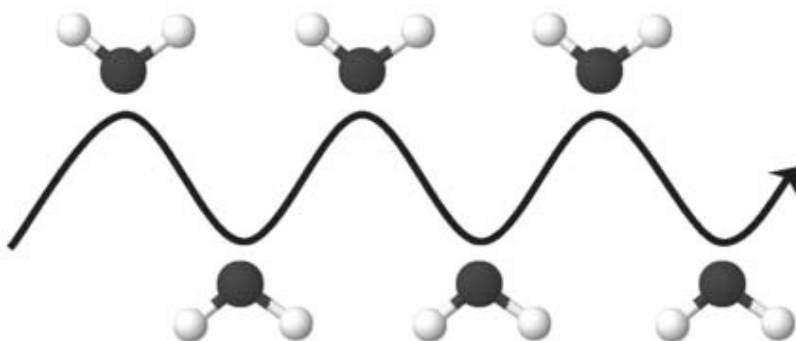


**Figure 1.14** Schematic representation of the microwave heating of water.

### 1.10.2 Application of Microwave on Polymeric Materials

In the last decade, microwaves have attracted the attention of chemists who have begun to apply this unconventional technique as a routine in their practice. The reduced time of processing under microwave conditions found for a great number of chemical reactions was the main reason that microwave techniques become so attractive for chemists. The result and advantages of microwave processing of material can be increase of productivity, improved product characteristics, uniform processing, less manufacturing space required, and controllability of the process. Microwave processing seems to be easily scaled up from a small batch process to a continuous process employing a conveyor. Besides ceramic, polymer processing forms probably the largest single discipline in microwave technology, and the methods and procedures used therein are certainly seen among the most developed. The past achievements in polymer synthesis such as free-radical polymerization, polyaddition as well as

polycondensation reactions, crosslinking and processing of polymeric materials with the stress on chemistry can be listed [112].

One of the first industrial applications of microwave radiation for the processing of polymeric materials was the vulcanization of rubber in the tire industry during the 1960s, with commercial application beginning late in that decade [113]. The principal mechanism of coupling of the microwave addition to the material occurred via carbon black fillers already present in many rubber formulations. Not all polymer materials are suitable for microwave processing. However, many polymers contain groups that form strong dipoles (e.g. epoxy, hydroxyl, amino, cyanate, etc.). Microwave processing can be used over a broad range of polymers and products, including thermoplastic and thermosetting resins, rubber, and composites.

In the field of synthetic polymer chemistry, microwave energy has been used for the polymerization of vinyl monomers [114], ring opening polymerization of caprolactam and caprolactone [115], condensation polymerization of polyesters [116], polyamides [117], and polyimides [118], as well as the curing of epoxy [119] and polyurethane resins [120].

### **1.11 Aim of the study**

Microwave-assisted synthesis and characterization of conducting polymer (**CP**) and/or crosslinked polymers (**CLP**) and/or white polymers (**WP**) and/or orange polymer (**OP**) and/or radical ion polymer (**RIP**) were to be achieved by using KOH with TCP, pyrrole and thiophene, in a very short time interval, in order to improve novel polymerization techniques, by studying the effects of heating time, microwave energy, amount of water and amount of KOH on percent conversion, structure and molecular weight of the polymers.

## CHAPTER 2

### EXPERIMENTAL

#### 2.1. Chemicals

##### 2.1.1. 2,4,6 – Trichlorophenol (TCP), Pyrrole(Py) and Thiophene(Th)

Analytical grade 2,4,6 – Trichlorophenol, Pyrrole and Thiophene were provided from Merck and was used without further purification.

##### 2.1.2. Potassium Hydroxide (KOH)

KOH produced by Merck, were used in the polymerization.

##### 2.1.3. Toluene

Toluene was provided from Merck and used as a solvent for the polymer.

##### 2.1.4. Ethyl Alcohol

Ethyl alcohol was commercially available technical grade and used as non-solvent for the polymers and used as precipitating reagent.

##### 2.1.5. Hydrochloric Acid

It was provided from Merck and used in the precipitation of the synthesized polymers to dissolve the by product salts formed during polymerization.

### **2.1.6. Deuterated Chloroform (CDCl<sub>3</sub>)**

CDCl<sub>3</sub> was provided from Merck and was used as a solvent to obtain NMR spectra of the polymers.

### **2.1.7. Potassium Bromide (KBr)**

Spectroscopic grade KBr was provided from Merck and was used to take FTIR spectra of polymers which were dispersed in KBr discs.

## **2.2. Apparatus and Instruments**

### **2.2.1. Microwave Oven**

Domestic microwave oven (BOSCH) works at 2.45 MHz and has a period of 10 seconds. It has several time intervals (1-25min) and microwave energies (90-900 watt) and it was used for polymerization.

### **2.2.2. Differential Scanning Calorimeter (DSC)**

Thermal behaviors of the polymers were obtained by using DuPont thermal analyst 2000 DSC 910S model differential scanning calorimeter. In order to obtain thermal behavior of the polymers, in the first run of the DSC analysis both of the samples were heated to 150 °C from room temperature with a heating rate of 10 °C/min then cooled to room temperature with a cooling rate of 10 °C/min to reduce the effect of unwanted contamination. At the second run, polymers were heated to 350 °C by the rate of 10 °C/min under nitrogen atmosphere.

### **2.2.3. Thermogravimetry Analysis and Fourier – Transform Infrared Spectrophotometer (TGA/FTIR) System**

Thermogravimetric analysis (TGA) is a technique that permits the continuous weighing of a sample as a function of temperature and/or as a function of time at a desired temperature. Weight losses of the polymers due to the increasing

temperature were determined by Perkin Elmer Pyris 1 TGA thermogravimetry analyzer coupled to Spectrum 1 FT-IR Spectrometer. Samples were heated from 30 °C to 800 °C with a heating rate of 10 °C/min. under nitrogen atmosphere.

#### **2.2.4. Fourier – Transform Infrared Spectrophotometer (FTIR)**

Infrared spectra of the samples were obtained on a Bruker IFS 66/S FTIR spectrometer in the 4000 – 400 cm<sup>-1</sup> region by dispersing the sample in KBr pellets.

#### **2.2.5. NMR Spectrophotometer**

<sup>1</sup>H NMR and <sup>13</sup>C NMR spectra of polymers were recorded on a Bruker Instrument NMR spectrometer (DPX-400) in deuterated chloroform and TMS as an internal reference.

#### **2.2.6. Mass Spectrometer**

Direct insertion probe pyrolysis mass spectrometry (DIP-MS) system consists of a 5973 HP quadrupole mass spectrometer coupled to a JHP SIS direct insertion probe (T<sub>max</sub>= 445 °C). This system provides fast scanning, self-tuning of experimental parameters and wide mass range. Mass spectra of the product was recorded at a scan rate of 2 scan/s in the mass range of 10-700 amu. Heating rate was 10 °C/min. and spectra were acquired at a rate of 2 scan/s using 70 eV electrons.

#### **2.2.7. Powder Diffraction X-ray**

Powder diffraction X-ray spectra of both washed and unwashed polymers were obtained by using computer controlled automatic Hunber-Guinner powder diffractometer with CoK $\alpha$  radiation obtained by using a voltage of 30 kV and a current of 7 mA.

### **2.2.8. Light Scattering**

Molecular weight, radius of gyration, and virial coefficient of polymers were determined at 37 °C by using Multi-angle light scattering spectrometer (Malvern 5000). The ALV/CG-3 Goniometer system is designed to perform dynamic and static light scattering analysis simultaneously.

### **2.2.9. ESR**

ESR spectra of the products were recorded by Bruker Xepr ELEXSY-580 spectrometer in quartz cell at room temperature where diphenylpicrylhydrazine was the reference.

### **2.2.10. SEM**

Analysis of the surface morphologies of all type polymers were done by using JEOL JSM- 6400 scanning electron microscope.

### **2.2.11. UV-Vis**

UV-Visible spectra of samples were obtained on Cary 100 UV-Visible Spectrophotometer in the 900–200 nm region by dissolving the sample in toluene and DMF.

### **2.2.12. Conductivity Measurement**

Conductivity measurements were performed both by two and four-probe techniques. The Four Probe Method is one of the standard and most widely used methods for the measurement of conductivity. The four osmium probes aligned in a colinear geometry. The error due to contact resistance, which is significant in the electrical measurement on semiconductors, is avoided by the use of two extra contacts (probes) between the current contacts. In this arrangement the contact resistance may all be high compared to the sample resistance, but as long as the resistance of the sample and contact resistance are small compared with

the effective resistance of the voltage measuring device (potentiometer, electrometer or electronic voltmeter), the measured value will remain unaffected. Due to equal pressure contacts, the arrangement is also especially useful for quick measurement on different samples or sampling different parts of the sample. Figure 2.1 demonstrates a simple four-probe measurement setup. Four equally spaced osmium tips touch the surface of polymer film taped on an insulating substrate. A known steady current is passed through the electrodes 1 and 4 and measured while the potential drop ( $\Delta V$ ) between contacts 2 and 3 is assessed.

Conductivity is calculated from the following equation,

$$\sigma = \ln 2 / (\pi R t) \quad (1)$$

where R is the resistance of the sample, and t is the thickness.

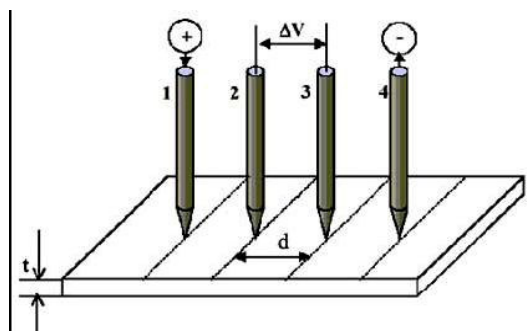


**Figure 2.1** Four-probe conductivity measurement set up.

### **2.3. Procedure**

Trichlorophenol (TCP) or pyrrole or thiophene, potassium hydroxide (KOH) and water were used as starting materials for the microwave-assisted polymerization.

#### **2.3.1. Synthesis of Polymers using TCP and KOH**

Microwave initiated polymerizations were performed at several time intervals (1-5 min), in different ranges of microwave energy (90-900 watt) and in various amounts of water (0.5-5 ml). Trichlorophenol (0.03 mol, 5.92 g) and KOH (0.03 mol, 1.68 g) were mixed by grinding and wetted by deionized water. Polymerization was performed in a Pyrex glass holder, loosely covered with a lid, inserted in a microwave oven working at 2.45 MHz and having a pulse period of 10 s. At the end of the reaction time intervals, the simultaneously resulting products were dissolved in 100 ml toluene by vigorous stirring. The insoluble black colored conducting polymer (**CP**) or white colored crosslinked polymer (**CLP**) were removed by filtration and washed several times by triple distilled hot water for purification. All the recovered precipitates were dried to a constant weight under vacuum.

#### **2.3.2. Synthesis of Polymers using Pyrrole and KOH**

Microwave initiated polymerizations were performed at several time intervals (1-25 min), in different ranges of microwave energy (90-900 watt) and in various amount of KOH ( $0.03-6 \times 10^{-4}$  mol) without water. Pyrrole (0.03 mol, 2.08 ml) and KOH ( $0.03-6 \times 10^{-4}$  mol, 1.68-0.034 g) were mixed and polymerization was performed in a Pyrex glass holder, loosely covered with a lid, inserted in a microwave oven working at 2.45 MHz and having a pulse period of 10 s. At the end of the reaction time intervals, the simultaneously resulting products were dissolved in 100 ml toluene by vigorous stirring. The insoluble black colored conducting polymer (**CP**) was removed by filtration and washed several times by triple distilled hot water for purification. The toluene soluble orange colored

radical ion polymer (**RIP**) was precipitated in ethanol. All the recovered precipitates were dried to a constant weight under vacuum.

### **2.3.3. Synthesis of Polymers using Thiophene and KOH**

Microwave initiated polymerizations were performed at several time intervals (1-25 min), in different ranges of microwave energy (90-900 watt) and in various amount of KOH ( $0.05-2 \times 10^{-4}$  mol) without water. Thiophene (0.05 mol, 4.00 ml) and KOH ( $0.05-2 \times 10^{-4}$  mol, 2.80-0.011 g) were mixed and polymerization was performed in a Pyrex glass holder, loosely covered with a lid, inserted in a microwave oven working at 2.45 MHz and having a pulse period of 10 s. At the end of the reaction time intervals, the simultaneously resulting products were dissolved in 100 ml ethanol by vigorous stirring. The insoluble black colored conducting polymer (**CP**) was removed by filtration and washed several times by triple distilled hot water for purification. The ethanol soluble white polymer (**WP**) and orange polymer (**OP**) were precipitated in toluene. All the recovered precipitates were dried to a constant weight under vacuum.

### **2.3.4. Characterization of the Polymers**

White colored, orange colored and radical ion polymers were characterized by FTIR,  $^1\text{H-NMR}$ ,  $^{13}\text{C-NMR}$ , TGA/ FTIR, DSC, SEM, ESR, UV-Vis, light scattering and mass spectrometer. Conducting and crosslinked polymers were characterized by FTIR, TGA/ FTIR, DSC, SEM, ESR, powder diffraction X-Ray and UV-VIS.

## CHAPTER 3

### RESULTS AND DISCUSSION

Microwave-assisted polymerizations were carried out at four different conditions:

1. A constant microwave energy and constant amount of water at different time intervals ranging from 1 to 25 min;
2. At constant time intervals and constant amount of water with variation of microwave energy ranging from 90 to 900 watt;
3. At constant time intervals and constant microwave energy with changing amount of water ranging from 0, 0.5 to 5 ml.;
4. At constant time intervals and constant microwave energy with changing amount of KOH ranging from 0.03, 0.05,  $2 \times 10^{-4}$  to  $6 \times 10^{-4}$  mol.

Percentage conversions values of each product were calculated by using following equation:

$$\text{Conversions (\%)} = \frac{\text{Weight of product}}{\text{Initial weight of monomer}} \times 100 \quad (1)$$

The %error is equal to  $\pm 0.6$ .

Results will be discussed under three topics. Each topic includes the results related to the synthesis and the characterization of the polymers which were synthesized with different monomer (TCP or pyrrole or thiophene) and Metal-hydroxide (KOH).

### 3.1. Synthesis of Polymer with TCP with KOH

Conducting polymer (**CP**) and/or crosslinked polymer (**CLP**) were synthesized from potassium 2,4,6-trichlorophenolate with microwave-assisted polymerization in a very short time interval. Polymerizations were performed at several time intervals (1-5 min), in different ranges of microwave energy (90-900 watt) and in various amount of water (0.5-5 ml).

The effect of polymerization time, energy, amount of water on the %conversions and %weight losses were shown in Table 3.1.1. With 0.5 cm<sup>3</sup> water, only **CP** was synthesized and showed a decreasing trend in % conversion up to 27.1% at 600 watt followed by an increase to 30.9% at 900 watt. The % WL generally increased slightly as the time and energy increased. At 900 watt % WL of **CP** was 62.8% and sharply decreased at 90 watt as 19.2%. As the water content increased to 5 cm<sup>3</sup>, **CLP** was the only synthesized product. The higher % conversion of **CLP** was observed at 180 watt as 85.9% and the minimum %WL at the same energy as 3.6%. Hence, the optimum conditions for **CP** and **CLP** were 90 watt for 5 min in 0.5 cm<sup>3</sup> water and 180 watt for 5 min in 5 cm<sup>3</sup> water having maximum values 38.9 and 85.9% respectively. In Figure 3.1.1, % conversion of **CP** and **CLP** are shown for each watt with maximum % conversions.

**Table 3.1.1** The effect of polymerization time and energy on the

% conversion and % weight loss of **CP** and **CLP** of TCP.

<b>90 W.</b>	<b>1min</b> 0.5 cm <sup>3</sup> w	<b>1min</b> 5 cm <sup>3</sup> w	<b>2min</b> 0.5 cm <sup>3</sup> w	<b>2min</b> 5 cm <sup>3</sup> w	<b>3min</b> 0.5 cm <sup>3</sup> w	<b>3min</b> 5 cm <sup>3</sup> w	<b>4min</b> 0.5 cm <sup>3</sup> w	<b>4min</b> 5 cm <sup>3</sup> w	<b>5min</b> 0.5 cm <sup>3</sup> w	<b>5min</b> 5 cm <sup>3</sup> w
<b>% CP</b>	-	-	15.8	-	19.5	-	30.1	-	<b>38.9</b>	-
<b>% CLP</b>	-	-	-	25.3	-	23.0	-	35.3	-	<b>46.6</b>
<b>% WL</b>	-	-	32.3	31.6	35.2	28.7	25.2	24.6	<b>19.2</b>	<b>16.9</b>
<b>180W.</b>	<b>1min</b> 0.5 cm <sup>3</sup> w	<b>1min</b> 5 cm <sup>3</sup> w	<b>2min</b> 0.5 cm <sup>3</sup> w	<b>2min</b> 5 cm <sup>3</sup> w	<b>3min</b> 0.5 cm <sup>3</sup> w	<b>3min</b> 5 cm <sup>3</sup> w	<b>4min</b> 0.5 cm <sup>3</sup> w	<b>4min</b> 5 cm <sup>3</sup> w	<b>5min</b> 0.5 cm <sup>3</sup> w	<b>5min</b> 5 cm <sup>3</sup> w
<b>% CP</b>	22.6	-	<b>30.6</b>	-	25.4	-	18.3	-	-	-
<b>% CLP</b>	-	28.9	-	48.5	-	72.4	-	<b>85.9</b>	-	-
<b>% WL</b>	41.3	32.7	<b>33.8</b>	26.2	39.0	19.5	38.2	<b>3.6</b>	-	-
<b>360W</b>	<b>1min</b> 0.5 cm <sup>3</sup> w	<b>1min</b> 5 cm <sup>3</sup> w	<b>2min</b> 0.5 cm <sup>3</sup> w	<b>2min</b> 5 cm <sup>3</sup> w	<b>3min</b> 0.5 cm <sup>3</sup> w	<b>3min</b> 5 cm <sup>3</sup> w	<b>4min</b> 0.5 cm <sup>3</sup> w	<b>4min</b> 5 cm <sup>3</sup> w	<b>5min</b> 0.5 cm <sup>3</sup> w	<b>5min</b> 5 cm <sup>3</sup> w
<b>% CP</b>	<b>32.6</b>	-	19.5	-	12.9	-	-	-	-	-
<b>% CLP</b>	-	50.2	-	<b>81.1</b>	-	44.9	-	-	-	-
<b>% WL</b>	<b>39.3</b>	31.3	44.6	<b>18.5</b>	55.1	38.4	-	-	-	-
<b>600 W.</b>	<b>1min</b> 0.5 cm <sup>3</sup> w	<b>1min</b> 5 cm <sup>3</sup> w	<b>2min</b> 0.5 cm <sup>3</sup> w	<b>2min</b> 5 cm <sup>3</sup> w	<b>3min</b> 0.5 cm <sup>3</sup> w	<b>3min</b> 5 cm <sup>3</sup> w	<b>4min</b> 0.5 cm <sup>3</sup> w	<b>4min</b> 5 cm <sup>3</sup> w	<b>5min</b> 0.5 cm <sup>3</sup> w	<b>5min</b> 5 cm <sup>3</sup> w
<b>% CP</b>	<b>27.1</b>	-	13.3	-	-	-	-	-	-	-
<b>% CLP</b>	-	55.2	-	<b>79.1</b>	-	-	-	-	-	-
<b>% WL</b>	<b>45.5</b>	32.4	62.7	<b>20.7</b>	-	-	-	-	-	-
<b>900 W.</b>	<b>1min</b> 0.5cm <sup>3</sup> w	<b>1min</b> 5 cm <sup>3</sup> w	<b>2min</b> 0.5 cm <sup>3</sup> w	<b>2min</b> 5 cm <sup>3</sup> w	<b>3min</b> 0.5 cm <sup>3</sup> w	<b>3min</b> 5 cm <sup>3</sup> w	<b>4min</b> 0.5 cm <sup>3</sup> w	<b>4min</b> 5 cm <sup>3</sup> w	<b>5min</b> 0.5 cm <sup>3</sup> w	<b>5min</b> 5 cm <sup>3</sup> w
<b>% CP</b>	<b>30.9</b>	-	11.3	-	-	-	-	-	-	-
<b>% CLP</b>	-	47.8	-	<b>64.9</b>	-	-	-	-	-	-
<b>% WL</b>	<b>62.8</b>	22.1	77.5	<b>10.6</b>	-	-	-	-	-	-

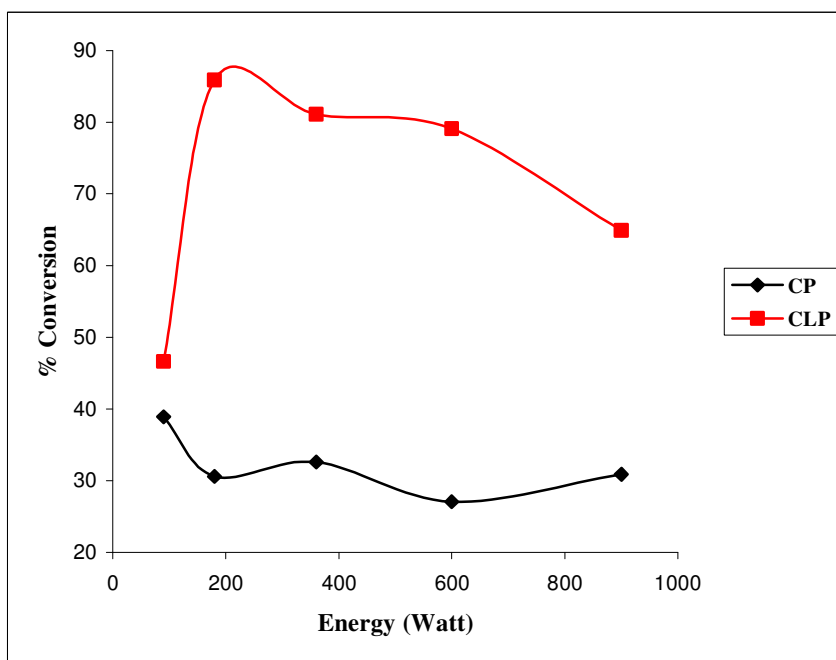


**Figure 3.1.1** % conversion of **CP** and **CLP**

### 3.1.2. Characterization

Fourier Transform Infrared Spectroscopy (FTIR) is an analytical technique used to identify organic (and in some cases inorganic) materials. This technique measures the absorption of various infrared light wavelengths by the material of interest. These infrared absorption bands identify specific molecular components and structures. Absorption bands in the range of 4000–1500 wavenumbers are typically due to functional groups (e.g. -OH, C=O, N-H, CH<sub>3</sub>, etc.). The region between 1500–400 wavenumbers is referred to as the fingerprint region. Absorption bands in this region are generally due to intra-molecular phenomena, and are highly specific for each material.

FTIR spectrum of **CLP** exhibited the characteristic absorptions at 852 cm<sup>-1</sup> (out of plane C-H bending), 1050-1200 cm<sup>-1</sup> (C-O-C stretching), 1170-1270 cm<sup>-1</sup> (C-O stretching), 1450 and 1560cm<sup>-1</sup> (C=C ring stretching), 3085 cm<sup>-1</sup> (aromatic C-H stretching) and 3590 cm<sup>-1</sup> (the phenolic end group) (Figure 3.1.2a).

FTIR spectrum of **CP** exhibited the peaks at  $3588\text{ cm}^{-1}$  ( the phenolic end group),  $3084\text{ cm}^{-1}$  (aromatic C-H stretching),  $1600\text{-}1460\text{ cm}^{-1}$  (C=C stretching of both benzenoid and quinoid structures),  $1280\text{-}1110\text{ cm}^{-1}$  (C-O stretching), and  $730\text{-}760\text{ cm}^{-1}$  (C-Cl stretching) (Fig. 3.1.2b) [121].

The FTIR spectrum of the evolved gas collected in a glass cell during polymerization, exhibited the peak at  $2450\text{ cm}^{-1}$  and  $1270\text{ cm}^{-1}$  related to  $\text{CO}_2$  and C=O stretching respectively (Figure 3.1.2c).

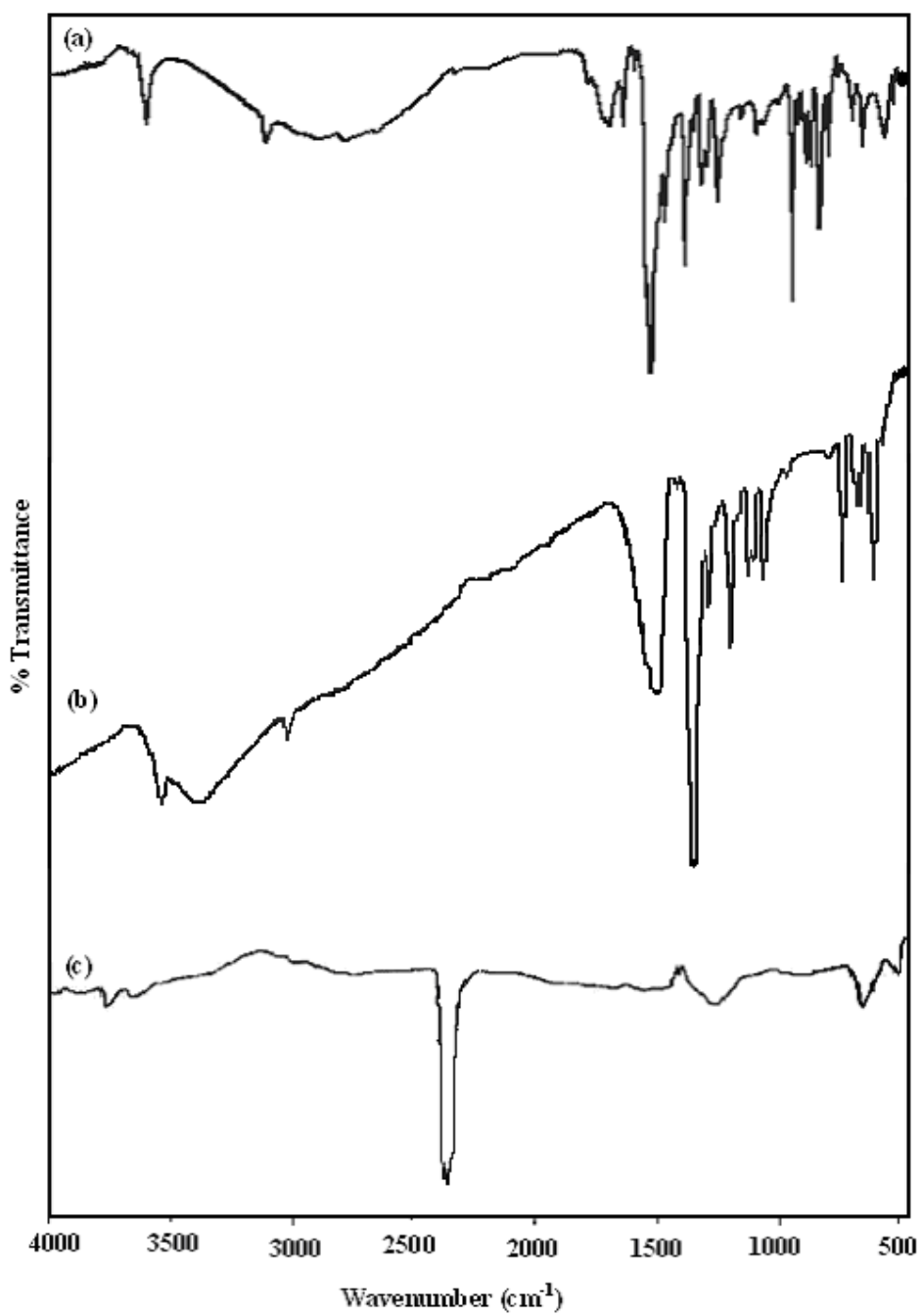


**Figure 3.1.2** FTIR spectra of (a) **CLP**, (b) **CP** and (c) released gases during polymerization.

The thermal properties of the synthesized polymers were studied with DSC and TGA. DSC thermograms of both **CP** and **CLP** were examined in the range 30 °C to 350 °C at a heating rate of 10 °C /min under nitrogen atmosphere. The glass transition temperatures were not observed for **CP** and **CLP** in the DSC thermograms (Figure 3.1.3 a and b)

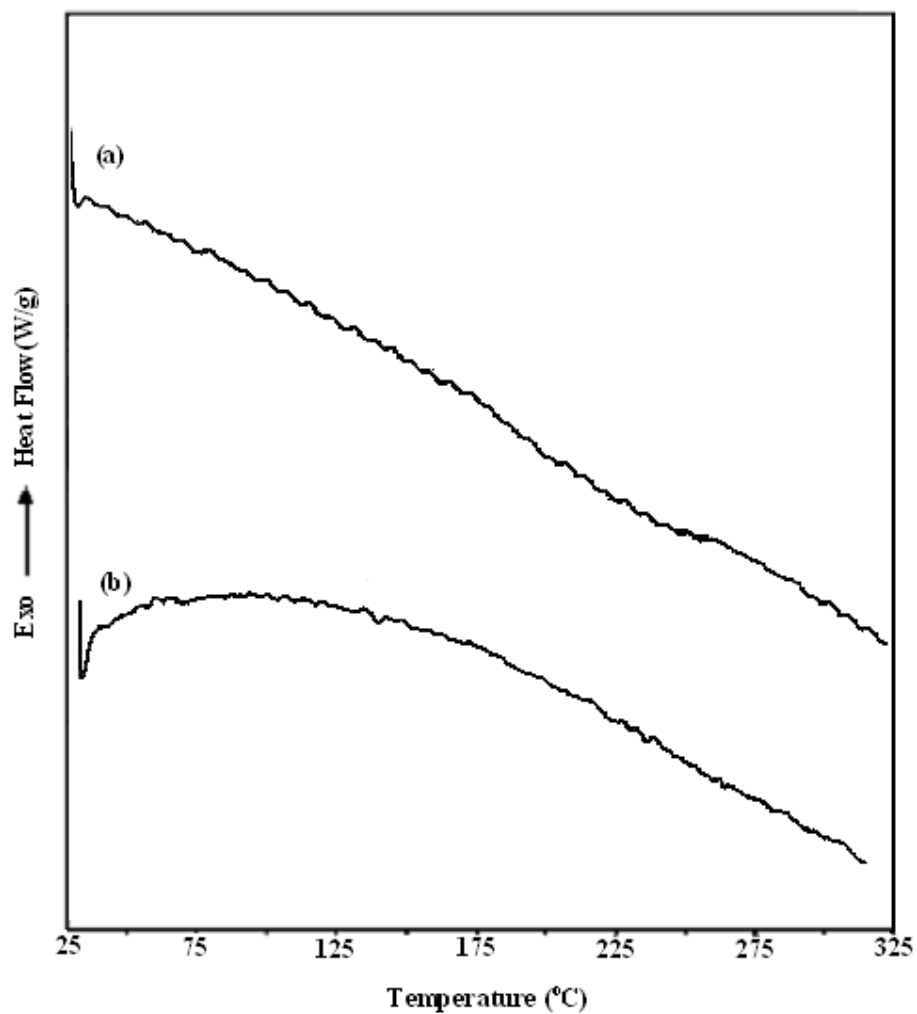
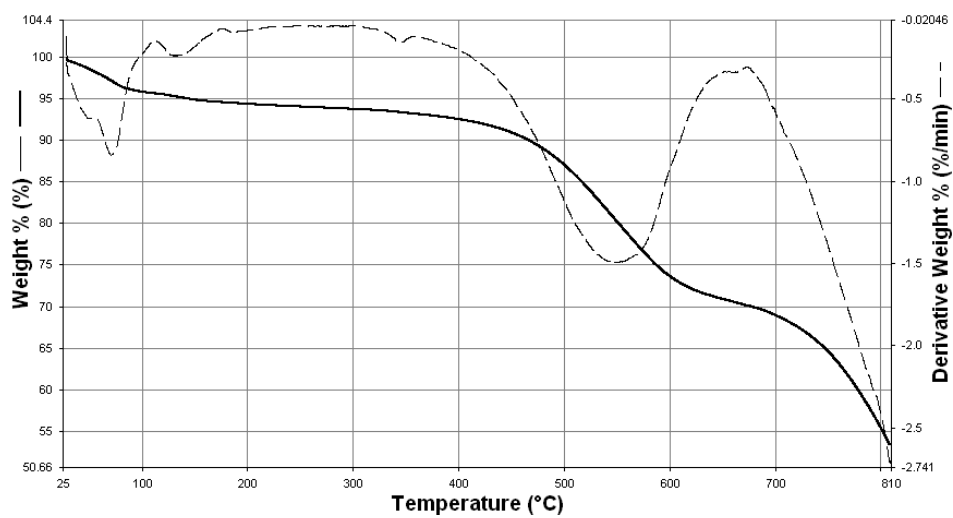


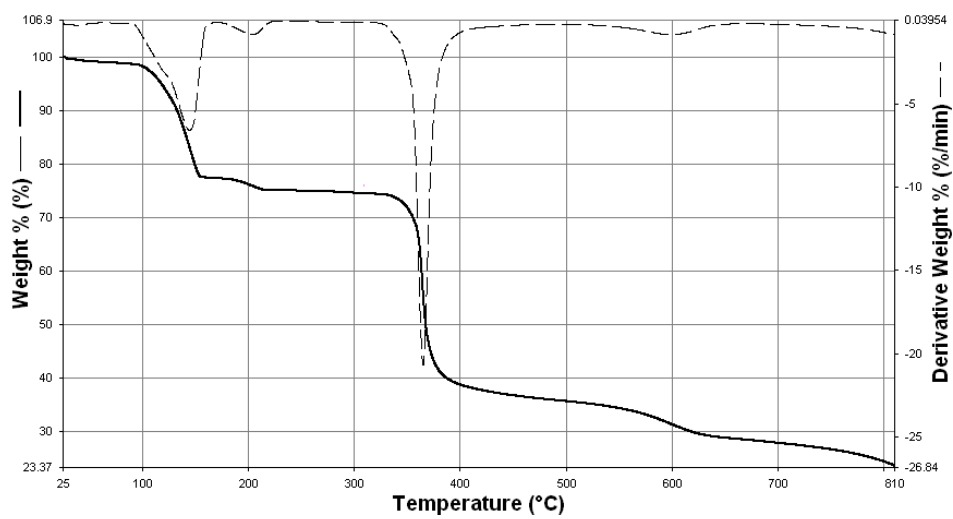
**Figure 3.1.3** DSC thermograms of (a) **CLP** and (b) **CP**

The TGA and DTG curves showed the thermal stability of **CP** in Figure 3.1.4a. Figure A1 from a to f showed the in situ FTIR spectrum of evolved volatile components at each mass loss of **CP**. For **CP**, decomposition occurred in three stages. 55 % **CP** remained when the temperature reached to 800 °C which showed the stability of polymer. In the first stage, the generation of H<sub>2</sub>O was observed over the whole range because of the trap water in cross-linked region of polymers. In the beginning stage of degradation around 90 °C, the characteristic peaks of H<sub>2</sub>O and CO<sub>2</sub> (2358 and 2309 cm<sup>-1</sup>) were observed with a 5% weight loss. The main degradation occurred around 450 °C with a weight loss of 20%. The characteristic peaks of 1,4 dichlorobenzene (1475, 1413, 1095-1010, 819 cm<sup>-1</sup>) and/or 1,2 dichlorobenzene (3080, 1575, 1460, 1256, 1130, 1044, 748 cm<sup>-1</sup>) were observed in the TGA-FTIR spectrum. In the third emission around 690 °C, characteristic bands of CO<sub>2</sub> and vinylchloride (1620, 1380-1270, 941, 730 cm<sup>-1</sup>) were observed.

In the case of **CLP**, sharp weight loss (22 %) observed up to 120 °C followed by a slight decrease up to 200 °C due to the trapped water. Figure A2 from a to d showed the in situ FTIR spectrum of evolved volatile components at each mass loss of **CLP**. The generation of H<sub>2</sub>O was observed over the whole range because of the trapped water in crosslinked region of polymers. In the beginning stage of degradation, the characteristic peaks of H<sub>2</sub>O (4000-3400, 1200-2000 cm<sup>-1</sup>) were observed with 22 % weight loss. In the second stage of degradation showed characteristic peaks of CO<sub>2</sub> (2358 and 2309 cm<sup>-1</sup>) with a weight loss of 35% at 350 °C. Finally, 5% weight loss observed at 600 °C. 29 % of **CLP** remained when the temperature reached to 750 °C (Figure 3.1.4b).



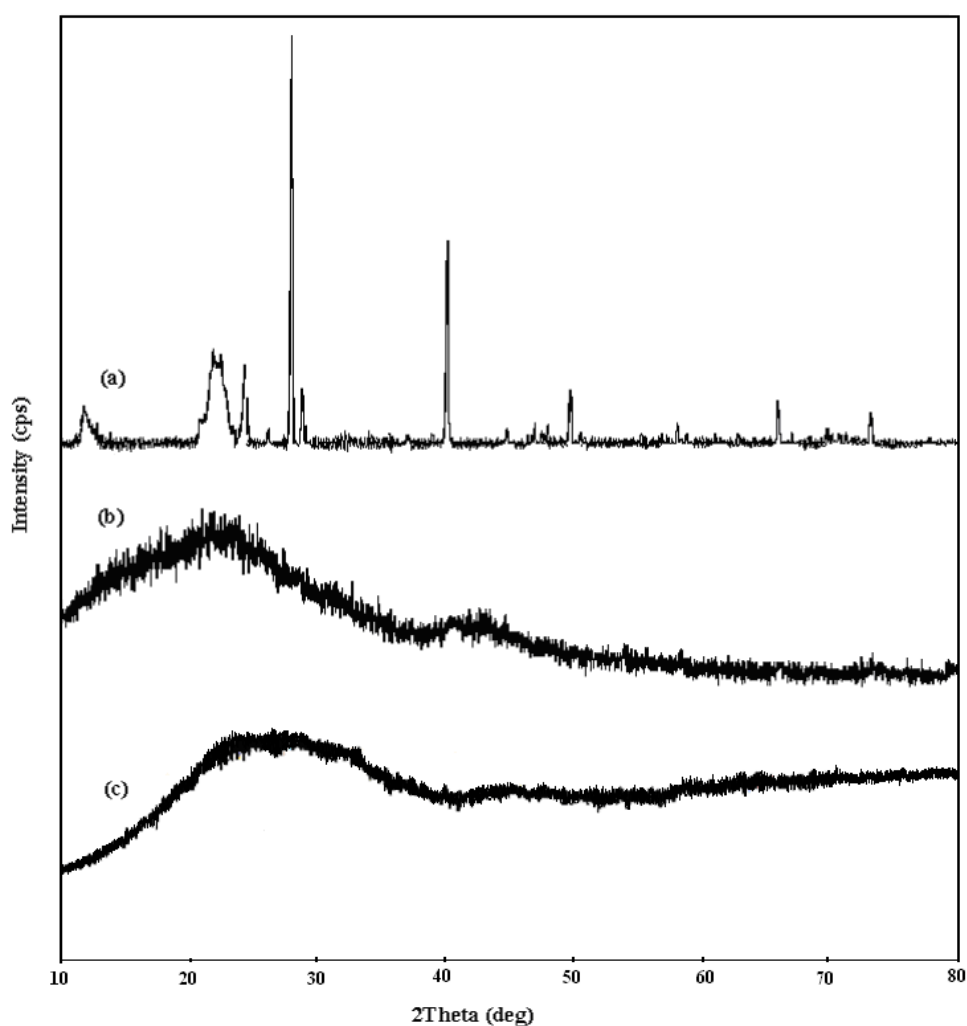
(a)



(b)

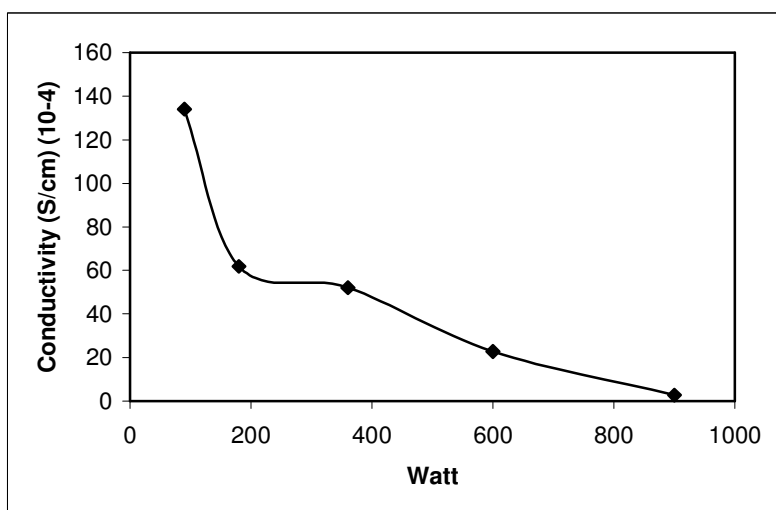
**Figure 3.1.4** TGA thermograms of (a) CP and (b) CLP.

Figure 3.1.5a showed the powder X-ray diffraction pattern of the unwashed **CP**. The powder diffraction X-ray spectrum of unwashed **CP** contained three strongest line of d-spacing of KCl (byproduct during the polymer synthesis). KCl could be indexed as cubic structure of KCl (JCPDS card no 73-0380C). **CP** was washed with hot water several times to removed all KCl. The washed **CP** having a broad line in the spectrum indicated an amorphous polymer (Figure 3.1.5b). For **CLP**, again broad X-ray spectrum of polymer was observed indicated the presence of amorphous polymer (Figure 3.1.5c).



**Figure 3.1.5** X-ray powder diffraction spectra of (a) unwashed **CP**, (b) washed **CP** and (c) **CLP**.

The direct synthesis of highly conducting polymers was achieved in the absence of applied doping process with microwave-assisted polymerization in a very short time sequence. Four probe conductivity measurements were performed on compacted disks of the polymers. The electrical conductivities of unwashed **CP** in the range from 90 to 900 watts were measured as  $13.4 \times 10^{-3}$ ,  $6.2 \times 10^{-3}$ ,  $5.3 \times 10^{-3}$ ,  $2.3 \times 10^{-3}$  and  $0.3 \times 10^{-3} \text{ S cm}^{-1}$ , respectively whereas **CLP** was insulator. As energy increased, the conductivities of **CP** were slightly decreased as shown in Figure 3.1.6. Conductivity of unwashed **CP** was higher than washed **CP**, indicating doping effect of KCl. **CP** synthesized at 90 watt washed with hot water for 3 times and dried to constant weight. The conductivity decreased to  $7.1 \times 10^{-4} \text{ S cm}^{-1}$ .



**Figure 3.1.6** The effect of energy on conductivity of **CP**.

ESR spectra of synthesized polymers studied at room temperature for the paramagnetic center's of the electronic structure of microwave-assisted **CP** and **CLP** revealed the signals with *g* values of 2.00346 and 2.00735 respectively (Figure 3.1.7a and b) which were very close to *g* values of free electron (2.0023).

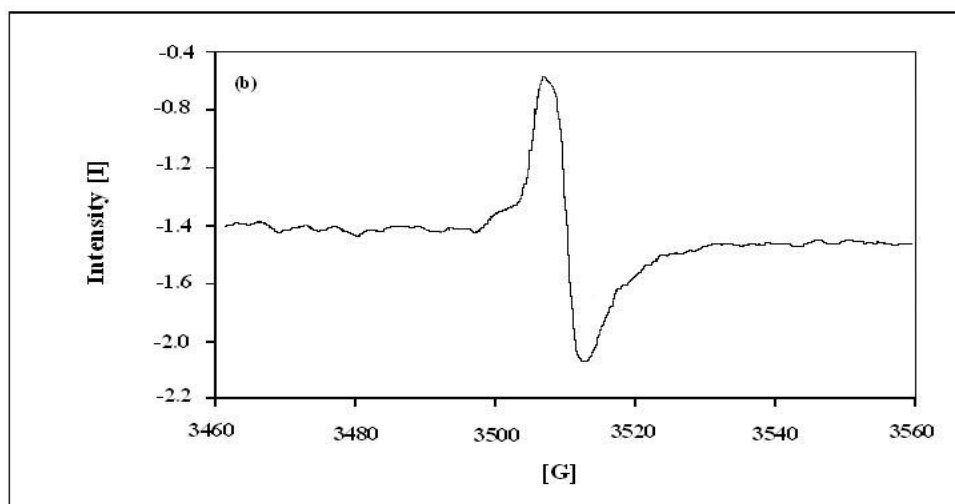
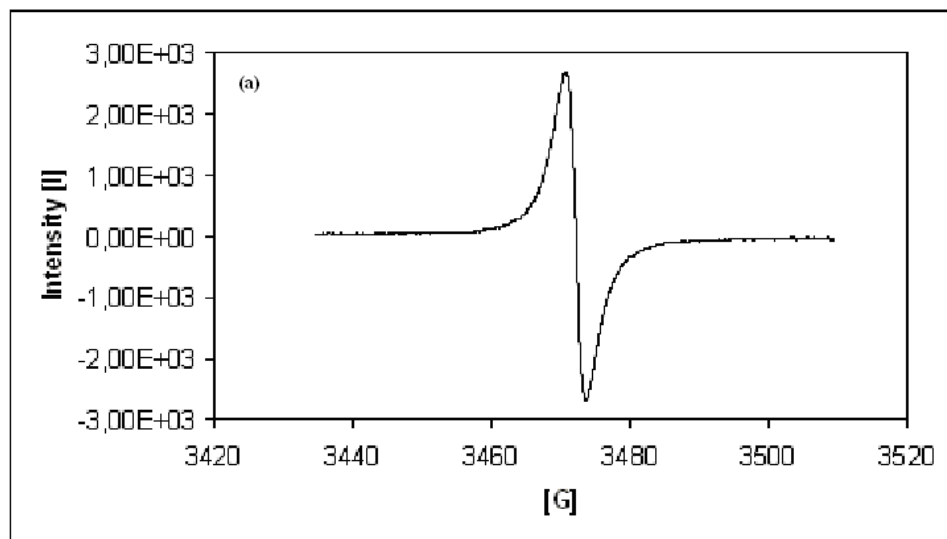


**Figure 3.1.7** ESR spectra of (a) **CP** and (b) **CLP** at room temperature.

The UV-Visible absorption spectra of monomer and crosslinked polymer dissolved in toluene were shown in Figure 3.1.8. The spectrum of monomer (TCP) showed single absorption maxima around 270 nm which could be correlated to absorption of benzene ring K-band (Figure 3.1.8a). However, in the spectrum of **CLP\***(soluble part of **CLP**), evolution of new band located around

323 nm was observed, which could be related to the  $n-\pi^*$  or  $\pi-\pi^*$  transition and the formation of polarons (Figure 3.1.8b).

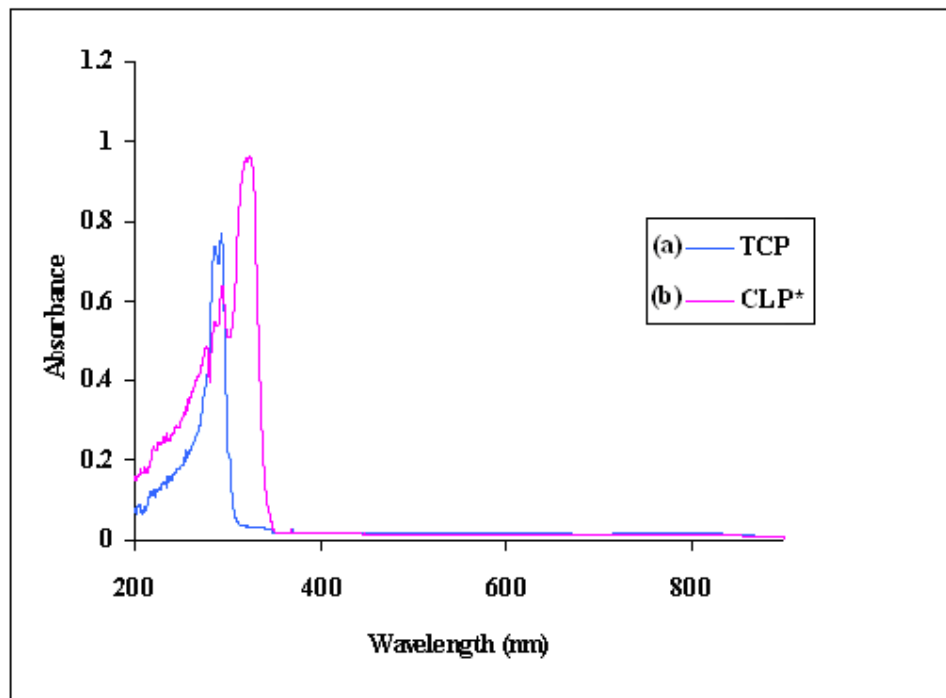


**Figure 3.1.8** UV-Vis spectra of (a) TCP and (b) **CLP\*** at room temperature.

Scanning Electron Microscopy (SEM) rasters a focused electron beam across a sample surface, providing high-resolution and long-depth-of-field images of the sample surface. Analysis of the surface morphologies of **CP** and **CLP** were carried out by scanning electron microscope (Figure 3.1.9a and d). The **CP** had sponge like structures (Figure 3.1.9a) whereas **CLP** had flake or needle like structure (Figure 3.1.9c). The X-ray microanalysis system detected the existence of O, Cl and C on all of **CP** and **CLP** whereas K detected on the unwashed **CP** (Figure 3.1.9b) and **CLP** (Figure 3.1.9d).

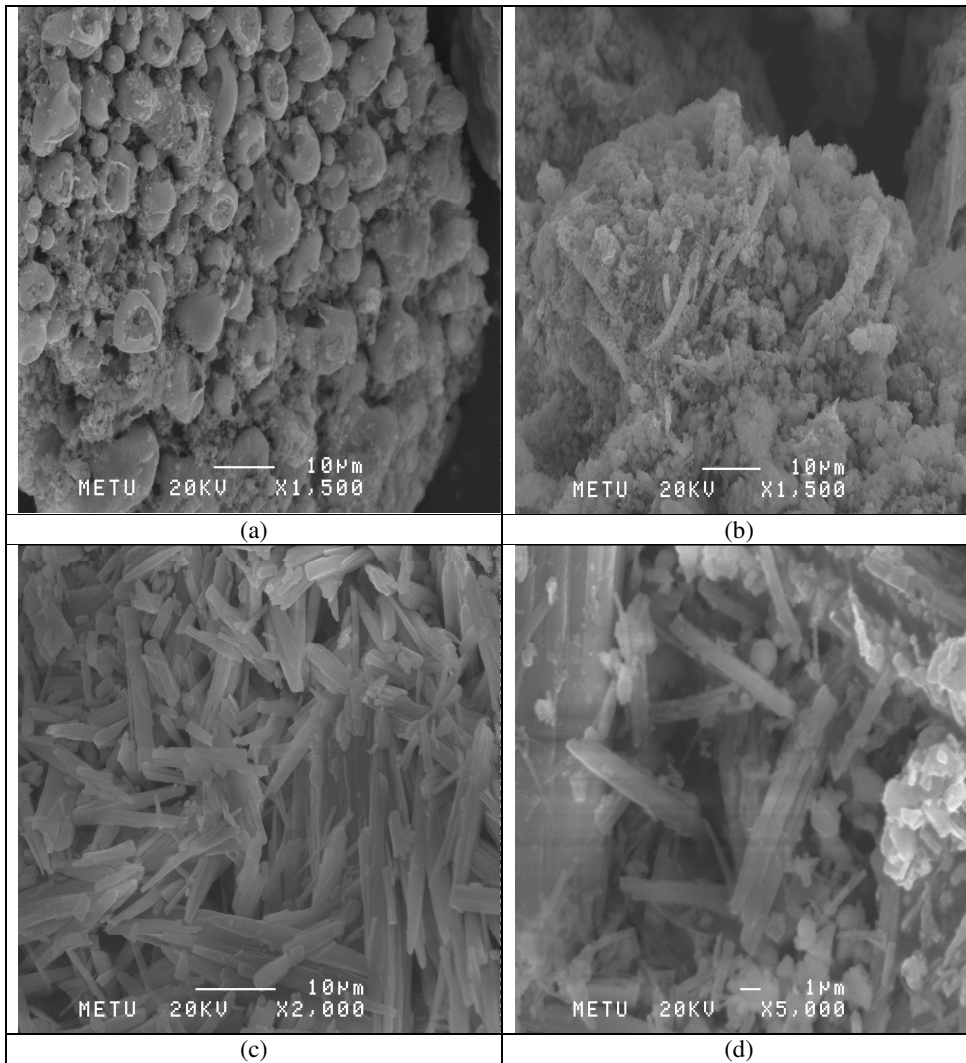


**Figure 3.1.9** SEM micrographs of (a) washed CP, (b) unwashed CP, (c) washed CLP and (d) unwashed CLP.

### 3.2. Synthesis of Polymer with Pyrrole and KOH

A microwave-assisted novel synthesis of conducting polymer (**CP**) and/or ion-radical polymer (**RIP**) were achieved from pyrrole and KOH with microwave energy in a very short time interval.

Table 3.2.1 listed the effect of polymerization time, energy and amount of KOH on the % conversions and polymerizations. The effect of amount of KOH on the polymerization was examined. For this purpose, high concentration of KOH (0.03 mol.) and low concentration of KOH ( $6 \times 10^{-4}$  mol.) were used with 0.03 mol. of monomer pyrrole. Polymerization was performed in the absence of water. For both 90 watt and 180 watt, synthesis of **RIP** and **CP**, whereas at 360, 600 and 900 watts synthesis of **CP** were achieved for both concentrations of KOH. At 90 watt, the polymers synthesized at the end of 6 minutes and polymerization continued upto 25 min. whereas in the range of 600-900 watt, the syntheses were achieved in between 3 to 5 minutes. With high concentration of KOH, % conversions of **RIP** at 90 and 180 watts were 54.2 % (6 min.) and 42.7 % (5 min.) respectively. In the case of low concentration of KOH, % conversions decreased to 34.3 % (6 min.) and 41.4 % (10 min.). Hence, the optimum condition for synthesis of **RIP** was at 90 watt for 6 min. having maximum % conversion value 54.2 %.

In the case of **CP** synthesized with high concentration of KOH, % conversion showed an increasing trend up to 180 watt with a value of 45.4 % in 15 min. period and followed by a decrease to 34.3 % at 900 watt in 4 min. On the other hand, maximum % conversion was achieved at 360 watt in 8 min as 47.0 % for **CP** synthesized with low concentration of KOH. Again a decrease was observed when energy increased to 900 watt with a 38.0 % conversion at the end of 5 min.

**Table 3.2.1** The effect of polymerization time, energy and amount of KOH  
on the % conversion and % weight loss of **CP** and **RIP** of pyrrole

<b>90 Watt</b>	<b>6min</b>	<b>8min</b>	<b>10min</b>	<b>15min</b>	<b>20min</b>	<b>25min</b>
% RIP	<b>54.2</b>	44.6	41.9	-	-	-
% CP	-	-	-	<b>35.7</b>	31.6	33.0
% WL	45.8	55.4	58.1	64.3	68.4	66.0
<b>% RIP</b>	<b>34.3</b>	25.6	-	-	-	-
<b>% CP</b>	-	-	28.2	31.6	<b>37.5</b>	26.4
<b>% WL</b>	55.7	74.4	71.8	68.4	62.5	73.6
<b>180Watt</b>	<b>5min</b>	<b>10min</b>	<b>15min</b>	<b>18 min</b>		
% RIP	<b>42.7</b>	32.4	-	-		
% CP	-	-	<b>45.4</b>	24.7		
% WL	57.3	57.6	56.6	75.3		
<b>% RIP</b>	25.2	<b>41.4</b>	-	-		
<b>% CP</b>	-	-	<b>40.6</b>	22.8		
<b>% WL</b>	74.8	58.6	59.4	77.2		
<b>360 Watt</b>	<b>4min</b>	<b>6min</b>	<b>8min</b>			
% CP	<b>39.5</b>	36.0	35.5			
% WL	60.5	64.0	64.5			
<b>% CP</b>	28.9	33.3	<b>47.0</b>			
<b>% WL</b>	71.1	66.7	53.0			
<b>600 Watt</b>	<b>3min</b>	<b>4min</b>	<b>5min</b>			
% CP	33.7	34.5	<b>35.1</b>			
% WL	66.3	65.5	64.9			
<b>% CP</b>	31.7	<b>43.2</b>	22.4			
<b>% WL</b>	68.3	56.8	77.6			
<b>900 Watt</b>	<b>3min</b>	<b>4min</b>	<b>5min</b>			
% CP	23.9	<b>34.3</b>	20.8			
% WL	76.1	65.7	79.2			
<b>% CP</b>	25.7	31.6	<b>38.0</b>			
<b>% WL</b>	74.3	68.4	62.0			

**RIP** and **CP** synthesized with high concentration of KOH

**RIP** and **CP** synthesized with low concentration of KOH

The optimum conditions for synthesis of **CP** were at 180 watt for 15 min, 360 watt for 8 min having maximum % conversion values 45.4 and 47.0 % respectively (Figure 3.2.1).

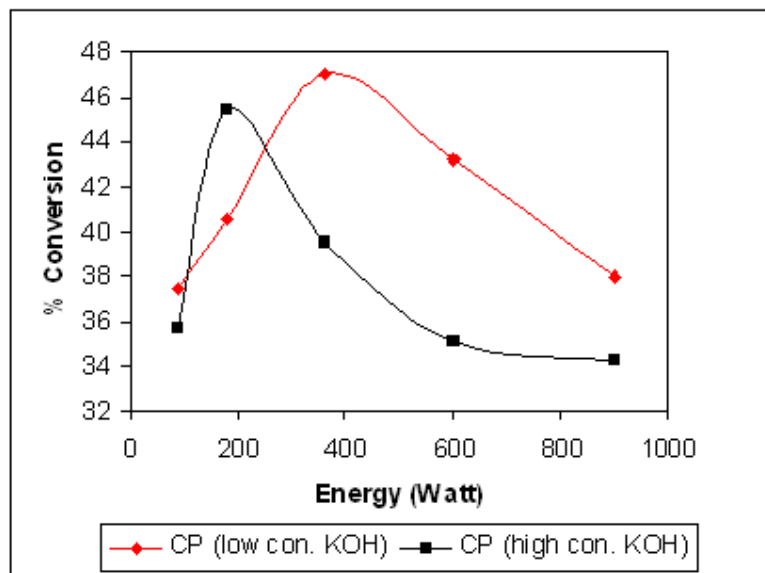


**Figure 3.2.1** % conversion of **CPs** of pyrrole at different concentration of KOH.

### 3.2.1 Characterization

FTIR spectrum of pyrrole monomer exhibited the characteristic absorptions at  $3400\text{ cm}^{-1}$  (N-H stretching vibration), the weak bands in the  $3130$  and  $3100\text{ cm}^{-1}$  (aromatic C-H stretching),  $1545\text{-}1580\text{ cm}^{-1}$  (C=C and C-N in-plane vibration), the conjugated double bonds of pyrrole ring absorb around  $1100\text{ cm}^{-1}$  as splitted into three peaks  $1014$ ,  $1072$  and  $1142\text{ cm}^{-1}$  (C=C ring stretching), (Figure 3.2.2a).

FTIR spectrum of **RIP** of pyrrole (Figure 3.2.2b) revealed the following absorptions at  $3396\text{ cm}^{-1}$  (N-H stretching vibration),  $3002\text{ cm}^{-1}$  (aromatic C-H stretching),  $1672\text{-}1550\text{ cm}^{-1}$  (C=C stretching),  $1460\text{ cm}^{-1}$  (C-N stretching),  $1389\text{ cm}^{-1}$  (C-H stretching),  $1105\text{-}1080\text{ cm}^{-1}$  (bending vibration of C-C and N-H),  $926\text{ cm}^{-1}$ ,  $815\text{ cm}^{-1}$ ,  $751\text{ cm}^{-1}$  (C-H out of plane deformation vibrations). Broadening of the peaks compared to pyrrole monomer and the peak intensities of  $1550\text{ cm}^{-1}$

against  $1460\text{ cm}^{-1}$  proved the formation of PPy oligomer. Since, peak intensities of  $1550\text{ cm}^{-1}$  against  $1460\text{ cm}^{-1}$  were associated with the C=C/C-C stretching mode of PPy, which related to the effective mean  $\pi$ -conjugation along the polymer chains. As the conjugation length increased, the intensity of the antisymmetric ring stretching mode at  $1550\text{ cm}^{-1}$  would decrease and the intensity of the symmetric mode at  $1460\text{ cm}^{-1}$  would increase. In other words, the lower the frequency, the longer the conjugation length of the PPy backbone [122, 123].

FTIR spectrum of **CP** of pyrrole (Figure 3.2.2c) showed the usual feature of PPy synthesized chemically [122], electrochemically [124] and by microemulsion [125] revealing the peak positioned at  $3220\text{ cm}^{-1}$  (N-H stretching vibration),  $3028\text{ cm}^{-1}$  (aromatic C-H stretching),  $1674 - 1563\text{ cm}^{-1}$  (C=C stretching),  $1413\text{ cm}^{-1}$  (C-N stretching),  $1297-1201\text{ cm}^{-1}$  (C-H deformation),  $1092\text{ cm}^{-1}$  (N-H bending),  $966\text{ cm}^{-1}$  and  $924\text{ cm}^{-1}$  (C-H in- plane and out of plane bending). FTIR spectrum of **CP** of pyrrole showed a monotonic decrease in transmittance at wavenumbers between  $4000$  to  $1700\text{ cm}^{-1}$  while the spectrum of pyrrole monomer remained flat in transmittance comparison with the spectrum of (Figure 3.2.2a). The reason was due to free-carrier absorption, which was characteristic of the conductivity state [123]. As seen from the FTIR spectrum of **RIP** the intensities of peaks at  $1550$  and  $1460\text{ cm}^{-1}$  were newly formed and low but in the spectrum of **CP** the peaks at  $1563$  and  $1413\text{ cm}^{-1}$  were well defined and the intensities of the band at  $1563\text{ cm}^{-1}$  decreased and the band at  $1413\text{ cm}^{-1}$  increased which indicated longer conjugation length of the PPy in **CP** compared to **RIP**. The results of the FTIR spectra were in good agreement with the results of the conductivity measurements.

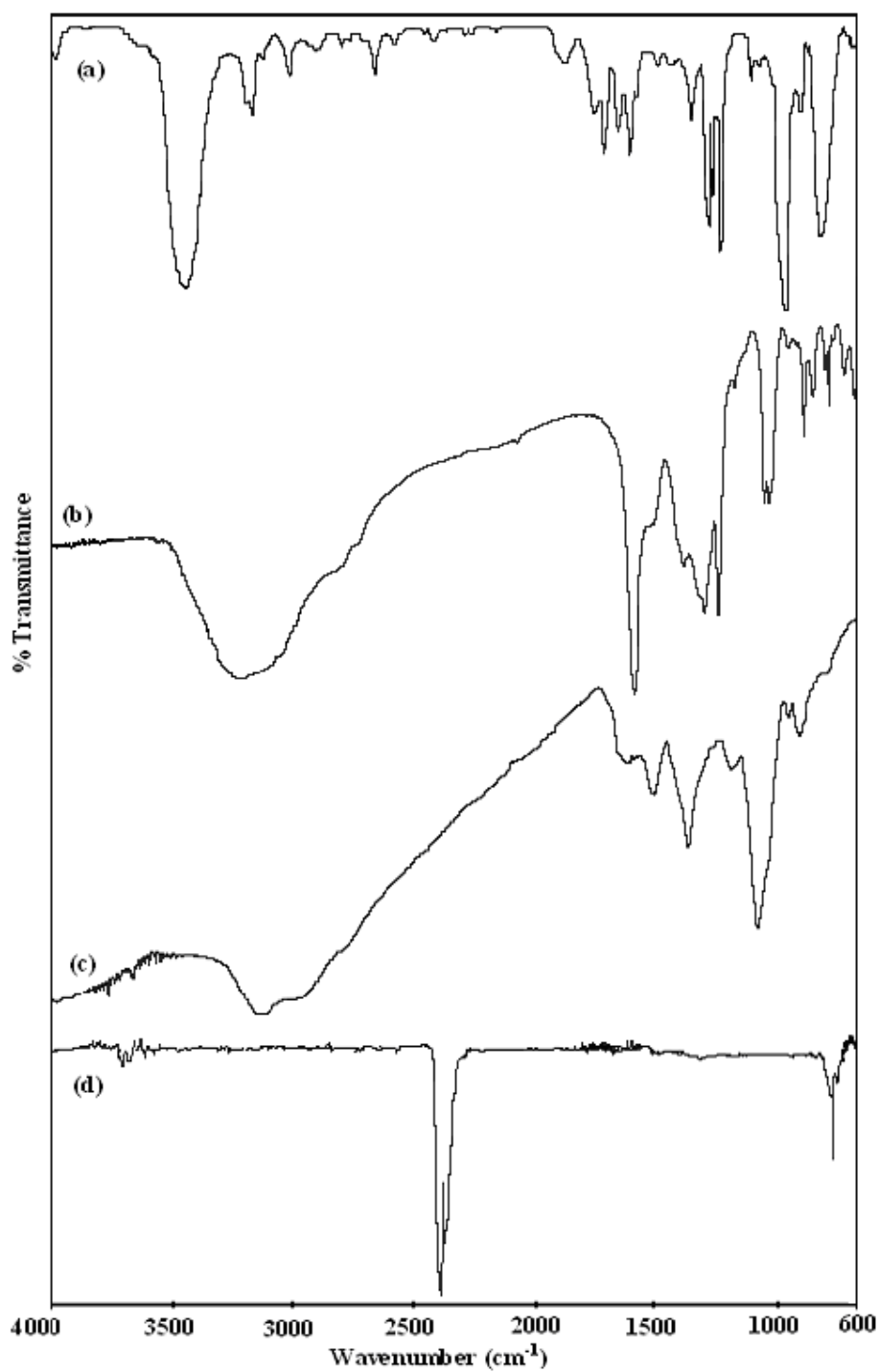


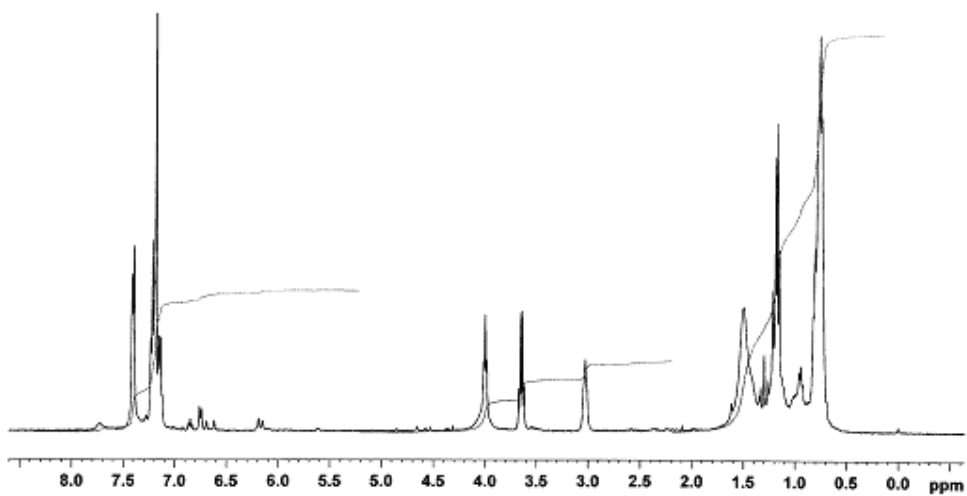
**Figure 3.2.2** FTIR spectra of (a) Pyrrole, (b) **RIP** of pyrrole, (c) **CP** (with low concentration of KOH) of pyrrole and (d) released gases during polymerization.

FTIR spectrum of **CP** of pyrrole synthesized with high concentration of KOH exhibited the similar peaks of **CP** of pyrrole synthesized with low concentration of KOH.

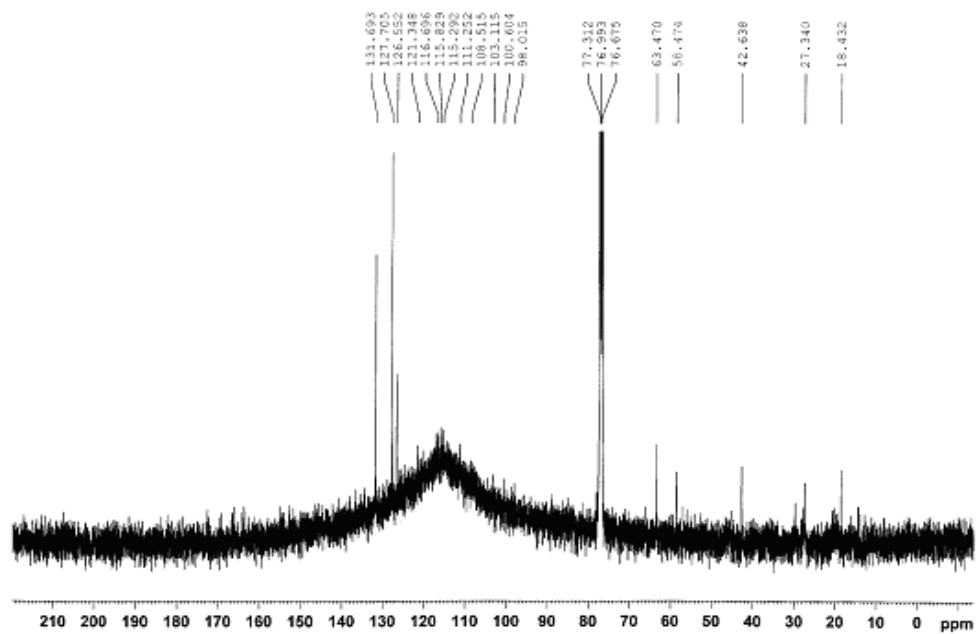
FTIR spectrum of the evolved gas collected in a glass cell during polymerization, exhibited the peak at  $2450\text{ cm}^{-1}$  ( $\text{CO}_2$ ) and  $1270\text{ cm}^{-1}$  (C=O stretching) (Figure 3.2.2d).

$^1\text{H}$  NMR of **RIP** and  $^{13}\text{C}$  NMR of **RIP** of pyrrole showed both aromatic and aliphatic peaks. The peaks at 7.4 ppm and 7.2 ppm in  $^1\text{H}$  NMR spectrum of **RIP** indicated the presence of polypyrrole in the structure. In some part of the structure, breakage of the pyrrole ring observed as seen in the aliphatic peaks (Figure 3.2.3a).

$^{13}\text{C}$  NMR of **RIP** of pyrrole showed a broad peak located around 115 ppm which again indicated the presence of polypyrrole (Figure 3.2.3b). It was well known that the  $\alpha$  and  $\beta$  carbons of the pyrrole monomer exhibited peaks at 117 and 108 ppm downfield relative to TMS [126]. The peaks at 126-127 and 103 ppm confirmed the presence of pyrrole moiety in the polymer, and the downfield shift of the  $\alpha$  carbons relative to monomeric pyrrole was consistent with the  $\alpha$ - $\alpha'$  linkages. The peak at 132 ppm would indicate the presence of some non-  $\alpha$ - $\alpha'$  linkages ( $\alpha$ - $\beta$  linkages) [127]. These results would correspond that the polypyrrole have predominantly  $\alpha$ - $\alpha'$  bonding but in some part of the ring there were  $\alpha$ - $\beta$  linkages. The presence of peaks at 117 and 108 ppm indicated that there were still unreacted pyrrole monomers in the polymeric matrix and polymerization would be continued.



(a)



(b)

**Figure 3.2.3** (a)  $^1\text{H}$  NMR of **RIP** and (b)  $^{13}\text{C}$  NMR of **RIP** of pyrrole.

In order to prove the presence of polypyrrole in the **RIP** of pyrrole, direct insertion probe mass spectrometry was used (Figure 3.2.4).

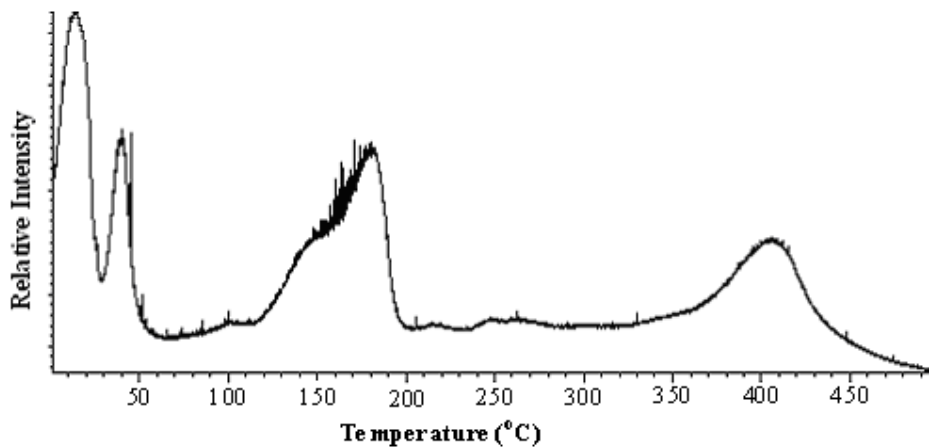
Direct pyrolysis of **RIP** yielded total ion current (TIC) curve, the variation of total ion yield as a function of temperature, with several peaks and shoulders (Figure 3.2.4a). Pyrolysis product peaks started to appear in the mass spectra even at initial stages pointing out adsorption of low molecular weight species. This behaviour could be explained either a complex thermal degradation mechanism and/or presence of more than one compound [128,129]. The low temperature peaks were mainly associated with solvent, unreacted pyrrole and KOH used for the synthesis. Peak that could be attributed to polymer degradation was appeared in the final stage of pyrolysis around 428 °C.

Figure 3.2.4b and c showed the direct and indirect pyrolysis mass spectra of **RIP** of pyrrole at 428 °C. Monomer and low-mass oligomer peaks were detected. Some selected fragments, with  $m/z$  values 18 Da ( $\text{H}_2\text{O}$ ), 43 Da (molecular ion of  $^+\text{CH}_2\text{-CH}_2\text{-NH}^-$ ), 44 Da ( $\text{CO}_2$  or  $^+\text{CH}_2\text{-CH}_2\text{-NH}_2$ ), 43 Da ( $\text{CH}_3\text{-CH}_2\text{-NH}_2$ ), 53 Da ( $\text{C}_3\text{H}_3\text{N}$ ), 66 Da (molecular ion of  $\text{C}_4\text{H}_3\text{NH}^+$ ), 67 Da (monomer pyrrole  $\text{C}_4\text{H}_5\text{N}$ ), 132 Da (dimer of pyrrole  $\text{C}_8\text{H}_6\text{N}_2$ ), 137 Da ( $\text{K}_2\text{CO}_3$ ).

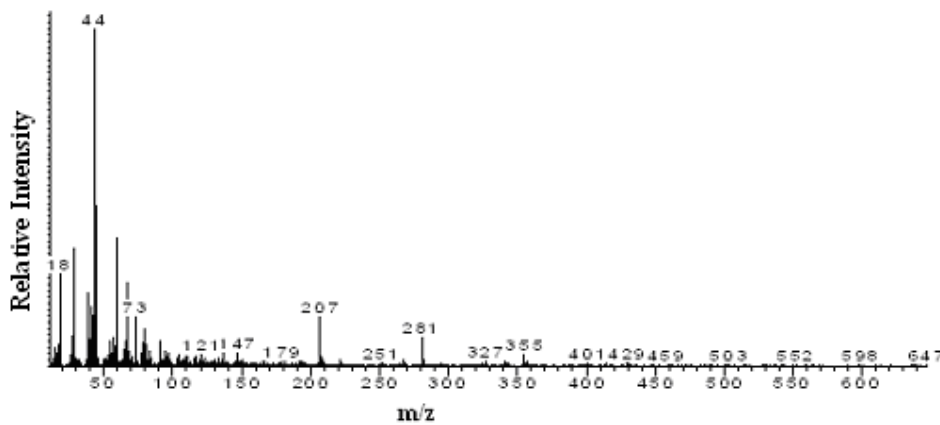
The peaks at  $m/z = 67$  Da and  $m/z = 132$  Da indicated the presence of pyrrole monomer and dimer, respectively in the structure of **RIP**. The peak at  $m/z = 66$  Da would be due to the unreacted pyrrole adsorbed on the polymer and proved that the polymerization would be continued and orange colored **RIP** would turn into black colored **CP** of pyrrole with higher conjugation length and conductivity.

The peak at  $m/z = 137$  Da was due to the  $\text{K}_2\text{CO}_3$  which was the decomposition product of  $\text{KHCO}_3$ .  $\text{KHCO}_3$  was found in the X-ray diffraction pattern of the unwashed **CP** (Figure 3.2.8a) and the byproduct of the reaction.  $\text{KHCO}_3$  decomposes at 100-200 °C into  $\text{K}_2\text{CO}_3$ ,  $\text{H}_2\text{O}$  and  $\text{CO}_2$  in the TGA spectrum of

**RIP** of pyrrole (Figure 3.2.6a). So the peaks at  $m/z = 18$  Da ( $H_2O$ ),  $m/z = 44$  Da ( $CO_2$ ) and  $m/z = 137$  Da ( $K_2CO_3$ ) were the decomposition products of  $KHCO_3$ .

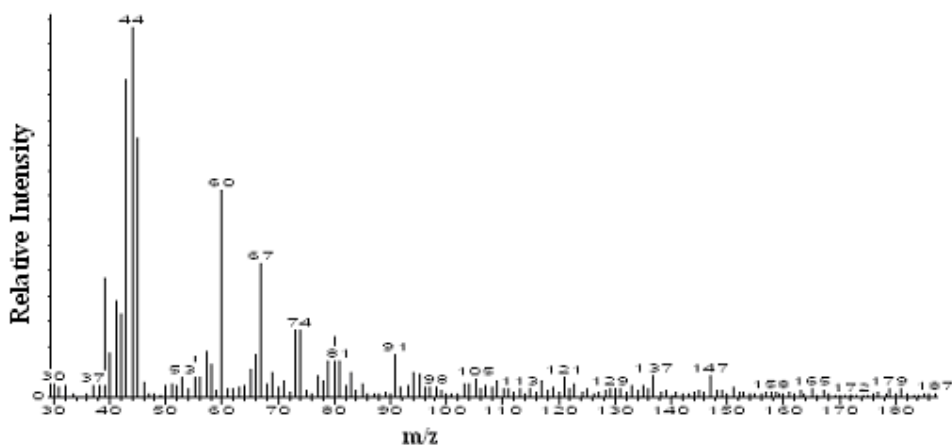


(a)



(b)

Figure 3.2.4 cont.



(c)

**Figure 3.2.4** (a) Ion-temperature profile of **RIP**, (b) Direct pyrolysis mass spectrum of **RIP** at 428 °C and (c) Indirect pyrolysis mass spectrum of **RIP** of pyrrole at 428 °C.

The thermal properties of the synthesized polymers were studied with DSC and TGA. The DSC thermogram of the **RIP** (Figure 3.2.5a) showed no glass transition temperature but a broad melting point at 190 °C which was in the melting range of  $\text{KHCO}_3$ . Glass transition temperature was also not observed for the washed **CP** of pyrrole (Figure 3.2.5b).

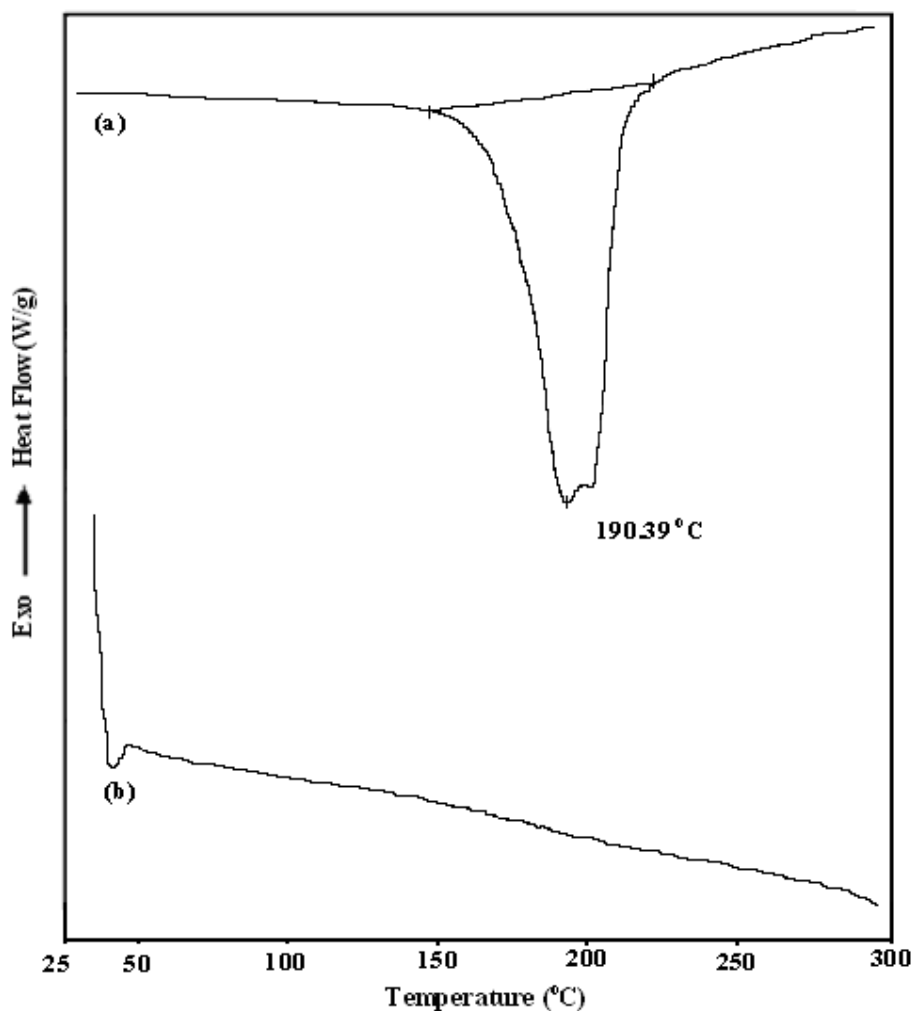
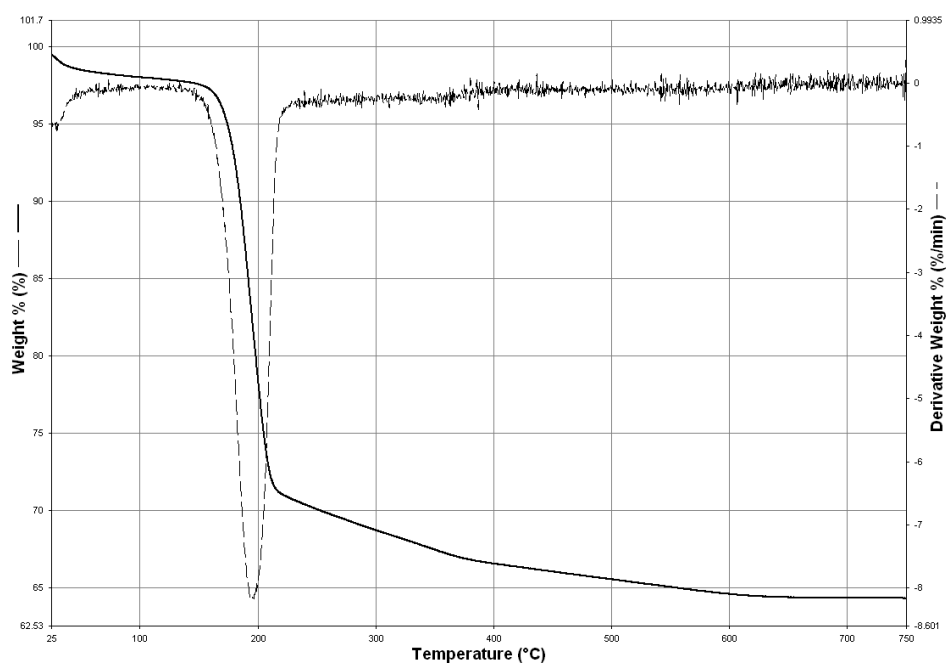


**Figure 3.2.5** DSC thermograms of (a) **RIP** and (b) **CP** of pyrrole.

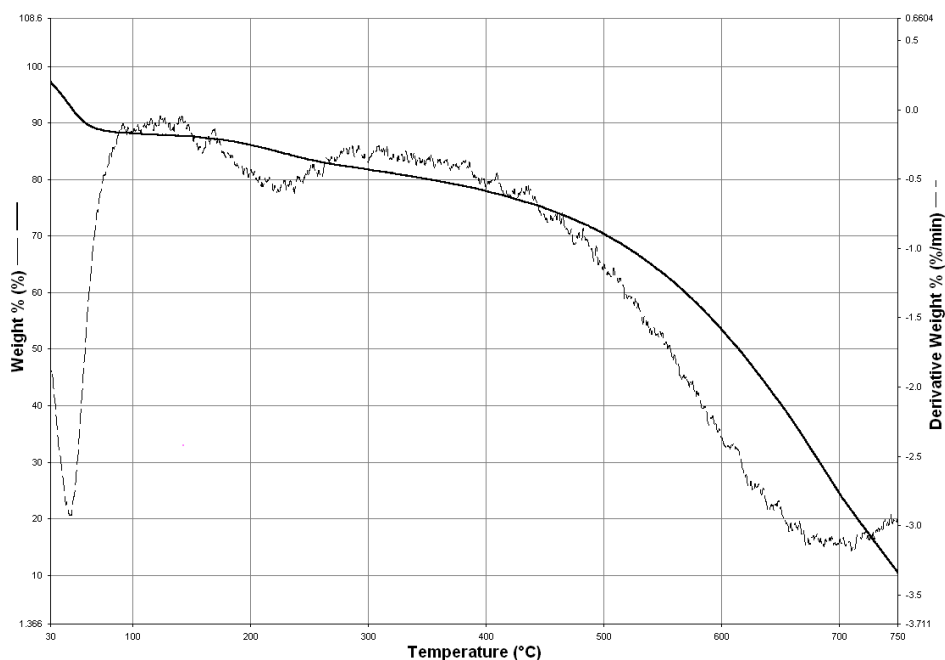
TGA weight loss curve and the corresponding derivative curve (DTG) for **RIP** of pyrrole was shown in Figure 3.2.6a. The main weight loss (25%) was observed at 190 °C which was due to the decomposition of  $\text{KHCO}_3$ . In situ FTIR spectrum of the evolved gases during the thermal gravimetric analysis showed characteristic peaks of  $\text{CO}_2$  which was one of the decomposition product of  $\text{KHCO}_3$  (Figure A3a). **RIP** showed a higher thermal stability and still having residues more than 60% beyond 800 °C.

TGA weight loss curve and the corresponding derivative curves (DTG) for **CP** was shown in Figure 3.2.6b. In the TGA thermogram, the **CP** of pyrrole, weight loss (10 %) observed up to 100 °C due to the trapped water. The second degradation occurred nearly 200 °C and then approximately 70 % of sample was lost when the temperature reached to 760 °C. The main weight loss was most probably due to the decomposition of the polymeric matrix.



(a)

Figure 3.2 6 cont.



(b)

**Figure 3.2.6** TGA thermograms of (a) **RIP** and (b) **CP** of pyrrole.

The effect of energy on conductivity of **CP** was determined. For this purpose, at each watt the conductivity of **CP** was measured by using substances with maximum % conversion (Figure 3.2.7). The conductivities of unwashed **CP** synthesized with low concentration of KOH (Figure 3.2.7a) in the range from 90 to 900 watts were measured as  $3.2 \times 10^{-4}$ ,  $8.8 \times 10^{-4}$ ,  $10.2 \times 10^{-4}$ ,  $16.5 \times 10^{-4}$ ,  $4.6 \times 10^{-4}$  S/cm, respectively. The maximum conductivity was measured at 600 watt as  $16.5 \times 10^{-4}$  S/cm. The conductivities of unwashed **CP** synthesized with high concentration of KOH (Figure 3.2.7b) were approximately 100 times higher than the conductivities of unwashed **CP** synthesized with low concentration of KOH. This was due to the formation of  $\text{KHCO}_3$  during polymerization. As concentration of KOH increased, the formation of byproduct increased which increased the conductivities. As watt increased, the conductivity of unwashed **CP**

synthesized with high concentration of KOH decreased from  $4.5 \times 10^{-2}$  S/cm to  $1.1 \times 10^{-2}$  S/cm. At 180 watt, **CP** was first washed with toluene and then with hot water and after drying for 3 days, the conductivity was  $5.5 \times 10^{-4}$  S/cm. But with the unwashed **CP**, the conductivity was increased to  $4.0 \times 10^{-2}$  S/cm as expected. The conductivity of **RIP** synthesized with high concentration of KOH at 90 watt 6 min. was measured as  $1.1 \times 10^{-5}$  S/cm.

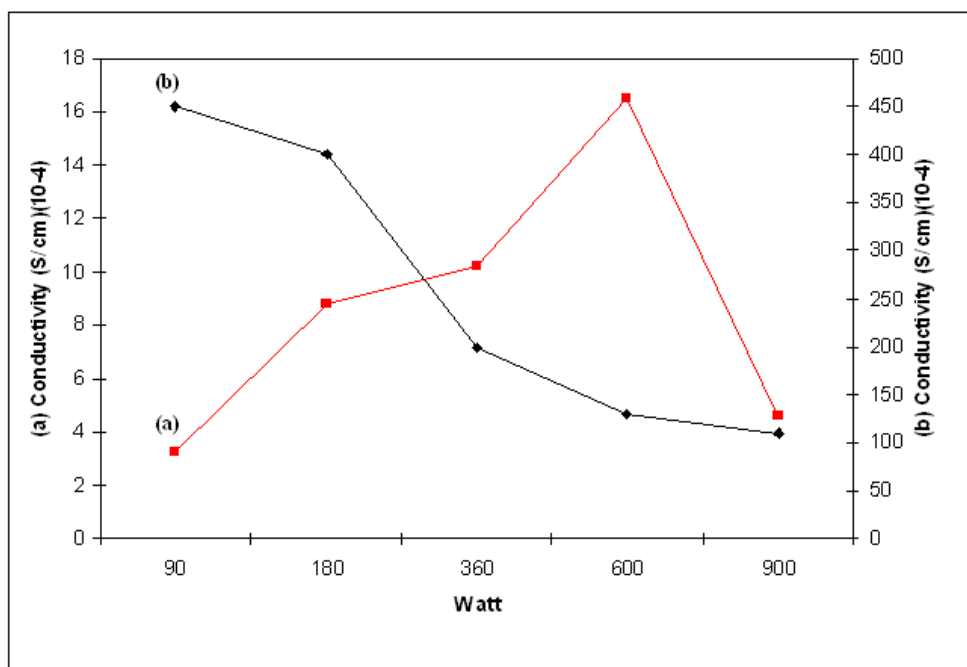


**Figure 3.2.7** The effect of energy on conductivity of **CP** of pyrrole (a) **CP** (with low concentration of KOH) and (b) **CP** (with high concentration of KOH).

Figure 3.2.8a showed the powder X-ray diffraction pattern of the unwashed **CP**. The diffraction peaks were in good agreement with those of  $\text{KHCO}_3$  crystals which could be indexed as the hexagonal structure of  $\text{KHCO}_3$  (JCPDS card no 50-09261). **CP** was washed with hot water in order to remove  $\text{KHCO}_3$  crystals trapped in the synthesized polymer. After that, a broad X-ray spectrum of polymer was observed indicated the presence of an amorphous polymer (Figure 3.2.8b).

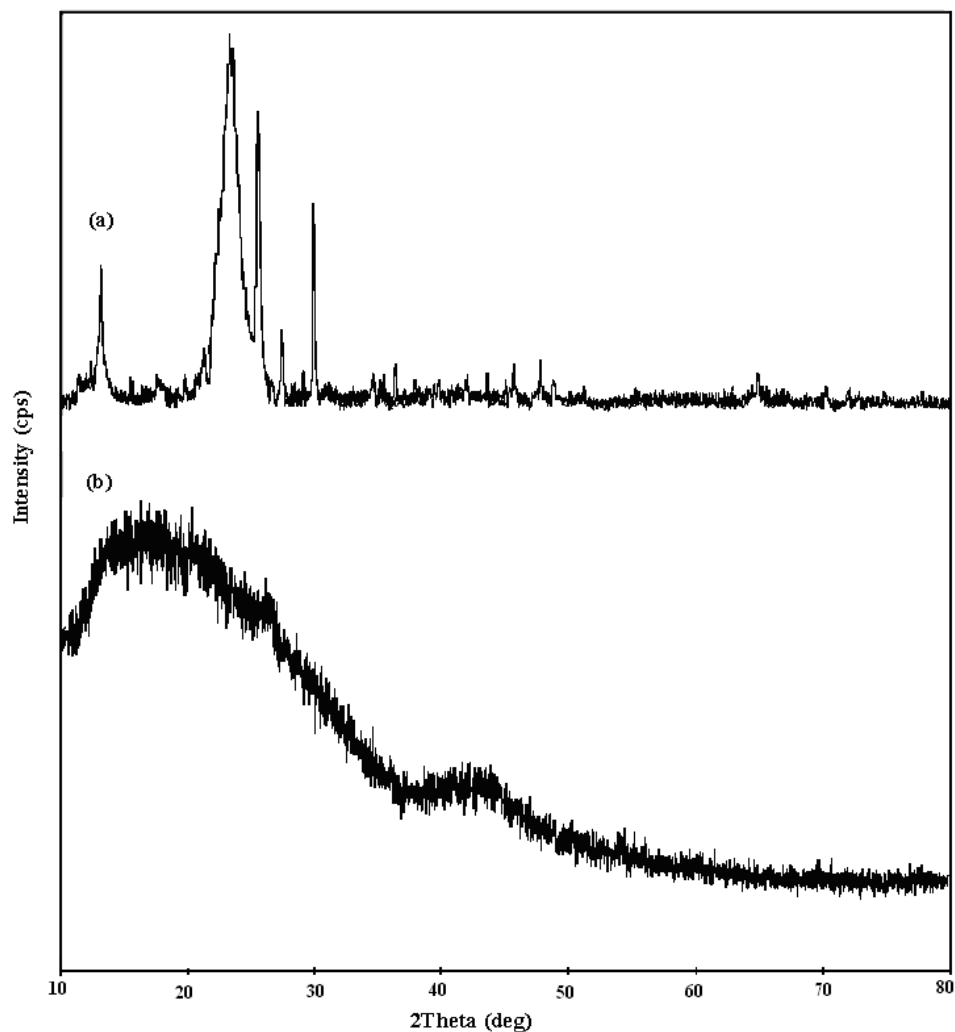


**Figure 3.2.8** X-ray powder diffraction spectra of (a) unwashed **CP** and (b) washed **CP** of pyrrole.

ESR spectrum was used in order to confirm the presence of radicals in synthesized polymers. ESR spectra of polymers were recorded at room temperature. As a result; **CP** was revealed one signal with  $g$  value of 2.005 (Figure 3.2.9a). But, for **RIP** of pyrrole two signals with  $g$  values of 2.186 and 1.999 were observed, respectively (Figure 3.2.9b and c).

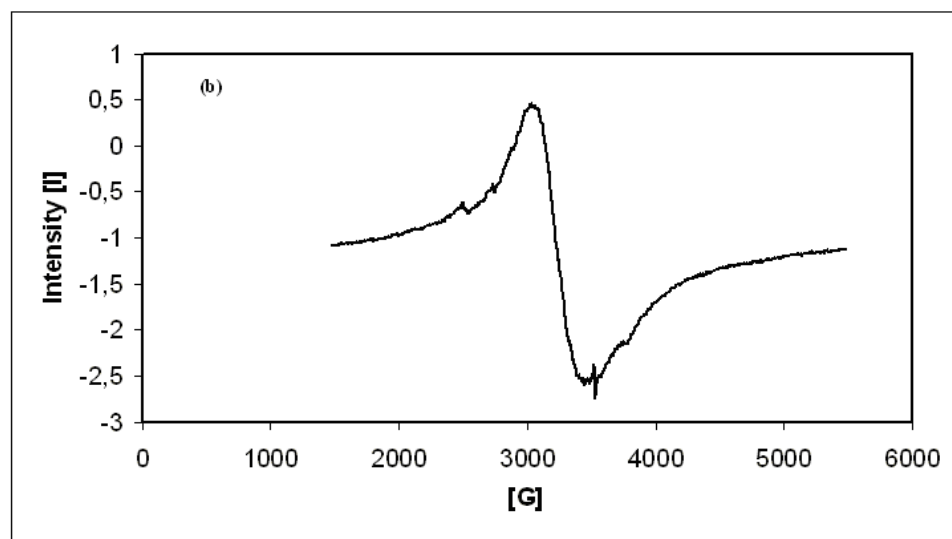
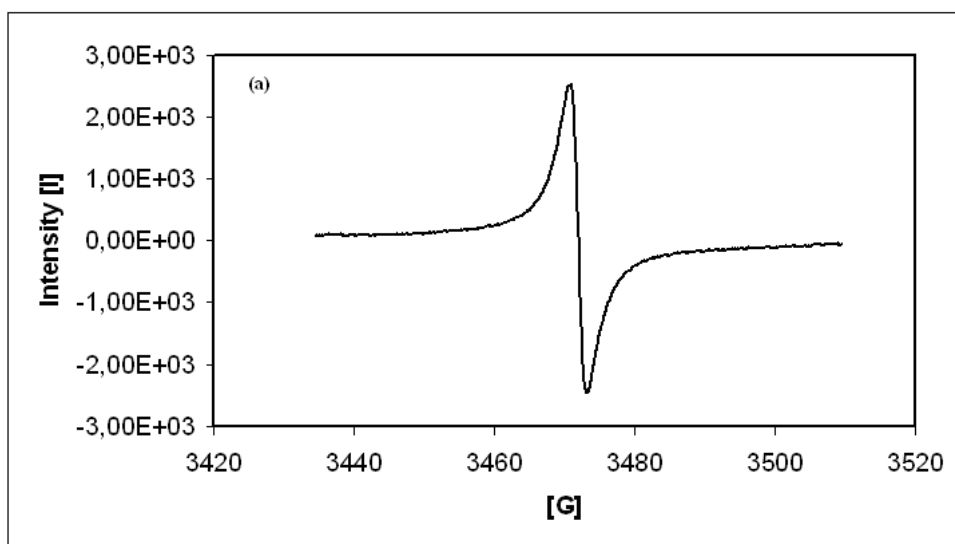
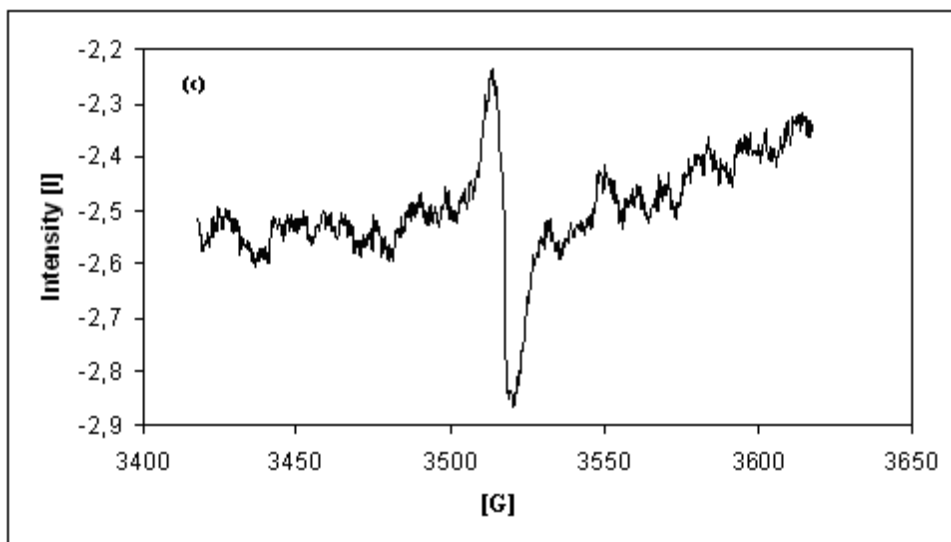
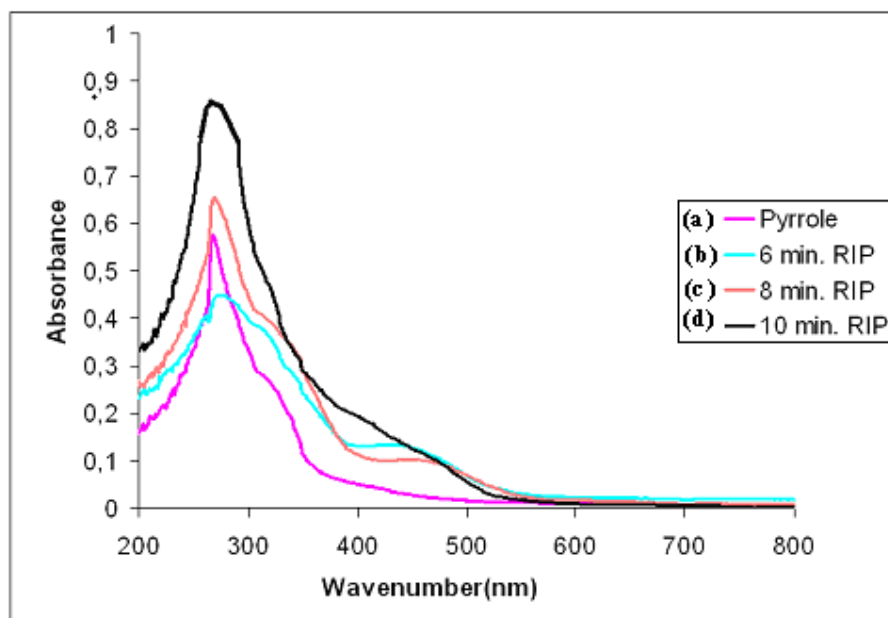


Figure 3.2.9 cont.



**Figure 3.2.9** ESR spectra of (a) **CP**, (b) **RIP** and (c) **RIP** of pyrrole at room temperature.

The UV-Visible absorption spectra of monomer pyrrole, synthesized **RIP** at 6, 8 and 10 minutes dissolved in N, N dimethylformamide were shown in Figure 3.2.10. The spectrum of pyrrole showed single absorption maxima around 270 nm which could be correlated to absorption of aromatics (Figure 3.2.10a). In the spectrum of **RIP** synthesized at the end of 6 min, the formation of polarons was observed for the soluble part of **RIP** with the evolution of new broad band located around 470 nm, which was related to the  $\pi$ - $\pi^*$  transition (Figure 3.2.10b). For **RIP** synthesized at the end of 8 min, again two bands were observed at 270 and 470 nm which indicated the formation of polarons (Figure 3.2.10c). However, in the UV-Visible absorption spectrum of **RIP** synthesized at the end of 10 min the formation of polarons decreased since the formation of **CP** of pyrrole began at that minute which was insoluble in DMF (Figure 3.2.10d).



**Figure 3.2.10** UV-Vis spectra of (a) Pyrrole, (b) 6 min. **RIP**, (c) 8 min. **RIP** and (d) 10 min. **RIP** of pyrrole at room temperature.

The scanning electron microscope images showed that polymers morphology were different. The existence of  $\text{KHCO}_3$  was observed on the surface of the unwashed **CP** (Figures 3.2.11a and c), like observed in X-ray spectrum. Tubular structures were observed on the edge of KOH in the SEM images of unwashed **CP** of pyrrole (Figures 3.2.11a and b). Washed **CP** showed cauliflower-like structure which is characteristic for polypyrrole (Figure 3.2.11d). The X-ray microanalysis system detected the existence of C and N in washed **CP** structure whereas K and O were detected in unwashed **CP**. The **RIP** of pyrrole contains hexagonal structures as surface morphologies. Honey comb figures were seen in the SEM images of **RIP** (Figures 3.2.11e and f).

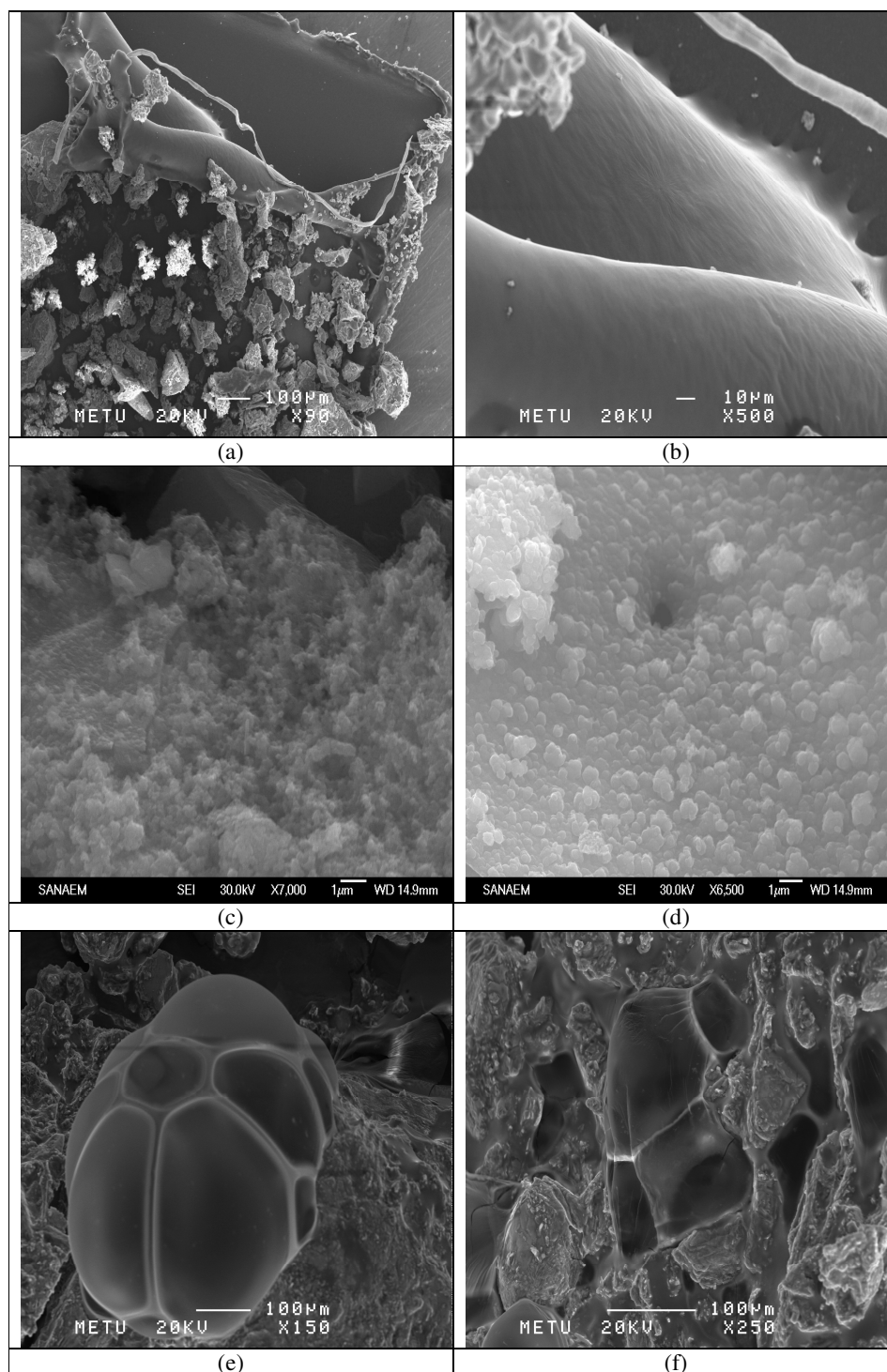


**Figure 3.2.11** SEM micrographs of (a), (b), (c) unwashed **CP**, (d) washed **CP**, (e) and (f) unwashed **RIP**.

### 3.3. Synthesis of Polymer with Thiophene and KOH

Microwave-assisted simultaneous novel synthesis of white polymer (**WP**), orange polymer (**OP**) and conducting polymer (**CP**) were achieved from thiophene and KOH. Polymerizations were performed by varying the time from 1 to 25 min, microwave energy from 90 to 900 watt.

The effect of polymerization time, energy and amount of KOH on the % conversions and % weight losses (WL) were listed in Table 3.3.1. Two different amounts of KOH (0.05 and  $2 \times 10^{-4}$  mol.) were used in 0.05 mol of monomer thiophene. At 90 watt orange and white polymers were obtained but in the range of 180 to 360 watts both white, orange and conducting polymers of thiophene were obtained for each amount of KOH. On the other hand, at high energies **CP** was the only product. In the range of 90-360 watt, generally % conversion slightly decreased for **WP** synthesized with both concentrations of KOH. The maximum % conversion of **WP** was obtained at 90 watt in 12 min with 28.9%. **OP** synthesized with high concentration of KOH showed no regular trend in % conversion and have a maximum value of 32.5% at 90 watt at the end of 15min. **OP** synthesized with low concentration of KOH showed an increasing trend upto 180 watt with 28.6 % conversion and then decreased to 22.4%.

% conversion of **CP** synthesized at different concentration of KOH in the range of 90-900 watt was shown in Figure 3.3.1. % conversion of **CP** synthesized with high concentration of KOH showed an increasing trend as microwave energy increased from 90 to 900 watt. On the other hand, % conversion increased slightly for **CP** synthesized with low concentration of KOH up to 39.3% followed by a decrease to 33.8% at 900 watt. Hence, the optimum condition for synthesis of **CP** was at 900 watt for 3 min with 0.05 mol KOH having maximum % conversion value 43.3%.

**Table 3.3.1** The effect of polymerization time, energy and amount of KOH

on the % conversion and % weight loss of **CP**, **WP** and **OP** of thiophene

<b>90 Watt</b>	<b>10min</b>	<b>12min</b>	<b>15min</b>	<b>20min</b>	<b>25min</b>
% WP	15.4	<b>28.9</b>	-	-	-
% OP	-	-	<b>32.5</b>	24.5	18.3
% WL	84.6	71.1	67.5	75.5	81.7
<b>% WP</b>	-	<b>24.7</b>	-	-	-
<b>% OP</b>	-	-	18.6	<b>25.3</b>	21.4
<b>% WL</b>	-	75.3	81.4	74.7	78.6
<b>180Watt</b>	<b>6min</b>	<b>8min</b>	<b>12min</b>	<b>16min</b>	
% WP	12.8	<b>20.7</b>	-	-	
% OP	-	-	<b>22.4</b>	-	
% CP	-	15.7	30.9	<b>34.1</b>	
% WL	87.2	63.6	46.7	65.9	
<b>% WP</b>	10.6	<b>17.6</b>	-	-	
<b>% OP</b>	-	-	<b>28.6</b>	-	
<b>% CP</b>	-	18.3	25.7	<b>29.5</b>	
<b>% WL</b>	89.4	64.1	45.7	70.5	
<b>360 Watt</b>	<b>4min</b>	<b>6min</b>	<b>8min</b>		
% WP	<b>19.3</b>	-	-		
% OP	-	<b>29.3</b>	-		
% CP	21.8	30.5	<b>35.7</b>		
% WL	58.9	40.2	64.3		
<b>% WP</b>	<b>15.5</b>	-	-		
<b>% OP</b>	-	<b>22.4</b>	-		
<b>% CP</b>	19.2	28.1	<b>30.3</b>		
<b>% WL</b>	65.3	49.5	69.7		
<b>600 Watt</b>	<b>3min</b>	<b>4min</b>	<b>5min</b>		
% CP	31.2	38.6	<b>42.4</b>		
% WL	68.8	61.4	57.6		
<b>% CP</b>	27.3	<b>39.3</b>	32.5		
<b>% WL</b>	72.7	60.7	67.5		
<b>900 Watt</b>	<b>2min</b>	<b>3min</b>	<b>4min</b>		
% CP	36.3	<b>43.3</b>	28.4		
% WL	63.7	56.7	71.6		
<b>% CP</b>	25.9	<b>33.8</b>	29.2		
<b>% WL</b>	74.1	66.2	70.8		

**WP, OP and CP** synthesized with high concentration of KOH

**WP, OP and CP** synthesized with low concentration of KOH

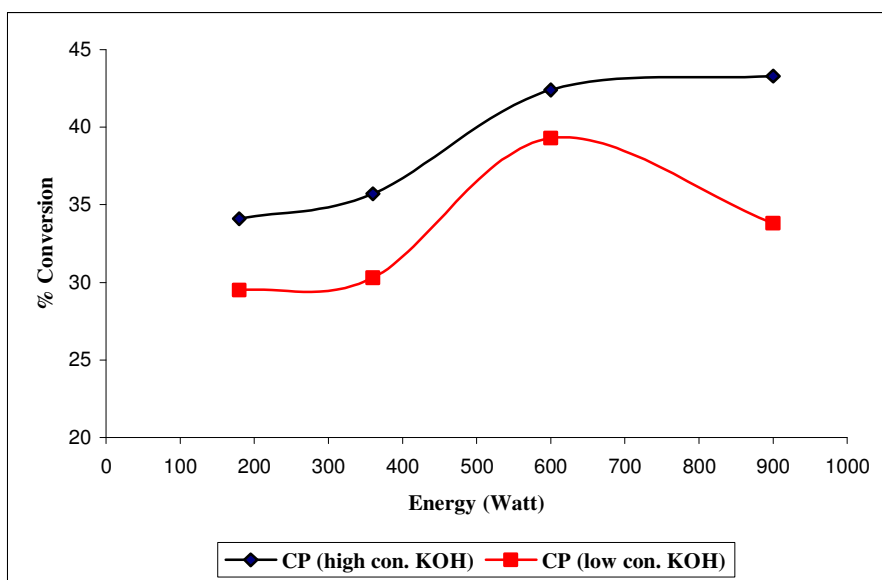


**Figure 3.3.1** % conversion of CPs of thiophene at different concentration of KOH

### 3.3.2 Characterization

FTIR spectrum of thiophene monomer exhibited the characteristic absorptions at  $3107\text{ cm}^{-1}$  ( $\text{C-H}_\alpha$  stretching vibration),  $3072\text{ cm}^{-1}$  (aromatic  $\text{C-H}_\beta$  stretching),  $1555\text{-}1480\text{ cm}^{-1}$  ( $\text{C=C}$  in-plane vibration), the conjugated double bonds of thiophene ring absorb at  $1407\text{ cm}^{-1}$ ,  $1080\text{ cm}^{-1}$ ,  $1033\text{ cm}^{-1}$  ( $\text{C=C}$  ring stretching),  $832\text{ cm}^{-1}$  ( $\text{C-H}_\alpha$  out of plane bending),  $712\text{ cm}^{-1}$  ( $\text{C-H}_\beta$  out of plane bending) (Figure 3.3.2a).

FTIR spectrum of CP of thiophene (Figure 3.3.2b) revealing the peak positioned at  $3176\text{ cm}^{-1}$  (aromatic  $\text{C-H}$  stretching),  $1640\text{ cm}^{-1}$ ,  $1448\text{ cm}^{-1}$  and  $1372\text{ cm}^{-1}$  (aromatic  $\text{C=C}$  and  $\text{C-C}$  ring stretching),  $1128\text{ cm}^{-1}$  ( $\text{C-C}$  deformation),  $1050\text{ cm}^{-1}$  ( $\text{C-H}$  in- plane bending deformation),  $883\text{ cm}^{-1}$  and  $830\text{ cm}^{-1}$  ( $\text{C-H}_\beta$  in- plane and out of plane bending),  $660\text{ cm}^{-1}$  ( $\text{C-S-C}$  stretching). Broadening of peaks in the spectra of CP of thiophene when compare to thiophene monomer indicate the formation of a polymeric material. Also, the spectrum of pure thiophene showed

the peak  $\alpha$ -CH out of plane bending at 832 and  $\alpha$ -CH stretching of the thiophene ring at 3107  $\text{cm}^{-1}$ , respectively. The analysis of the spectrum suggests  $\alpha$ - $\alpha'$  couplings of the thiophene rings. The intensity of the bands due to the  $\alpha$ -CH stretching of thiophene ring in the spectrum of Figure 3.3.1a is reduced in the spectrum of **CP** (Figure 3.3.2b). Two new bands related to C-H $_{\beta}$  out of plane bending of 2,5 disubstituted thiophene and C-S stretching appeared at 830 and 660  $\text{cm}^{-1}$ , respectively. Beside these indications, the broad conjugation band at 1640  $\text{cm}^{-1}$  implies not only the polymerization but also the conductivity [130]. **CP** synthesized with high concentration of KOH revealed the similar FTIR spectra of the **CP** synthesized with low concentration of KOH.

FTIR spectrum of the evolved gas collected in a glass cell during polymerization, exhibits the peak at 2450  $\text{cm}^{-1}$  ( $\text{CO}_2$ ) and 1270  $\text{cm}^{-1}$  (C=O stretching) (Figure 3.3.2c).

FTIR spectrum of **WP** of thiophene (Figure 3.3.3a) exhibited the peaks at 3067  $\text{cm}^{-1}$  (aromatic C-H stretching), 2938 and 2606  $\text{cm}^{-1}$  (aliphatic C-H stretching), 1623  $\text{cm}^{-1}$  (C=C stretching), 1395 and 1370  $\text{cm}^{-1}$  (C=C in-plane vibrations of thiophene ring), 1106  $\text{cm}^{-1}$  (C=S vibration), 1003  $\text{cm}^{-1}$  (C=S vibration or S=O stretching), 972  $\text{cm}^{-1}$  (C-H out of plane vibration), 830  $\text{cm}^{-1}$  (C-H $_{\beta}$  out of plane bending), 702  $\text{cm}^{-1}$  (C-H out of plane deformation), 662  $\text{cm}^{-1}$  (C-S-C stretching).

FTIR spectrum of **OP** of thiophene (Figure 3.3.3b) was revealing the peak positioned at 3017-2941  $\text{cm}^{-1}$  (C-H stretching), 1738  $\text{cm}^{-1}$  (C=O stretching), 1379  $\text{cm}^{-1}$  (C=C in plane vibration), 1230- 1206  $\text{cm}^{-1}$  (C-O-C stretching), 1124  $\text{cm}^{-1}$  (C-O stretching or C=S vibration), 995  $\text{cm}^{-1}$  (C-H out of plane vibration), 879-854  $\text{cm}^{-1}$  (C-H out of plane deformation), 670  $\text{cm}^{-1}$  (C-S-C stretching).

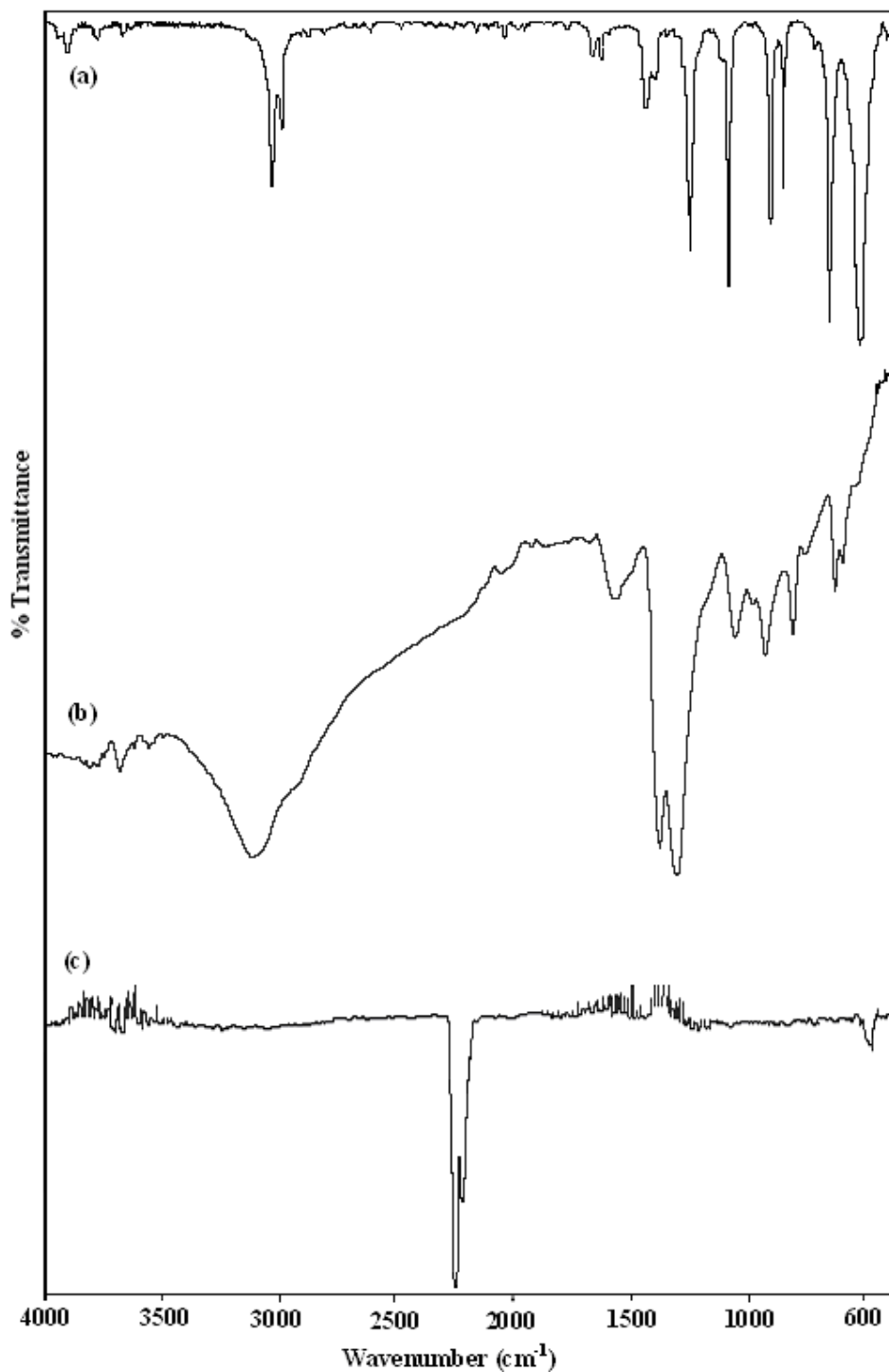


**Figure 3.3.2** FTIR spectra of (a) Thiophene, (b) **CP** (with low concentration of KOH) and (c) released gases during polymerization.

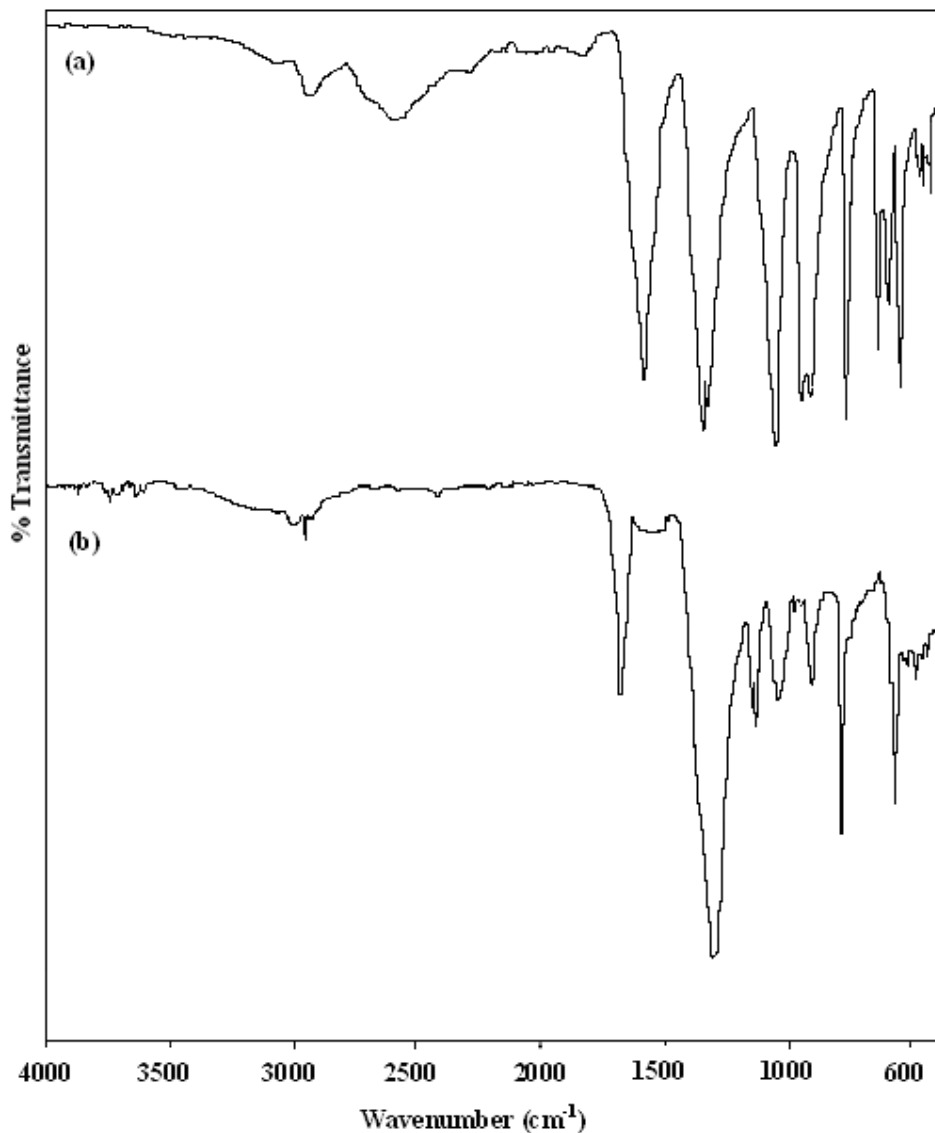
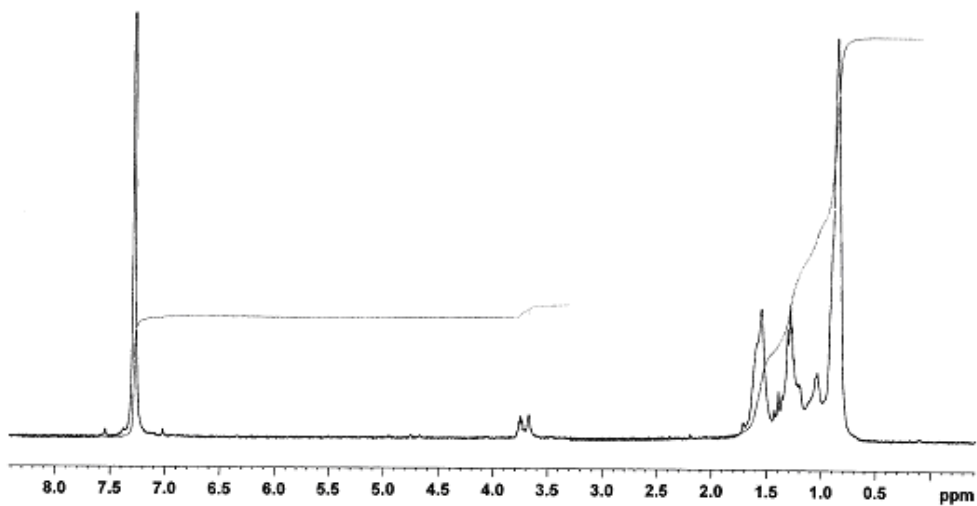


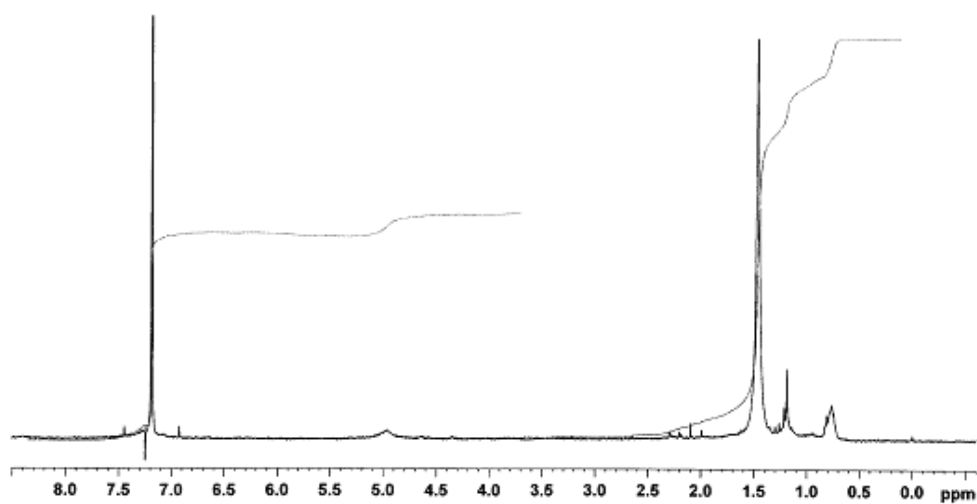
**Figure 3.3.3** FTIR spectra of (a) white polymer **WP** and (b) orange polymer **OP** of thiophene.

In the  $^1\text{H}$  NMR of **WP** and **OP** both aromatic and aliphatic peaks were observed indicating that in some part of both polymers thiophene ring opened during polymerization (Figure 3.3.4a and b). The peaks at 7.3 ppm indicated the aromatic thiophene rings in both **WP** and **OP**. However, the peaks at 3.7 ppm, 1.6 ppm, 1.3 ppm, 1 ppm, 0.8 ppm in  $^1\text{H}$  NMR of **WP** and the peaks at 1.5 ppm,

1.3 ppm, 0.7 ppm in  $^1\text{H}$  NMR of **OP** indicated the breakage of the thiophene ring in some part of the polymer.



(a)



(b)

**Figure 3.3.4** (a)  $^1\text{H}$  NMR of **WP** and (b)  $^1\text{H}$  NMR of **OP** of thiophene.

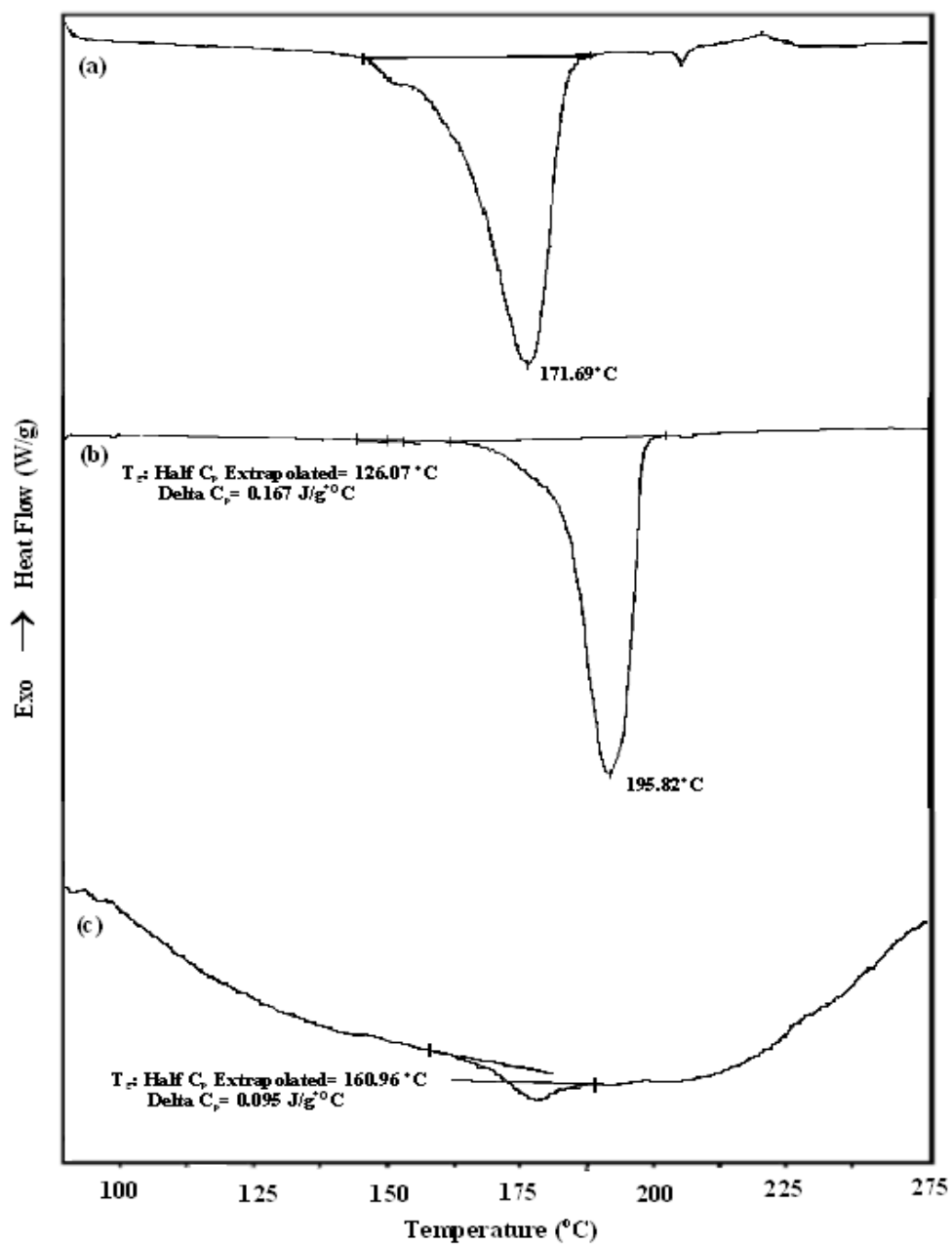


**Figure 3.3.5** DSC thermograms of (a) CP, (b) white polymer WP and (c) orange polymer OP of thiophene.

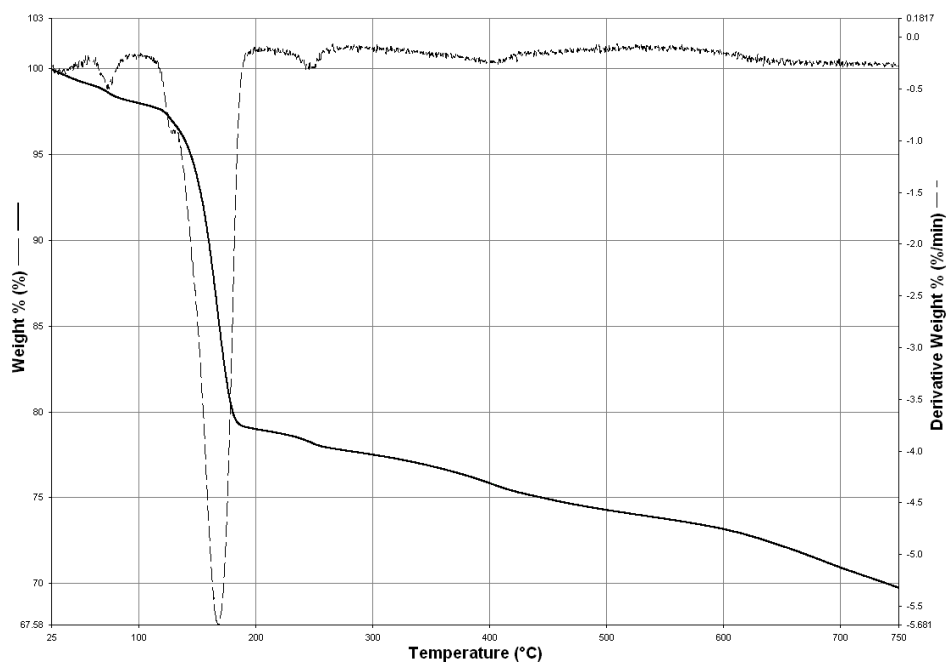
DSC thermograms of both **CP**, **WP** and **OP** of thiophene were examined in the range 30 °C to 275 °C at a heating rate of 10 °C/min (Figure 3.3.5). Glass transition ( $T_g$ ) was not observed in the DSC thermogram of **CP** as expected (Figure 3.3.5a) but a broad melting at 172 °C was observed. DSC thermogram of **WP** exhibited two thermal events; a glass transition ( $T_g$ ) at about 126 °C and a decomposition at about 196 °C (Figure 3.3.5b). The decomposition can be due to the decomposition of  $\text{KHCO}_3$  which is the byproduct of reaction. In the DSC thermogram of **OP** of thiophene (Figure 3.3.5c) a glass transition ( $T_g$ ) at about 161 °C was seen indicating high rigidity of polymer.

The TGA and DTG curves of **CP** of thiophene showed high thermal stability and still having residues of 69 % at 750 °C (Figures 3.3.6a). Small weight loss (3 %) observed up to 120 °C due to the trapped water coming from the solvent, followed by a sharp decrease (17%) in weight loss at 180 °C. The main degradation at this temperature was most probably because of side products produced during reaction.

TGA weight loss curve and the corresponding derivative curves (DTG) for **WP** of thiophene were shown in Figure 3.3.6b. No weight loss was observed for **WP** up to 185 °C and was stable up to 750 °C. In situ FTIR spectra of the evolved gases during the thermal gravimetric analysis indicated the evolution of  $\text{CO}_2$  and  $\text{H}_2\text{O}$  at 185 °C (Figures A.4a). 26% weight loss was observed at that temperature due to the decomposition of byproduct  $\text{KHCO}_3$  which gave  $\text{CO}_2$  and  $\text{H}_2\text{O}$ . **WP** still had residues of 72% beyond 750 °C.

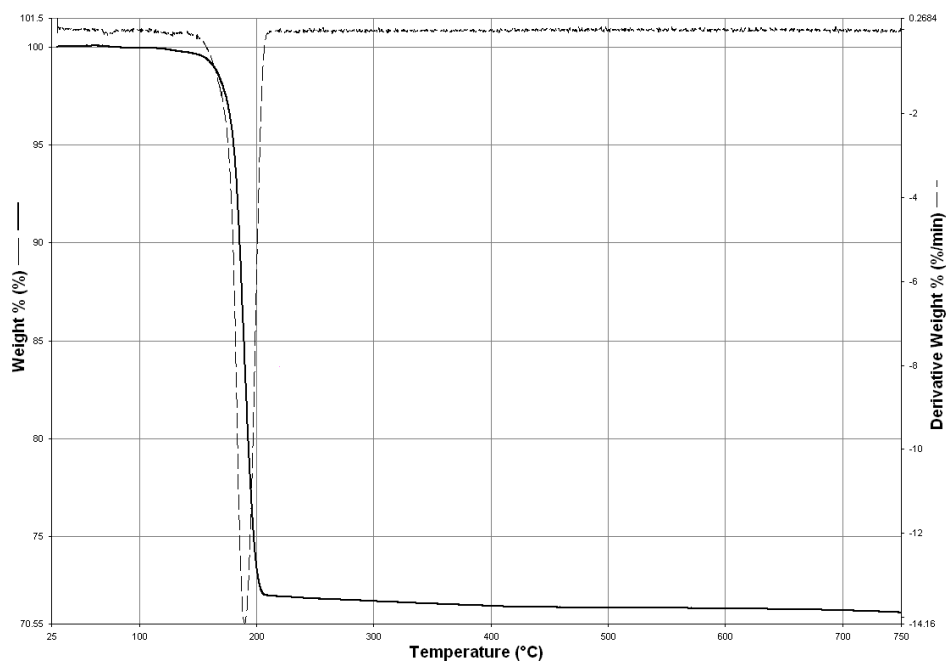
Small weight loss (3%) was observed for **OP** of thiophene at 100 °C and then a sharp loss of 15% around 185 °C and then followed by a 40 % lost when the temperature reached to 500 °C. Decomposition occurs in three stages with the small weight loss around 100 °C and 185 °C and main degradation around 450 °C (Figure 3.3.6c). In the beginning stage of degradation, trapped water was lost. In the second stage of degradation showed characteristic peaks of  $\text{CO}_2$  (2358 and 2309  $\text{cm}^{-1}$ ) (Figures A.5a) which was again due to the decomposition of  $\text{KHCO}_3$ .

Finally beyond 450 °C, the decomposition of polymeric matrix was observed. **OP** indicated a high thermal stability and still having residues of 55 % beyond 750 °C.

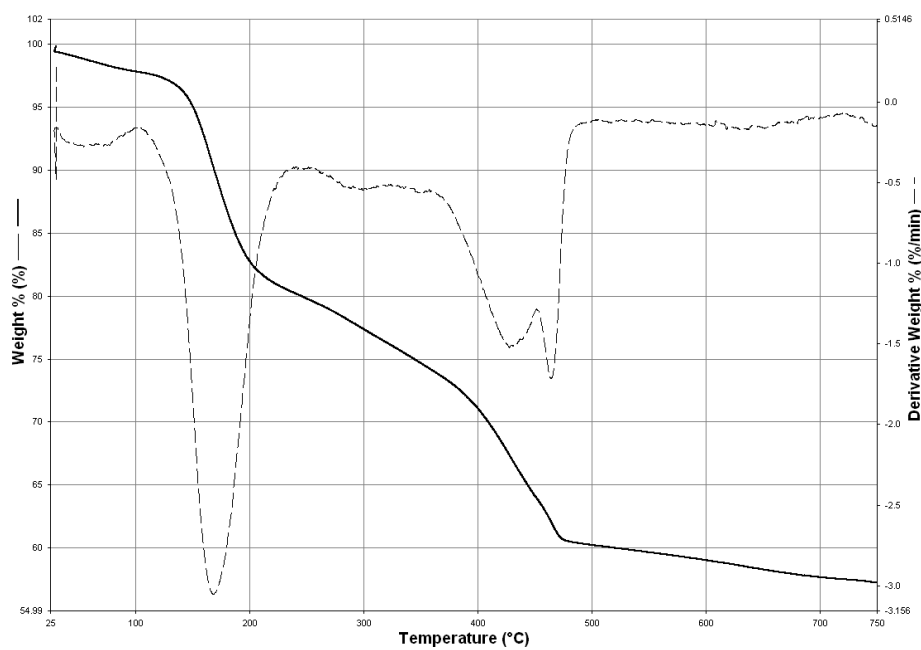


(a)

Figure 3.3.6 cont.



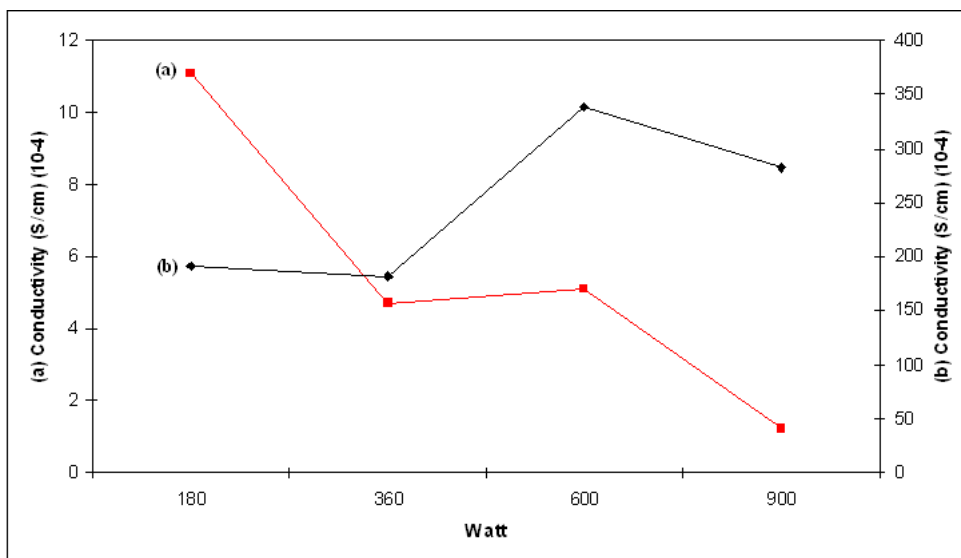
(b)



(c)

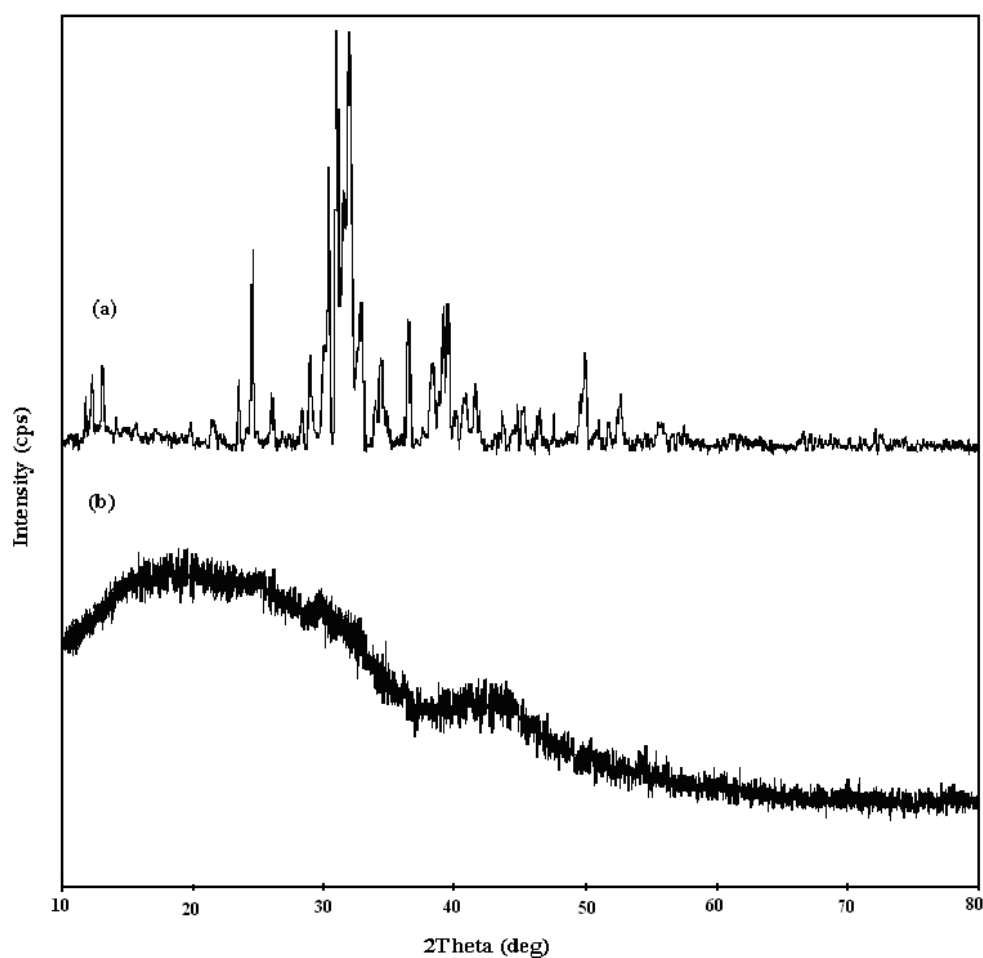
**Figure 3.3.6** TGA thermograms of (a) **CP**, (b) **WP** and (c) **OP** of thiophene.

Two and four probe conductivity measurements were performed on compacted disks of the polymers. The effect of energy on the electrical conductivities of unwashed **CP**s of thiophene was shown in Figure 3.3.7. At 90 watt no **CP** were observed for different amounts of KOH. The conductivities of unwashed **CP** synthesized with low concentration of KOH (Figure3.3.7a) in the range from 180 to 900 watts were measured as  $11.1 \times 10^{-4}$ ,  $4.7 \times 10^{-4}$ ,  $5.1 \times 10^{-4}$ ,  $1.2 \times 10^{-4}$  S/cm, respectively. As seen from the graph, the conductivities decrease as energy increase for **CP**. The conductivities of **CP** of thiophene synthesized with high concentration of KOH (Figure3.3.7b) were higher than the one synthesized with low concentration of KOH which could be due to the higher formation of byproduct,  $K_2S_5$ . The maximum conductivity was observed at 600 watt as  $3.4 \times 10^{-2}$  S/cm and as energy increased, conductivities increased. Always, conductivity of washed **CP** was lower than unwashed **CP**. **WP** and **OP** of thiophene showed no conductivity.



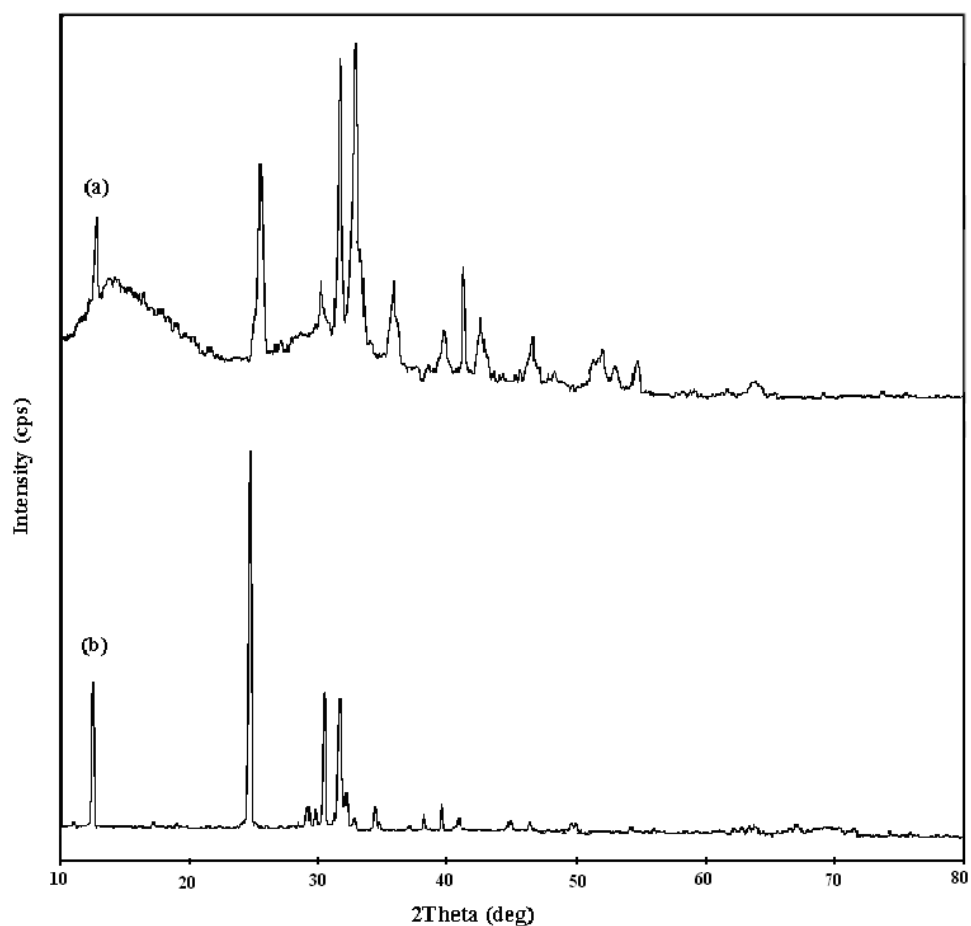
**Figure 3.3.7** The effect of energy on conductivity of **CP** of thiophene (a) **CP** (with low concentration of KOH) and (b) **CP** (with high concentration of KOH).

The powder X-ray diffraction pattern of the unwashed **CP** of thiophene indicated the presence of dipotassium pentasulfide ( $K_2S_5$ ) in the polymeric matrix. The diffraction peaks were in good agreement with those of  $K_2S_5$  crystals which could be indexed as the orthorhombic structure of  $K_2S_5$  (JCPDS card no 30-0993C) (Figure 3.3.8a). **CP** was washed with hot water in order to remove  $K_2S_5$  crystals trapped in the synthesized polymer. Then, a broad X-ray spectrum of polymer was observed indicated the presence of an amorphous polymer (Figure 3.3.8b).



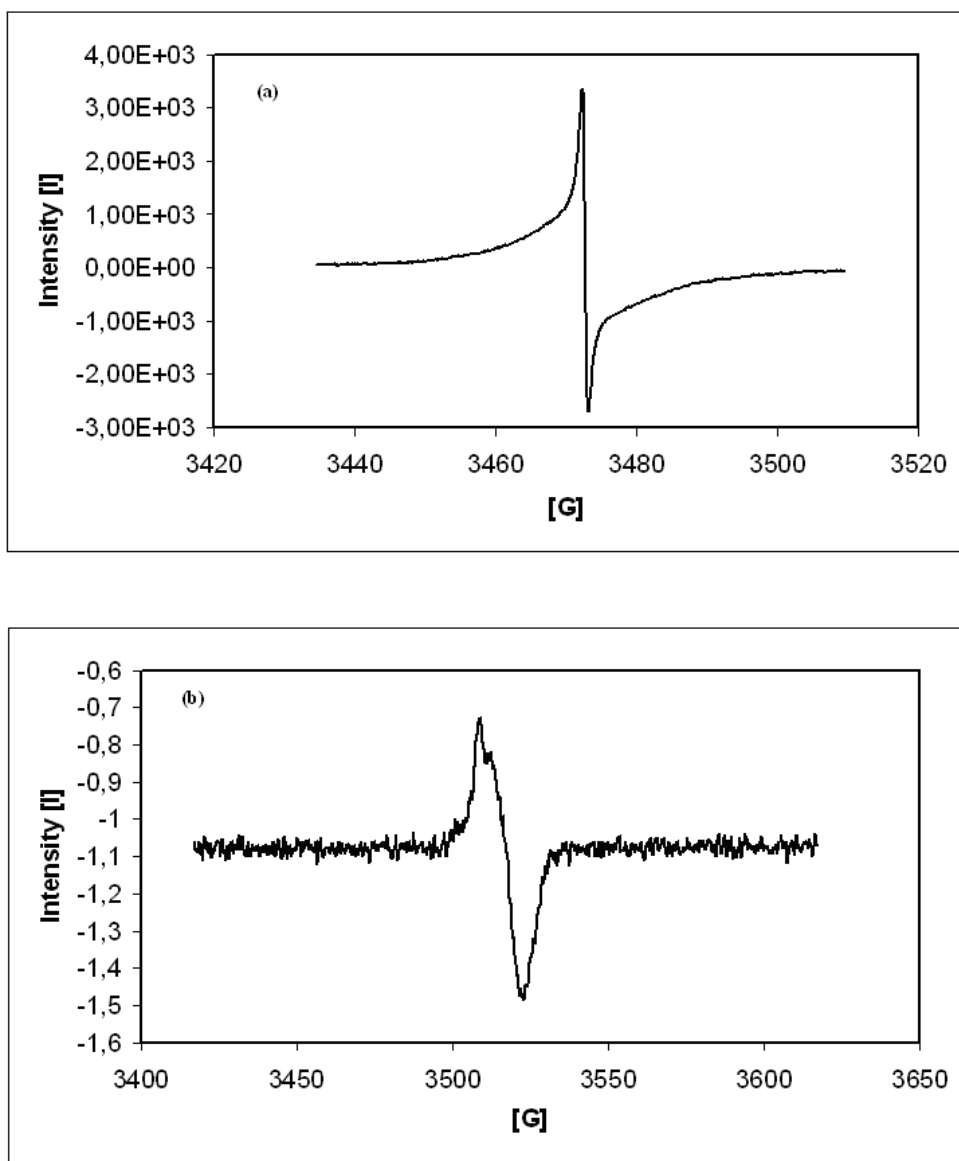
**Figure 3.3.8** X-ray powder diffraction spectra of (a) unwashed **CP** and (b) washed **CP** of thiophene.

Figure 3.3.9a showed the powder X-ray diffraction pattern of the unwashed **WP** of thiophene. Monoclinic structure of  $\text{KHCO}_3$  crystal was observed (JCPDS card no 70-1168A). For **OP** of thiophene, again the diffraction peaks were in good agreement with those of Kalicinite ( $\text{KHCO}_3$ ) crystals which could be indexed as the monoclinic structure of  $\text{KHCO}_3$  (JCPDS card no 12-0292N) (Figure 3.3.9b). **WP** and **OP** of thiophene were water soluble polymers so no washing was done.



**Figure 3.3.9** X-ray powder diffraction spectra of (a) unwashed **WP** and (b) unwashed **OP** of thiophene.

ESR spectra of **CP** and **OP** of thiophene revealed the signals with  $g$  values of 2.0035 and 2.00 respectively (Figure 3.3.10a and b) which were very close to  $g$  values of free electron (2.0023). No signal was observed in the ESR spectrum of **WP** of thiophene.



**Figure 3.3.10** ESR spectra of (a) **CP** and (b) **OP** at room temperature.

The surface morphologies of all type of polymers were analyzed by scanning electron microscope (Figure 3.3.11). The morphology of washed **CP** of thiophene presented a compact cauliflower-like structure (Figure 3.3.11a). The X-ray microanalysis system detected the existence of S and C on **CP** whereas K and O detected on the unwashed **CP** (Figure 3.3.11b). **WP** of thiophene showed a rod like structure formed on the edge of KOH paticules (Figure 3.3.11c and d). X-ray microanalysis indicated the presence of C, O and S on the rod but K was observed on the edges (Figure 3.3.11e and f). **OP** of thiophene had both fiberic (Figure 3.3.11g) and globular-like structures (Figure 3.3.11h).

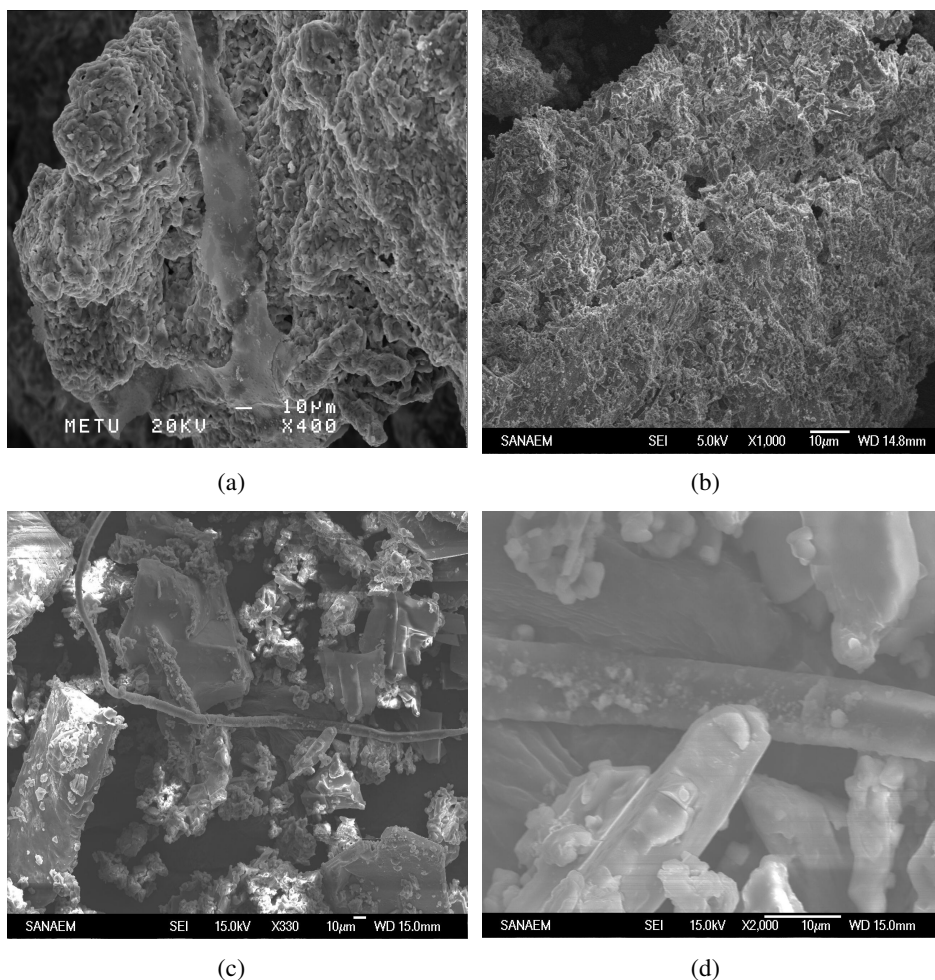
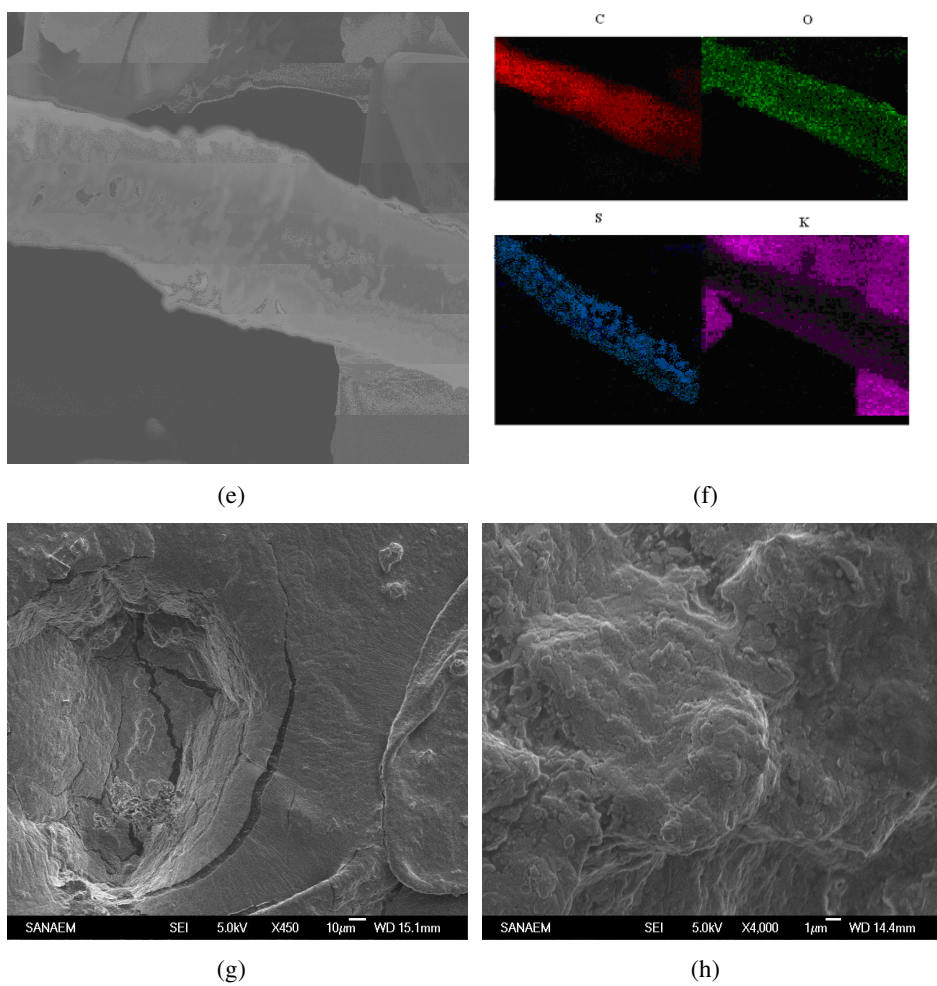


Figure3.3.11cont.



**Figure 3.3.11** SEM micrographs of (a) washed **CP**, (b) unwashed **CP**, (c) and (d) **WP**, (e) **WP**, (f) X-ray microanalysis of **WP**, (g) and (h) **OP** of thiophene.

## CHAPTER 4

### CONCLUSION

In this study, microwave-assisted syntheses of different type of polymers were achieved simultaneously from TCP, pyrrole, thiophene with KOH in a very short time interval for the first time. Polymers were achieved either at constant microwave energy with different time intervals (1 - 25 min) or at constant time intervals with different microwave energy (90-900 watt), in various water contents (0, 0.5, 5 ml) and in various concentrations of KOH ( $0.03$ ,  $0.05$ ,  $2 \times 10^{-4}$ ,  $6 \times 10^{-4}$  mol.) at constant time intervals and microwave energy.

In the synthesis of polymers from potassium 2,4,6-trichlorophenolate, conducting polymer **CP** and crosslinked polymer **CLP** were achieved in water and characterized by FTIR, TGA/ FTIR, DSC, SEM, ESR, UV-Vis, and X-ray diffraction analysis. Microwave-assisted polymerization was achieved very rapidly (1 to 5 min) compared to previously used electrochemical and chemical methods (3 to 48 hours). In addition, induction period for the polymerization was very short (less than 2 min at 90 watt and 1 min at higher watts) when compared to the syntheses in solution or in solid state. The effects of heating time, microwave energy and amount of water on polymer synthesis and on the % conversion were investigated. The optimum conditions for **CP** and **CLP** were 90 watt for 5 min in  $0.5 \text{ cm}^3$  water and 180 watt for 5 min in  $5 \text{ cm}^3$  water having maximum values 38.9 and 85.9% respectively.

In the synthesis of polymers from potassium hydroxide and pyrrole, conducting polymer **CP** and radical ion polymer **RIP** were achieved and characterized by FTIR, TGA/ FTIR, DSC, SEM, ESR, UV-VIS,  $^1\text{H-NMR}$ ,  $^{13}\text{C-NMR}$  and X-ray diffraction analysis. When the effects of amount of KOH, heating time,

microwave energy on the polymerization and on the % conversion examined, the optimum conditions for **CP** and **RIP** were observed at 360 watt with  $6 \times 10^{-4}$  mol KOH at the end of 8 min and at 90 watt with 0.03 mol. KOH at the end of 6 min. having maximum % conversion values of 47.0 % and 54.2 % respectively.

In the synthesis of polymers from potassium hydroxide and thiophene, conducting polymer **CP**, white polymer **WP** and orange polymer **OP** were achieved and characterized by FTIR, TGA/ FTIR, DSC, SEM, ESR,  $^1\text{H-NMR}$ , and X-ray diffraction analysis. The optimum conditions for **CP**, **WP** and **OP** were at 900 watt with 0.05 mol KOH at the end of 3 min., at 90 watt with 0.05 mol KOH at the end of 12 min. and at 90 watt with 0.05 mol KOH at the end of 15 min. having maximum % conversion values of 43.3 %, 28.9% and 32.5% respectively.

In the previous studies of the polymerization of sodium trichlorophenolate and potassium tribromophenolate simultaneous synthesis of poly (dichlorophenylene oxide), CP and poly (dibromophenylene oxide), orange-colored radical ion polymer (RIP) and CP were achieved respectively by microwave initiation [100, 121]. In the present study, poly(dichlorophenylene oxide) was not synthesized but regioselectively synthesis of **CP** and white insoluble **CLP** were achieved for the first time. The effects of monomer (TBP or TCP) and metal-hydroxides (NaOH or KOH) on polymer synthesis and on the optimum % conversion were;

- Percent conversions of **CP** are:

TCP- NaOH > TCP-KOH > TBP-KOH

- Conductivities of unwashed **CP** are:

TBP- KOH > TCP-NaOH > TCP-KOH

For the first time, microwave-assisted synthesis of conducting polypyrrole **CP** and **RIP** was achieved from KOH and pyrrole. **RIP**, an intermediate step for the

synthesis of conducting polypyrrole, was isolated and characterized in solid state for the first time.  $^{13}\text{C}$ -NMR results indicated that the polypyrrole have predominantly  $\alpha$ - $\alpha'$  bonding but in some part of the ring there were  $\alpha$ - $\beta$  linkages. The presence of peaks at 117 and 108 ppm indicated that there were still unreacted pyrrole monomers in the polymeric matrix and polymerization would be continued. In the mass spectrum, the peaks at  $m/z = 67$  Da and  $m/z = 132$  Da indicated the presence of pyrrole monomer and dimer, respectively in the structure of **RIP**. In UV-Vis spectrum, evolution of new broad band around 470 nm, related to  $\pi$ - $\pi^*$  transition, formation of polarons. Formation of bipolaron was not observed.

For the first time, microwave-assisted synthesis of conducting polythiophene **CP**, **WP** and **OP** were achieved from KOH and thiophene. The analysis of the FTIR spectra suggests that  $\alpha$ - $\alpha'$  coupling of thiophene rings in conducting polythiophene. High Tg value of **WP** (Mw: 985) and **OP** indicated high rigidity.

The direct syntheses of highly conducting polymers were achieved in the absence of applied doping process in a very short time sequence with microwave-assisted polymerization.

- The order of decreasing conductivity values of **CP** are:

Pyrrole- KOH > Thiophene-KOH > TCP-KOH.

The powder diffraction X-ray spectra of unwashed **CPs** contained always peaks of by products ( $\text{KCl}$ ,  $\text{KHCO}_3$  and  $\text{K}_2\text{S}_5$ ) and washed **CPs**, having a broad line, indicating amorphous polymers.

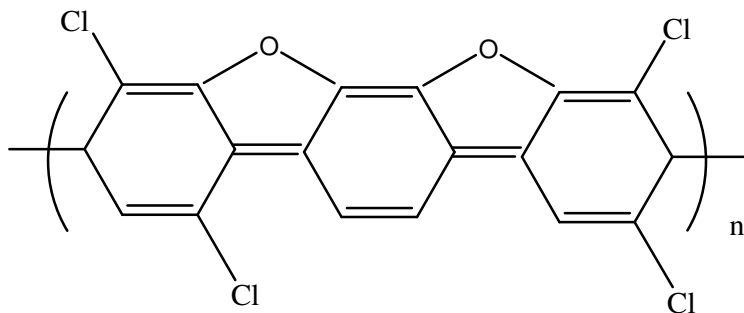
ESR spectrum of **RIP**, **CLP**, **CP** and **OP** products were revealed the signals very close to g values of free electron.

Analysis of the surface morphologies of all polymer types indicated sponge like (**CP**-TCP), cauliflower like (**CP**-Py, **CP**-Th), flake or needle like (**CLP**-TCP),

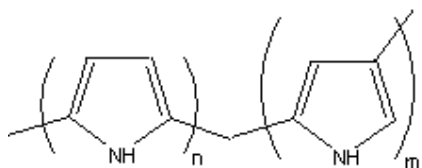
hexagonal (**RIP-Py**), rod like (**WP-Th**) and fibrillar or globular (**OP-Th**) structures.

The proposed structures for CPs are:

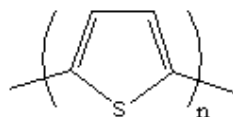
**CP (TCP)**



**CP (Py)**



**CP (Th)**



## REFERENCES

- [1] Skotheim, T.A., Handbook of Conducting Polymers, Marcel Dekker: New York, 1986.
- [2] Doblhofer, K. and Rajeshwar, K, Handbook of Conducting Polymers. eds Skotheim, T.A., Elsenbaumer, R.A and Reynolds, J.R., New York: Marcel Dekker, 1998. Ch 20
- [3] Shirakawa, H., Louis, E.J., Heeger, A.J. and Chiang, C.K., J. Chem. Soc., Chem. Commun., 578, 1977.
- [4] Skotheim, T.A., Elsenbaumer, R.L. and Reynolds, J.R., Handbook of Conducting Polymers, Marcel Dekker: New York, 1998.
- [5] Chen, S. A. and Tsai, C. C., Macromolecules, 26, 2234, 1993.
- [6] Wei, Y., Tian, J., MacDiarmid, A. D., Masters, J. G., Smith, A. L. and Li, D., J. Chem Soc. Commun., 7, 552, 1994.
- [7] Beadle, P., Armes, S.P., Gottesfeld, S., Mombourquette, C., Houlton, R., Adwers, W. D. and Agrew, S. F., Macromolecules, 25, 2526, 1992
- [8] Somanathan, N. and Wegner, G., Ind. J. Chem., 33A, 572, 1994.
- [9] Malhotra, B. D., Ghosh, S. and Chandra, R., J. Appl. Polym. Sci., 40,1049, 1990.
- [10] Negler, B. R., Laxmeshwar N. B. and Santhanam, K. S. V., Ind. J. Chem., 33A, 547, 1994.
- [11] Annapoorni, S., Sundaresan, N. S., Pandey, S. S. and Malhotra, B. D., J. Appl. Phys., 74,2109, 1993.
- [12] Kumar, D. and Sharma, R.C., Eur.Polym. J., 34, 1053, 1998.
- [13] Caddick, S., Tetrahedron, 51, 10403, 1995.
- [14] Shaktawat, V., Jain, N., Saxena, R., Saxena, N. S., Sharma, K. and Sharma, T. P., Polm. Bull., 57, 535, 2006.
- [15] Wessling, B., Chem Innovation, 31, 34, 2001.
- [16] Galal, A., Atta, N. F. and Mark, H. B., ACS Symposium Series, 690, 210, 1998.

- [17] Kaiser, A. B., *Adv. Mater.*, 13, 927, 2001.
- [18] Bredas, J. L., Chance, R. R. and Silbey, R., *Phys. Rev., Part B*, B26(10), 5843, 1982.
- [19] Tourillon, G. , Gourier, D., Garnier, P. and Vivien, D. , *J. Phy. Chem.*, 88, 1049, 1984.
- [20] Chiang, C. K., Fincher, Jr. C. R., Park, Y. W. , Heeger, A. J. , Shirakawa, H., Louis, E. J. and MacDiarmid, A. G., *Phys. Rev. Lett.* 39, 1098, 1977.
- [21] Kanatzidis, M. G., *Chem. Eng. News*, 68(49), 36, 1990.
- [22] Ziemelis, K. E. , Hussain, A. T. , Bradley, D. D. C. , Friend, R. H. , Rilhe, J. and Wegner, G., *Phys. Rev. Lett.*, 66, 2231, 1991.
- [23] Mort, N.F., Davis, E.A., *Electronic Processes in Non-Crystalline Materials*, Clarendon Press, Oxford, 1979.
- [24] Rodriguez, J., Grande H. J. and Otero T.F., *Handbook of Organic Conductive Molecules and Polymers*, John Wiley & Sons, 2, 415, 1997.
- [25] Vidal, J.C., Garcia, E. and Castillo, J.R., *Anal. Chim. Acta*, 385 1-3, 213, 1999.
- [26] Kincal, D., Kamer, A., Child, A.D. and Reynold, J.R., *Synth. Met.*, 92, 53, 1998.
- [27] Jerome, C., Labaye, D., Bodart, I. and Jerome, R., *Synth. Met.*, 3, 101, 1999.
- [28] Smela, E., *J. Micromech. Microeng.* 9, 1, 1999.
- [29] Yang, S.C., Liu, H. and Clark, R.L., *PCT Int. Appl. WO 99 22,380(CI.H01 B1/00)*.
- [30] Takamatsu, T. and Taketani, Y., *Jpn. Kokai. Tokyo Koho JP11 121, 279[99 121, 279]*
- [31] Wang L., Li X. and Yang Y., *Reac. and Funct. Polym.*, 47, 125, 2001.
- [32] Oh, E.J., Jang, K.S. and MacDiarmid, A.G., *Synth. Met.* 125, 297, 2002.
- [33] Salmon, M., Kanazawa, K., Diaz, A. F. and Krounbi, M., *J. Polym. Lett.*, 22, 187, 1982.
- [34] Henry, M.C., Hsueh, C.C., Timko, B.P. and Freunda, M.S. *J. Electrochem.Soc.* 148, 155, 2001.

- [35] Kanazawa, K., Diaz, A. F., Gill, W. D., Grant, P. M., Street, G. B. and Gadrini, G. P., *Synth. Met.*, 1, 329, 1980.
- [36] Genies, E. M., Bidan, G. and Diaz, A. F., *J. Electroanal. Chem.*, 149, 101 1983.
- [37] Jones, S. "Polypyrroles," in *Encyclopedia of Polymer Science and Engineering*, 13, 42, Wiley, New York 1988.
- [38] Armes, S. P., *Synth. Met.*, 20, 365, 1987.
- [39] Ayad, M. M., *Polym Int.*, 35, 35, 1994.
- [40] Przulski, J., Zagorska, M., Pron, A., Kucharski, Z. and Suwalski, J., *J. Phys. Chem Solids*, 48, 635, 1987.
- [41] Ayad, M. M., *J. Polym. Sci.: Polym. Chem.*, 32, 9, 1994.
- [42] Chen, X., Devaux, J., Issi, J. P. and Billaud, D., *Polym. Eng. Sci.*, 35, 642, 1995.
- [43] Walker, J. A., Warren, L. F. and Witucki, E. F., *J. Polym. Sci: Polym. Chem*, 26, 1285, 1988.
- [44] Machida, S., Miyata, S. and Techagumpuch, A., *Synth. Met.*, 31, 311, 1989.
- [45] Chan, H. S. O., Hor, T. S. A., Ho, P. K. H., Tan, K. L. and Tan, B. T. G., *J. Macromol. Sci. Chem*, A27, 1081, 1990.
- [46] Nakata, M., Taga, M. and Kise, H., *Polym. J.*, 24, 437, 1992.
- [47] Bhattacharya, A. and De, A., *J.M.S. Rev. Macromol. Chem. Phys.* C39 (1), 17, 1999.
- [48] Audebert, P., Aldebert, P. and Girault, N., *Synth. Met.* 58, 251, 1993.
- [49] Gardini, G. P., *Advances in Heterocyclic Chemistry*. 15, 67, 1973.
- [50] Reynolds, J. R., *Chem. Tech.*, 8, 440, 1988.
- [51] Kuwabata, S., Okamoto, K. and Yoneyama, H., *J. Chem. Soc., Faraday Trans. 1- 84*, 2317, 1988.
- [52] Kim, D.Y., Lee, J.Y., Kim, C.Y., Kang, E.T. and Tan, K.L., *Synth. Met.*, 69, 501, 1995.
- [53] Takeoka, S., Hara, T., Yamamoto, K. and Tsuchida, E., *Chem. Lett.*, 253 1996.

- [54] Ansari, R. and Wallace, G.G., *Polymer*, 35, 2372, 1994.
- [55] Singh, R., Narula, A.K., Tandon, R.P., Rao, S.U.M., Panwar, V.S., Mansingh, A. and Chandra, S., *Synth. Met.* 79, 1, 1996.
- [56] Aeiyaich, S., Zaid, B. and Lacaze, P.C., *Electrochim. Acta*, 44-17, 2889, 1999.
- [57] Meyer, V. *Chem. Ber.*, 16, 1465, 1883.
- [58] Meisel, S. L., Johnson, G. C. and Hartough, H. D., *Am. Chem. Soc.*, 72, 1910, 1950.
- [59] Yamamoto, T., Sanechika, K. and Yamamoto, A, *Polym. Sci., Polym. Lett. Ed.*, 18, 9, 1980.
- [60] Lin, J. W.P. and Dudek, L., P. J. *Polym. Sci., Polym. Chem. Ed.*, 18, 2869, 1980.
- [61] Yamamoto, T., Morita, A., Maruyama, T., Zhou, Z. H., Kanbara, T. and Saneckika, K., *Polym. J. (Tokyo)*, 22, 187, 1990.
- [62] Hotz, C. Z., Kovacic, P. and Khoury, I. A., *J. Polym. Sci., Polym. Chem. Ed.*, 21, 2617, 1983.
- [63] Kobayashi, M., Chen, J., Chung, T. C., Moraes, F., Heeger, A. J. and Wudl, F., *Synth. Met.*, 9, 77, 1984.
- [64] Yamamoto, T., Osakada, K., Wakabayashi, T. and Yamamoto, A., *Makromol. Chem., Rapid Commun.*, 6, 671, 1985.
- [65] Yamamoto, T., Morita, A., Miyazaki, Y., Maruyama, T., Wakayama, H., Zhou, Z.H., Nakamura, Y., Kanbara, T., Sasaki. S. and Kubota, K. *Macromolecules*, 25, 1214, 1992.
- [66] McCullough, R. D., Williams, S. P. and Jayaraman, M., *Polym. Prepr., Am. Chem. Soc., Div. Polym.Chem.*, 35, 190, 1994.
- [67] KoBmehl, G. and Chatzitheodorou, G., *Makromol. Chem., Rapid Commun.*, 2, 551, 1981.
- [68] Sugimoto, R., Takeda, S., Gu, H. B. and Yoshino, K., *Chem. Express*, 1, 635, 1986.
- [69] Leclerc, M., Diaz, F. M. and Wegner, G., *Makromol. Chem.*, 190, 3105, 1989.

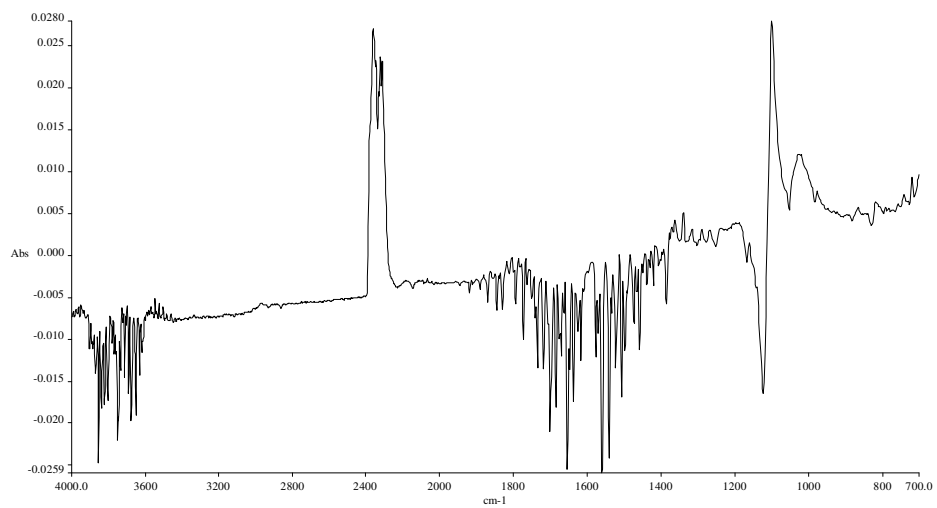
- [70] Leclerc, M. and Daoust, G., *Chem. Soc., Chem. Commun.*, 273, 1990.
- [71] Ikenoue, Y., Saida, Y., Kira, M., Tomozawa, H., Yashima, H. and Kobayashi, M., *J. Chem. Soc., Chem. Commun.*, 1694, 1990.
- [72] Yoshino, K., Hayashi, S. and Sugimoto, R., *Jpn. J. Appl. Phys.*, 23, L899, 1984.
- [73] Berlin, A., Pagani, G. A. and Sannicolo, F., *J. Chem. Soc., Chem. Commun.*, 1663, 1986.
- [74] Enzel, P. and Bein, T., *J. Chem. Soc., Chem. Commun.*, 1326, 1989.
- [75] Diaz, A. *Chem. Scr.*, 17, 145, 1981.
- [76] Roncali, J. *Chem. Rev.*, 92, 71, 1992.
- [77] Tourillon, G. and Gamier, F., *Electroanal. Chem.*, 135, 173, 1982.
- [78] Kaneto, K., Kohno, Y., Yoshino, K. and Inuishi, Y., *J. Chem. Soc., Chem. Commun.*, 382, 1983.
- [79] Yasser, A., Roncali, J. and Gamier, F., *Macromolecules*, 22, 804, 1989.
- [80] Sato, M., Tanaka, S. and Kaeriyama, K., *J. Chem. Soc., Chem. Commun.*, 713, 1985.
- [81] Hotta, S., Rughooputh, S. D. D. V., Heeger, A. J. and Wudl, F. *Macromolecules*, 20, 212, 1987.
- [82] Herman, F.M., Norman, G. G. and Norbert, M. B., *Encyclopedia of Polymer Science and Technology*, John Wiley and Sons, Vol. 10, 1969.
- [83] Solomons Graham, T. W., *Organic Chemistry*, John Wiley and Sons, 5 Ed., 937, 1992.
- [84] Salamone, J. C., *Polymeric Materials Encyclopedia*, CRC Press, Vol. 8, 5731, 1996.
- [85] Vogt, L. H. Jr., Wirth, J. G. and Finkbeiner, H. L., *Org. Chem.*, 34(2), 273, 1969.
- [86] Concise, *Encyclopedia of Polymer Science and Engineering*, John Wiley And Sons, 870, 1068, 1990.
- [87] Blanchard, H. S., Finkbeiner, H. L. and Russell, G. A., *J. Polym. Sci.*, 58, 469, 1962.

- [88] Hunter, W. H., Olson, A. O. and Daniels, E. A., J. Am. Chem. Soc., 38, 1761, 1916.
- [89] Hunter, W. H. and Joyce, F. E., J. Am. Chem. Soc., 39, 2640, 1917.
- [90] Hunter, W. H. and Seyfried, L. M., J. Am. Chem. Soc., 43, 151, 1921.
- [91] Hunter, W. H. and Dahlen, M. A., J. Am. Chem. Soc., 54, 2456, 1932.
- [92] Staffin, G. D., Price, C. C., J. Am. Chem. Soc., 82, 3632, 1960.
- [93] Hay, A.S., J. Polym. Sci. 58, 581, 1962.
- [94] Harrod, J.F., Can. J. Chem., 47 (4), 637, 1969.
- [95] Harrod, J.F., Carr, B.G. and Van Gheluwe, P., Macromolecules, 6, 498, 1973.
- [96] Türker, L., Kısakürek, D., Şen, Ş., Toppare, L. and Akbulut, U., J. Polym. Sci. Phys. Ed., 26, 2485, 1988.
- [97] Saçak, M., Akbulut, U., Kısakürk, D., Türker and L., Toppare, L., J. Polym. Sci. Chem. Ed., 27, 1599, 1989.
- [98] Kısakürek, D., Aras, L. and Şanlı, O., J. Pure and Appl. Sci. 23(2), 49, 1990.
- [99] Kısakürek, D., Şen, Ş., Aras, L., Türker, L. and Toppare, L., Polymer, 32 (7), 1323, 1991.
- [100] Çakmak, O., Baştürkmen, M. and Kısakürek, D., Polymer 45, 5451, 2004.
- [101] Çelik, B.G. and Kısakürek, D., J. Appl. Polym. Sci., 102, 5427, 2006.
- [102] Çelik, B.G. and Kısakürek, D., Designed Monomers and Polymers, in press.
- [103] Walker, K.A., Markoski, L.J., Deete, G.A., Spilman, G.E., Martin, D.C. and Jeffrey S. Moore, J.S., Polymer, 35, 5012, 1994.
- [104] Dusek, K. and M. Duskova, M., Prog. Polym. Sci., 25, 1215, 2000.
- [105] Dusek, K., Network formation. In: Meijer HEH, editor. Processing of Polymers, Material Science and Technology, vol. 13. Weinheim: Verlag Chemie, 401, 1997.
- [106] Wiesbrack, F., Hoogenboom, R. and Schubert, U. S., Macromol. Rapid Commun., 25, 1739, 2004.
- [107] Parodi, F., Physical and chemistry of microwave processing, in Comprehensive Polymer Science: The Synthesis, Characterization, Reactions

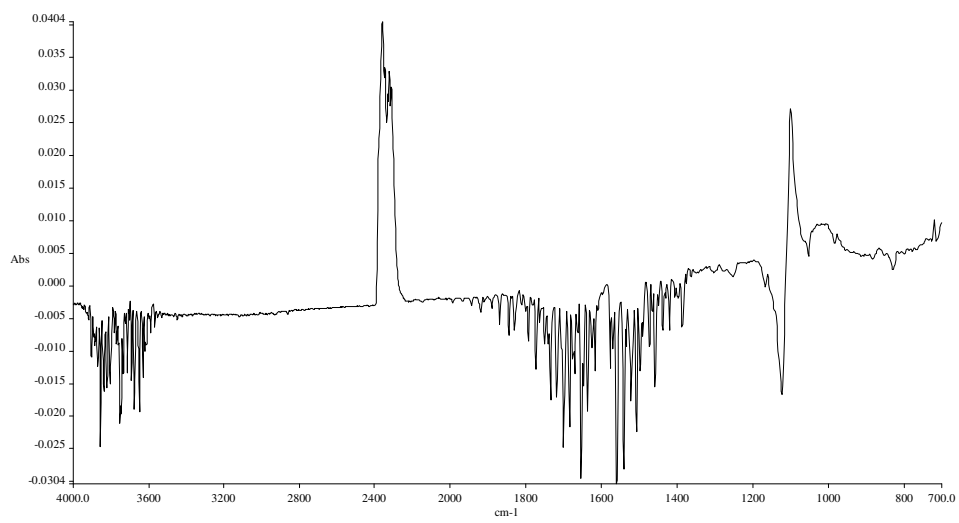
- and Applications of Polymers, Allen G. and Bevington J. C., New York: Pergamon, 2, 669, 1996.
- [108] Boey, F. Y. C., Gosling, I. and Lye, S. W., Processing problems and solutions for an industrial automated microwave curing system for a thermoset composite, Proc. 9th Intern. Conf. Composite Materials, Madrid, 651, 1993.
- [109] Hayes, B. L., Microwave synthesis: Chemistry at the speed of light, CEM Publishing, Matthews, 2002.
- [110] Kappe, C. O., Angew. Chem. Int. Ed., 43, 6250, 2004.
- [111] A. de la Hoz et al., Chem. Soc. Rev., 34,164, 2005.
- [112] Bogdał, D., Penczek, P., Pielichowski, J. and Prociak, A., Microwave Assisted Synthesis, Crosslinking, and Processing of Polymeric Materials, Adv. Polym. Sci. 163, 193, 2003.
- [113] Chabinsky, I. J., The practice of Microwave Preheating Rubber Prep Stocks in Compression and Transfer Molding Operations, 34-36, 188,1983.
- [114] Teffal M. and Gourdenne, A., Eur Polym J,19, 543, 1983.
- [115] Fang, X., Simone, C.D., Vaccaro, E., Huang, S.J. and Scola D.A, J. Polym. Sci. A: Polym Chem, 40, 2264, 2002.
- [116] Hong, U.H., Wei , J., Dhulipala, R. and Howley, M.C., Chem. Trans.,21,587, 1991.
- [117] Pourjavadi, A., Zamanlu, M. R. and Zohurian-Mehr, M.J., Angew. Makromol. Chem., 269, 54, 1999.
- [118] Lewis, D. A., Summers, J. D., Ward, T. C. and McGrath, J. E., J. Polym. Sci. A: Polym Chem, 30, 1647, 1992.
- [119] Mijovic, J. and Wijaya, J., Polym. Compos., 11, 184, 1990.
- [120] Silinski, B., Kuzmycz, C. and Gourdenne, A., Eur. Polym. J., 23, 273, 1987.
- [121] Çelik, B.G. and Kısakürek, D., Synth. Met., in press
- [122] Mathys, G.I. and Truong, V. T., Synth. Met., 89,103, 1997.
- [123] Lei, J., Cai, Z. and Martin, C. R., Synth. Met., 46, 53, 1992.
- [124] Kang, H. R. and Jo, N. J., High Per. Poly., 18,665,2006.

- [125] Yan, F., Xue, G. and Zhou, M., *J. Appl. Polymer Sci.*, 77, 135, 2000.
- [126] Jones, R.A and Bean, G. P., *Chemistry of Pyrroles*, Academic Press, Inc., New York, 1977, Ch.11.
- [127] Clarke, T. C., Scott, J. C. and Street, G. B., *J. Res. Develop.*, 27-4, 313, 1983.
- [128] Uyar, T., Toppare, L. and Hacaloğlu, J., *Synth. Met.*, 123, 335, 2001.
- [129] Uyar, T., Toppare, L. and Hacaloğlu, J., *Synth. Met.*, 119, 307, 2001.
- [130] Yagcı, Y., Yılmaz, F., Kıralp, S. and Toppare, L., *Macromol. Chem. Phys.*, 206, 1178, 2005.

## APPENDIX

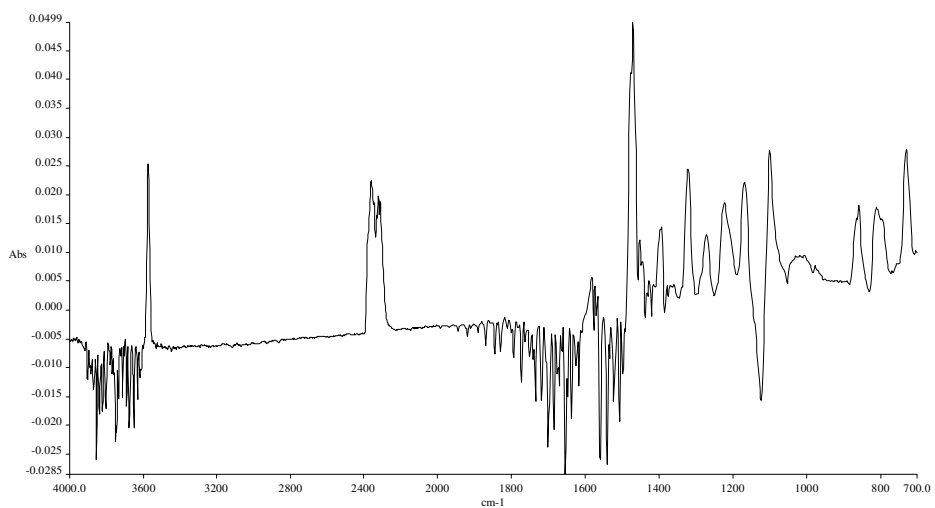


(a)

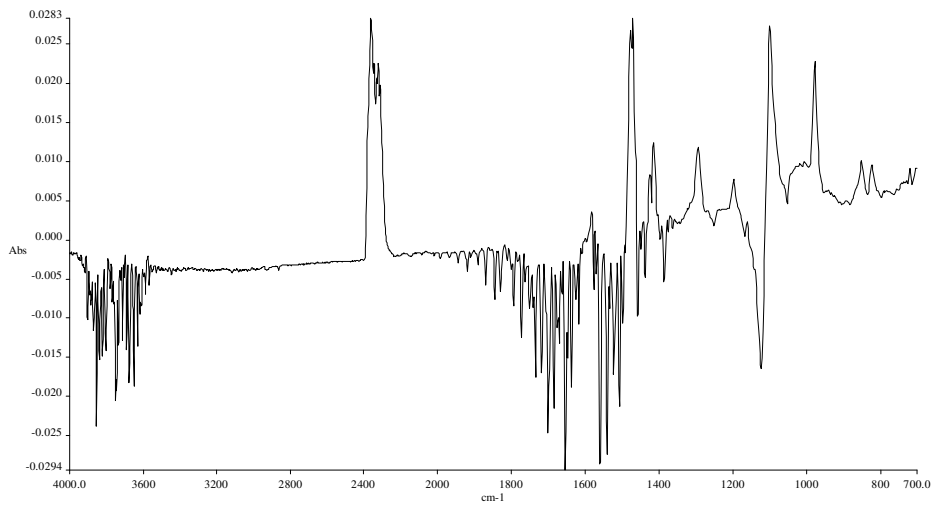


(b)

Figure A.1 cont.

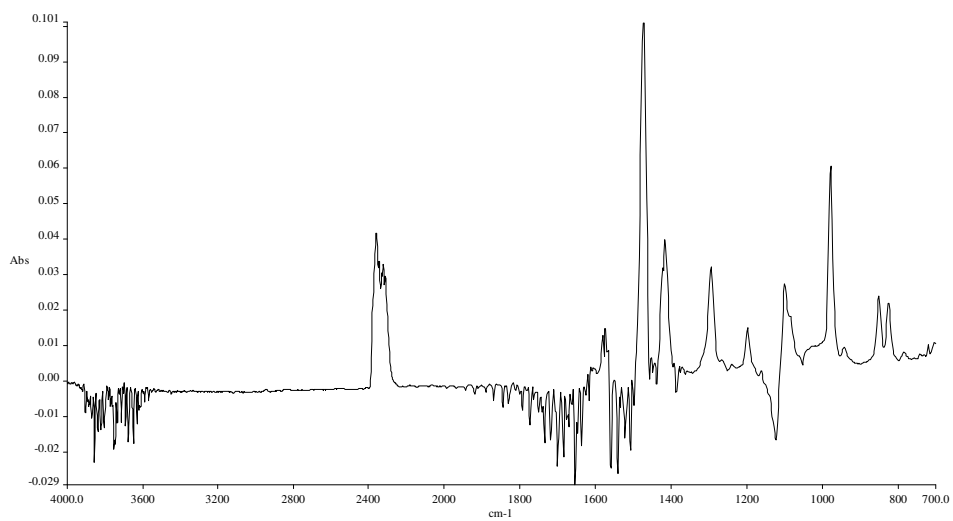


(c)

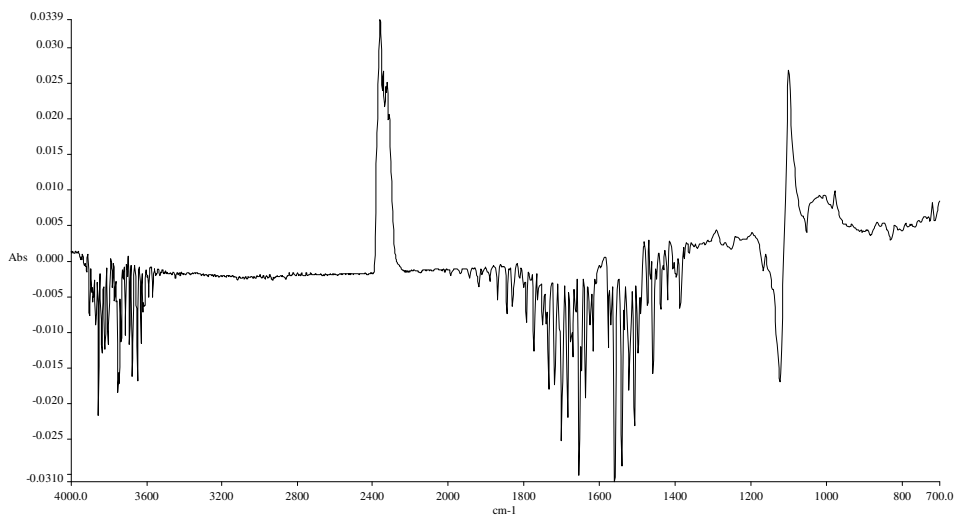


(d)

Figure A.1 cont.

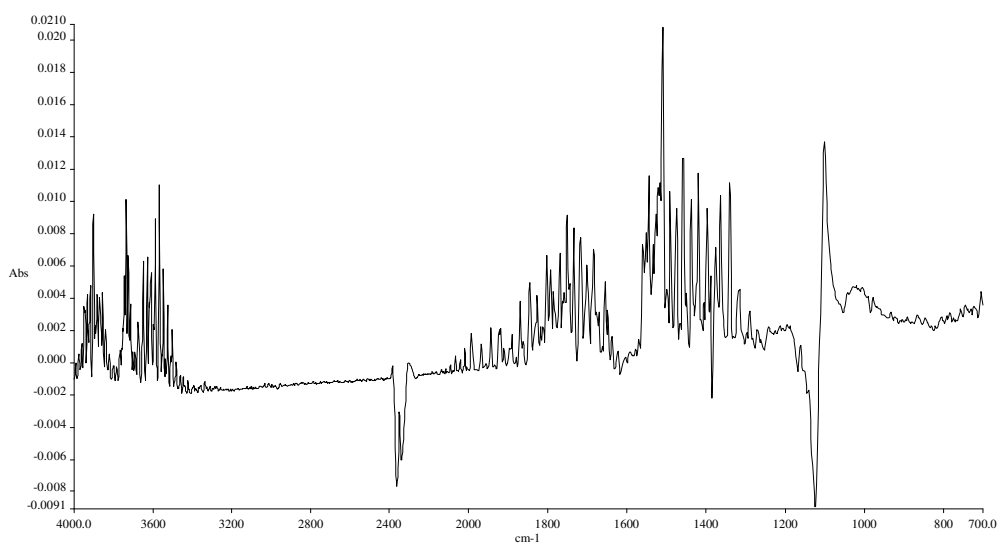


(e)

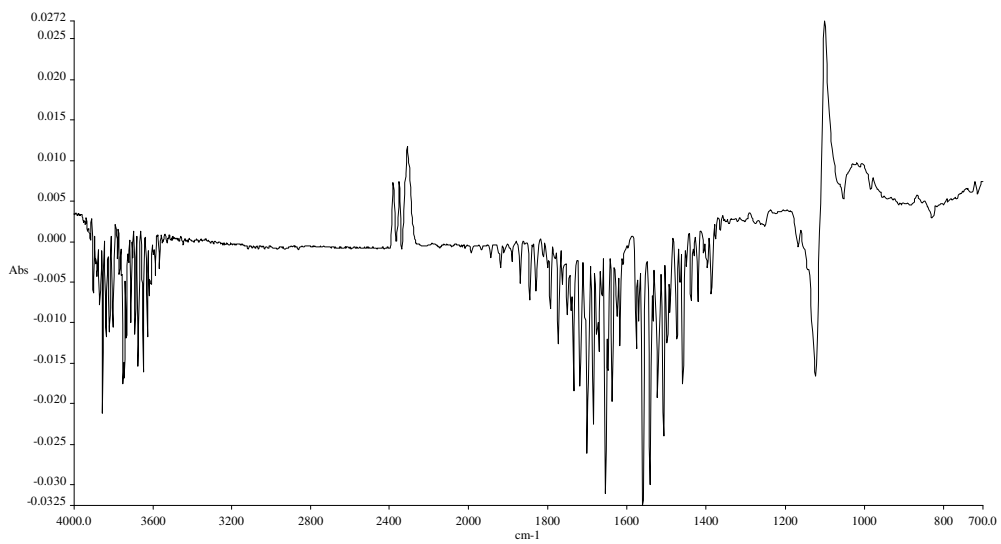


(f)

**Figure A 1.** In situ FTIR spectrum of evolved volatile components during TGA of CP synthesized from potassium 2,4,6-trichlorophenolate at (a) 31 °C (b) 166 °C (c) 360 °C (d) 453 °C (e) 562 °C (f) 795 °C.

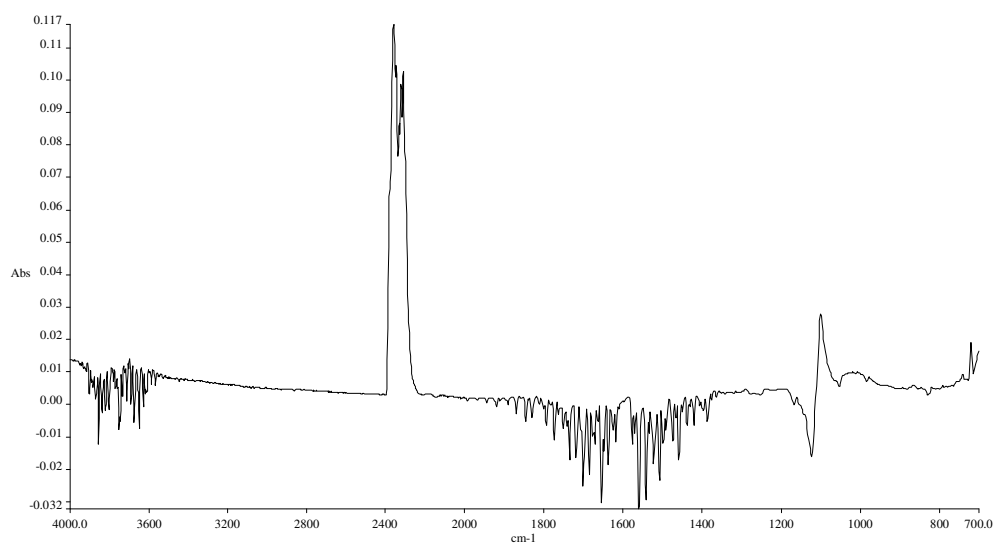


(a)

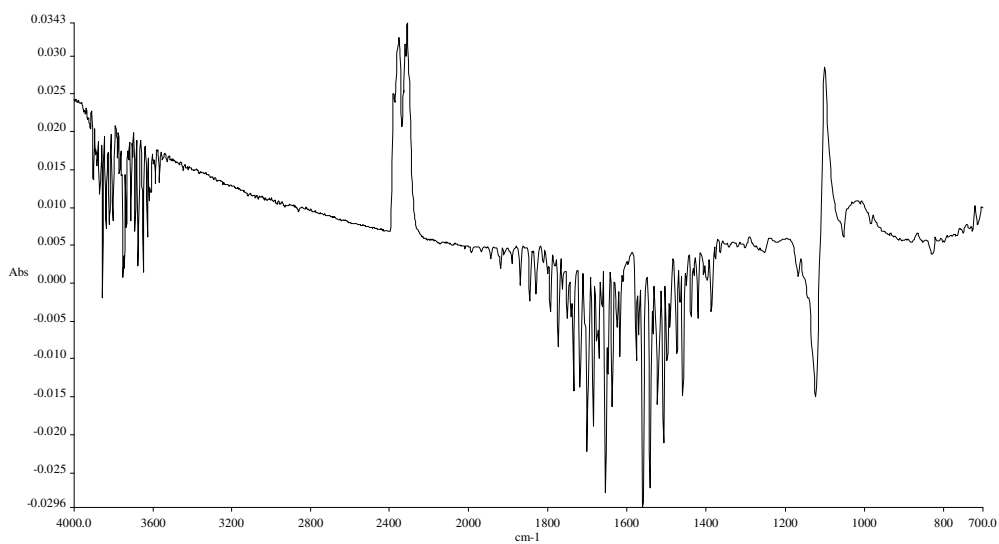


(b)

Figure A.2 cont.

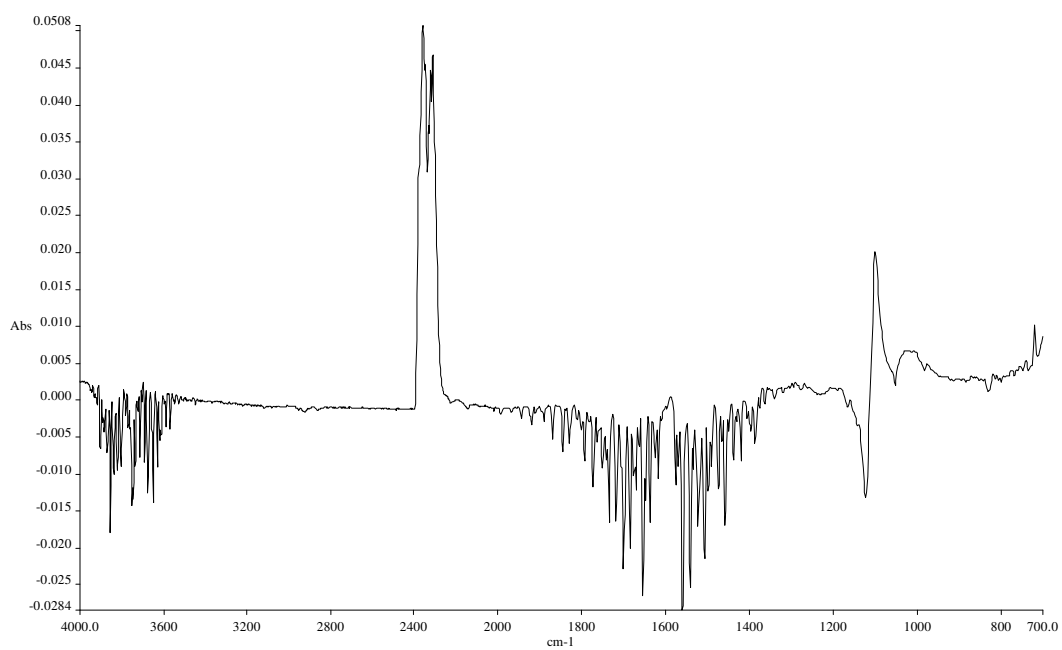


(c)



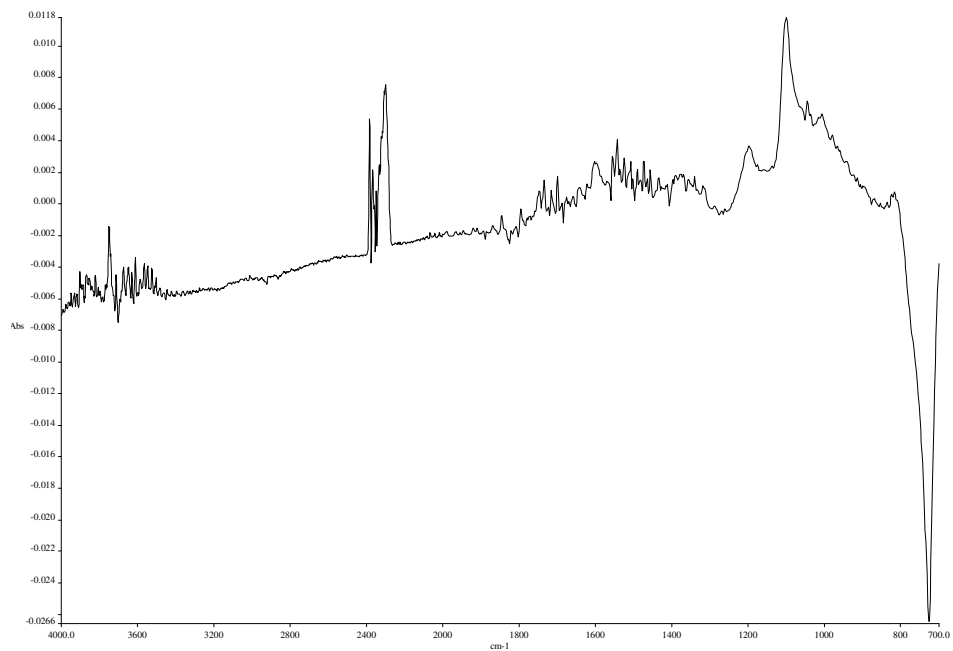
(d)

**Figure A 2.** In situ FTIR spectrum of evolved volatile components during TGA of CLP synthesized from potassium 2,4,6-trichlorophenolate at (a) 120 °C (b) 403 °C (c) 578 °C (d) 802 °C.



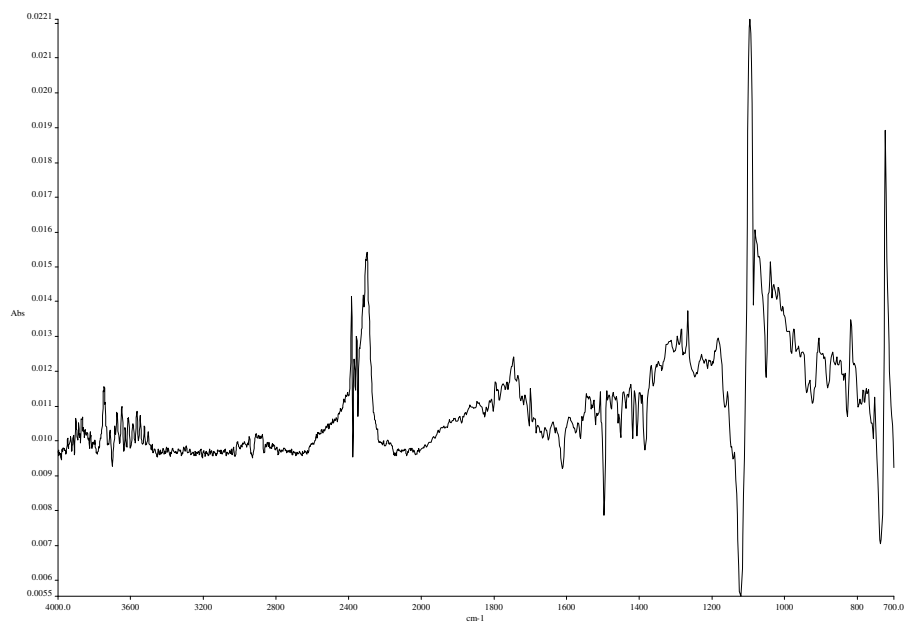
(a)

**Figure A 3.** In situ FTIR spectrum of evolved volatile components during TGA of **RIP** synthesized from pyrrole and KOH at (a) 190 °C



(a)

**Figure A 4.** In situ FTIR spectrum of evolved volatile components during TGA of **WP** synthesized from KOH and thiophene at (a) 185 °C



(a)

**Figure A 5.** In situ FTIR spectrum of evolved volatile components during TGA of orange polymer **OP** synthesized from KOH and thiophene at (a) 45 °C.

## CURRICULUM VITAE

### PERSONAL INFORMATION

Surname, Name: Güngör(Ünsal), Müfide Elif  
Nationality: Turkish (TC)  
Date and Place of Birth: 06 February 1974, Ankara  
Marital Status: Married  
Phone: +90 312 430 49 83  
Email: elif.gungor@taek.gov.tr

### EDUCATION

Degree	Institution	Year of Graduation
MS	METU Chemistry	2000
BS	METU Chemistry	1998
High School	Private Arı College	1992

### WORK EXPERIENCE

Year	Place	Enrollment
2006-Present	TAEK	Chemist
1998-2006	METU Department of Chemistry	Research Assistant

### FOREING LANGUAGES

Advanced English

### PUBLICATIONS

1. Zora, M. and Gungor, M. E., *Tetrahedron Lett.*, 42, 4733, 2001.